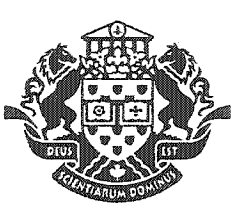

Université d'Ottawa · University of Ottawa

Université d'Ottawa · University of Ottawa

FACULTÉ DES ÉTUDES SUPÉRIEURES ET POSTDOCTORALES

FACULTY OF GRADUATE AND POSTDOCTORAL STUDIES

EKICI, Özgür

AUTEUR DE LA THÈSE - AUTHOR OF THESIS

M.A.Sc. (Electrical Engineering)

GRADE - DEGREE

School of Information Technology and Engineering

FACULTÉ, ÉCOLE, DÉPARTEMENT - FACULTY, SCHOOL, DEPARTMENT

TITRE DE LA THÈSE - TITLE OF THE THESIS

Capacity Analysis of CDMA in Multi-Beam Mobile Satellite Systems

A. Yongacoglu

DIRECTEUR DE LA THÈSE - THESIS SUPERVISOR

EXAMINATEURS DE LA THÈSE - THESIS EXAMINERS

C. D'Amours	R. Hafez

J.-M. De Koninck, Ph.D.

LE DOYEN DE LA FACULTÉ DES ÉTUDES SUPÉRIEURES ET POSTDOCTORALES — SIGNATURE — DEAN OF THE FACULTY OF GRADUATE AND POSTDOCTORAL STUDIES

CAPACITY ANALYSIS OF CDMA IN MULTI-BEAM MOBILE SATELLITE SYSTEMS

By

Özgür Ekici, B. A. Sc.

A thesis submitted to the

Faculty of Graduate and Postdoctoral Studies

in partial fulfillment of the requirements of the degree of

Master of Applied Sciences

in Electrical and Computer Engineering

Ottawa-Carleton Institute for Electrical and Computer Engineering

School of Information Technology and Engineering

Faculty of Engineering

University of Ottawa

May 2003

Your file Votre référence
ISBN: 0-612-90068-1
Our file Notre référence
ISBN: 0-612-90068-1

Abstract

Satellite communication is a valuable option in regions having low population densities, where mobile users do not have access to terrestrial communication systems. In this thesis, the design considerations of multi-beam satellite CDMA systems are treated. In communication systems, higher capacities can be obtained by efficiently using the available frequency spectrum. Satellite systems can achieve the high spectrum efficiency by using multi-beams.

The first issue emphasized in this thesis is that of co-channel interference in multi-beam systems. Similar to the terrestrial systems, in multi-beam satellite systems co-channel interference is created by interfering users within the wanted user's own cell as well as users in the other cells using the same operational frequency. One possible way to decrease the co-channel interference is to separate the co-channel cells by introducing bigger frequency reuse clusters, however this reduces the spectral efficiency. The dependence of the co-channel interference on the spot-beam contour is explained and it is shown that by appropriately choosing the cluster size and spot-beam contour, a better system performance than the full frequency reuse can be obtained in satellite CDMA systems. Hence the impact of cluster size on the capacity is carefully investigated.

Another important issue in applying the CDMA scheme is the problem of unequal received power levels. The capacity of a CDMA system is maximized in uplink when all transmitted signals are received at equal power to obtain the specified signal to interference power ratio. In view of the fact that power control techniques cannot perfectly compensate for power fluctuations in mobile communications channels, the capacity of the system is reduced. The performance of a multi-beam satellite CDMA system using perfect and imperfect power control are calculated and compared. Probability density functions and cumulative distribution functions of user bit energy-to-interference density ratios are obtained and used for system capacity calculations. Additionally, the link margins and outage probability of systems are estimated for different loadings and power control errors.

LIST OF FIGURES

LIST OF TABLES

LIST OF ABBREVIATIONS

ACeS	Asia Cellular Satellite
AWGN	Additive white Gaussian noise
BER	Bit error rate
BPSK	Binary-phase shift keying
cdf	cumulative distribution function
CDMA	Code division multiple access
EAST	Euro African Satellite Telecommunications
ELM	Excess link margin
FDMA	Frequency division multiple access
FEC	Forward error correcting
GEO	Geostationary satellite
HEO	Highly elliptic orbit
IPC	Imperfect power control
LEO	Low earth orbits
LM	Link margin
OCI	Other cell interference
PCE	Power control error
PG	Processing gain
pdf	probability density function
PPC	Perfect power control
MAI	Multiple access interference
QPSK	Quadri-phase shift keying
SIR	Signal to interference power ratio
SINR	Signal to interference noise power ratio

TDMA	Time division multiple access

LIST OF SYMBOLS (in order of appearance)

ε	Elevation angle
ϑ	Nadir angle
ψ	The earth central angle
d	Slant range
h	The satellite altitude
R_e	The radius of earth
ϕ	Power flux density
ϕ_{uni}	Uniform power flux density
f_0	Operational frequency
P_t	Transmitted signal power
G	Antenna gain
D	The diameter of the antenna aperture,
λ	The wavelength
η	Antenna efficiency
A_r	Receiver antenna area
P_r	Received signal power
L_0	Free-space path loss
$J_1(.)$	The Bessel function of the first kind and first order
$J_3(.)$	The Bessel function of the first kind and third order
θ	The off-axis angle
θ_{3dB}	One-sided 3dB beam-width
f	Other-cell-interference factor

θ_i, θ_j	Deflection angles of interfering user signals, relative to center of a particular spot-beam
Ψ_j	Receive angle of interfering signal from other spot-beam, Relative to center of its own spot-beam
N	Number of active users, randomly distributed over uniformly sampled spot-beam
P_0	Received power level with perfect power control
I_{inter}	Inter-cell interference
I_{intra}	Intra cell interference
η	Background thermal noise power
N_0	One-sided thermal noise power spectral density
W	Signal bandwidth
R	Bit rate
E_b/I_{tot}	Bit energy-to-total interference power density ratio
V	Voice activity factor
E_b/I_{req}	Required bit energy-to-total interference power density ratio
$N_{\max}$	Maximum user capacity of a spot-beam
E_b/N_0	Bit energy-to-thermal noise spectral density ratio
K	Convolutional code constraint length
$\sigma(.)$	Standard deviation
$m(.)$	Mean value
γ, ζ	Gaussian distributed random variables
p_{out}	Outage probability
P_I	Interference power

Δ_k	Denial or acceptance parameter of mobile user k in capacity calculation
n	Spot-beam ring number in the cellular layout
R_{3dB}	Spot-beam radius having 3dB gain decrease on its contour
$f_{3\text{-Cell}}$	Other cell interference factor of 3-cell cluster frequency reuse
$f_{4\text{-Cell}}$	Other cell interference factor of 4-cell cluster frequency reuse
$f_{7\text{-Cell}}$	Other cell interference factor of 7-cell cluster frequency reuse
r	Distance from spot-beam center
$P_{\text{no-deg}}$	Total power required for the users uniformly distributed in the spot-beam without PPC
P_{spot}	Total power required for a spot-beam of certain gain decrease on its contour with PPC
P_{ext}	Extra power supplied from the satellite for compensating the spot-beam antenna gain roll-off relative to no-degradation power

ACKNOWLEDGEMENTS

My special thanks go to my superviser, Prof. Dr. Abbas Yongacoğlu for his support, advice, and patience, without his directions this thesis could not have been done.

I would like to thank to my fellow graduate students and friends; Miss. Güneş Karabulut, Mr. Tunçer Baykaş, Mr. Gürkan Kurtoglu, Mr. Tolga Kurt, Mr. Onur Kutlukaya, Mr. Emre Erkmen and Mr. İstemi Faruk Özkan. Special thanks are extended to Mr. Angelo Raimondo and Mr. Mohammed Elbadri for their tireless encouragement and support

My deepest thanks go to my family for their moral support during all phases of this project. The patience and sacrifice of my mother, father, brother and sister throughout my studies can never be forgotten.

To my family and to my only love Katarina...

Aileme...

Chapter 1

INTRODUCTION AND OUTLINE

A satellite is a specialized wireless receiver/transmitter that is launched by a rocket and placed to an orbit around the earth. Satellite communication is the process of transmitting information by utilizing the satellites around the world. In satellite communications the objective is to achieve ever increasing ranges and capacities with the lowest possible cost. Massive quantity of new satellite systems that have been implemented recently, or are to be implemented in the near future such as ACeS for Asia, EAST for Africa, Thuraya for Middle East and Globalstar for worldwide coverage [Lut00] demonstrate the importance of satellites in communications.

1.1 Problem Statement

Satellite communication systems have certain advantages as well as limitations compared to terrestrial ones. One of the chief advantages of satellite system, perhaps the most significant one, is to have large coverage area. Another advantage of satellite systems, compared to terrestrial ones is that, satellite networks can be established in a relatively short time and has a flexible architecture. Table 1-1 enumerates comparisons of both communication systems.

Table 1-1 Comparison of terrestrial and satellite mobile radio systems

Terrestrial mobile radio systems	Satellite mobile radio systems
Covered areas grow gradually with the deployment of the infrastructure	Large areas can be covered quickly
High bandwidth efficiency because of small radio cells	Low bandwidth efficiency
Short round-trip-delay (important in power control)	Long round-trip-delay
No world-wide usage because of incompatible standards	Worldwide usage
Suitable for urban environments	Suitable for rural environments

From the comparisons made, we can conclude that terrestrial mobile radio systems are cost effective for limited areas with high user population and traffic density, whereas mobile satellite systems are cost effective for large areas with low user population and limited traffic density.

In mobile communication systems, the major restriction of having a large capacity is the limited spectrum. In terrestrial communication systems, the same frequency channels are used many times in different cells and this is termed frequency reuse. In satellite mobile radio systems, the frequency reuse is accomplished by utilizing multi-beams. The coverage area is divided into several regions, each of which is served by a different satellite spot-beam.

In multi-beam satellite systems, the reuse of radio channels, whose purpose is to increase the spectrum efficiency of the system, is the cause of one of the main performance impairment. That is, the multiple access interference (MAI). In order to successfully design any frequency reuse system, it is imperative to understand and analyze the effects of the MAI on the system performance.

Another important issue that needs to be addressed in satellite communications is the power control. Because of the length of the round trip propagation delay inherent on a satellite channel, and inability of power control schemes to track out fast variations due to multi-path fading, one has to include the power control error in the capacity calculations.

In satellite communications, it is possible to use frequency division multiple access (FDMA) or time division multiple access (TDMA) schemes for multi-beam systems. However, they have major disadvantages particularly from frequency reuse perspective. Furthermore TDMA scheme requires high instantaneous power. Considering also that 3rd Generation cellular systems are employing code division multiple access (CDMA), the most promising multiple access technique for multi-beam mobile satellite system is CDMA Hence in this thesis we will consider only CDMA systems.

1.2 Thesis Objectives

In this thesis, the capacity of a satellite-based mobile communications system employing CDMA technique is presented. GEO satellite system utilizing multi-beam antenna is described and the system parameters that affect the system performance are explained.

The motivation behind this thesis is to investigate the interaction between the system design parameters that are used in CDMA multi-beam satellite systems. The performance of a CDMA system is mainly limited by two factors: MAI and power control accuracy.

The first issue that is considered is the MAI. In a multi-beam satellite system or a multi-satellite system with overlapping beams, the estimation of the MAI becomes much more complex. An argument advocating that the interference coming from the mobile users in the adjacent cells are much more critical for satellite systems than for terrestrial cellular systems will be justified. Proper performance evaluation of the MAI requires information about satellite spot-beams: their number, configuration, and the beam roll off characteristics. This raises issues such as frequency assignment and frequency re-use between spot-beams and it becomes a more challenging problem requiring detailed analysis.

The concept of other cell interference (OCI) will be introduced as a major system parameter representing the MAI characteristic of the CDMA multi-beam satellite systems.

A detailed explanation will be provided regarding that one possible way to decrease the OCI is to introduce bigger frequency reuse clusters. Using different operational frequencies in adjacent cells reduces the MAI. The trade off between the capacity gain due to decreased OCI and the capacity loss due to reduced spectral efficiency will be presented and it will be shown that in satellite CDMA systems better performance can be obtained by introducing frequency reuse clusters rather than full frequency reuse.

In terrestrial communication systems, in addition to frequency reuse, one can decrease the MAI by increasing the separation of cells. The idea behind this approach is the attenuation of the signal

power by a distance power law. However, in satellite systems, the isolation between the spot-beams can be accomplished by increasing the spot-beam contour. Usually, the spot-beam contour is defined by a 3 dB decrease of antenna gain. Higher beam isolation leading to less interference can be achieved by choosing a larger gain decrease at spot-beam contour. The thesis will also address that by selecting a larger gain decrease at spot-beam contour, one can increase the capacity per beam. We will present that despite the increased capacity per beam, the overall system capacity would decrease due to less spectral efficiency (e.g. representing the constant serving area with fewer beams).

The second issue that is studied for system performance is Power Control Error (PCE). We will explain the limitation of the imperfect power control (IPC) on the system capacity. We will give the outage probability expression and system capacity degradation due to PCE. Furthermore, we will evaluate the system link margin (LM), which gives an idea about the applicability of the system.

1.3 Thesis Outline

Chapter 2 provides basic properties of a satellite multi beam system. An explanation of the earth-satellite geometry, geometric relations between satellite and mobile users on earth will be introduced. There will also be an introduction of spot-beam antenna gain characteristics used in GEO satellite. The radio links in satellite communications is defined. The concept of the hexagonal radio cell pattern, cellular layout and frequency reuse policies are discussed. We introduced the interference model and MAI calculation method. We conclude the chapter by giving the satellite mobile channel characteristics.

In Chapter 3, theoretical capacity calculations of CDMA satellite systems are introduced. Firstly we consider the capacity of single beam systems. By the introduction of the other cell interference originated from other beams, we then calculate multiple beam system capacity. Further expansion of capacity calculation for practical systems is assessed by taking into account the PCE. It will

later be shown that a system capacity highly depends on the PCE. Finally outage probability calculation of the system is given.

Simulation results are provided in Chapter 4. Initially, perfectly power controlled system capacities are evaluated. In PPC, Single beam satellite system considered first. In multi beam system capacity evaluations, systems with different parameters are then evaluated. The effects of cellular layout, beam overlap value, frequency reuse and beam loading on satellite system capacity are calculated. Another critical system parameter, satellite power requirement for PPC is evaluated in this section as well.

After considering perfectly power controlled users, PCE is introduced to capacity calculations of the system. The consequences of different PCEs on the system capacities are evaluated. We conclude the section with outage probability calculations and excess link margin evaluations of realistic systems.

In Chapter 5; summary, conclusion, contributions and recommendations for future work are presented.

Chapter 2

BASIC CONCEPTS OF MULTI-BEAM MOBILE SATELLITE CDMA SYSTEMS

In this chapter, we will review the basic properties and definitions of the multi-beam mobile satellite CDMA systems and present the system model that we will employ. We will indicate the differences of satellite CDMA systems from terrestrial ones and identify the characteristics of the multi-beam satellite CDMA system that we will use to evaluate the performance.

In order to have accurate performance evaluation of a communication system, it is vital to give all the system structure details that affect the overall performance and capacity. In satellite multi-beam communications, we can count several factors that influence the overall performance, e.g., satellite constellations, spot-beam antenna gain pattern, and multi-beam cellular layout.

The aim of this chapter is to give brief descriptions of the system parameters that we will use in the system performance evaluation.

2.1 Satellite - Earth Geometry

This section deals with basic geometric relations between satellite and mobile user terminals on earth. The geometry of a satellite and a user terminal on earth is illustrated in the Figure 2-1. We will use this model to calculate the interference level the mobile users experience and capacity of satellite systems. In this thesis, we will focus on a single Geostationary Satellite (GEO) with multi-beam generation property instead of considering multiple-satellite constellations. One of the important parameters of the system, the coverage area, is defined by geometric relations of the satellite and earth with assumption of flat surface.

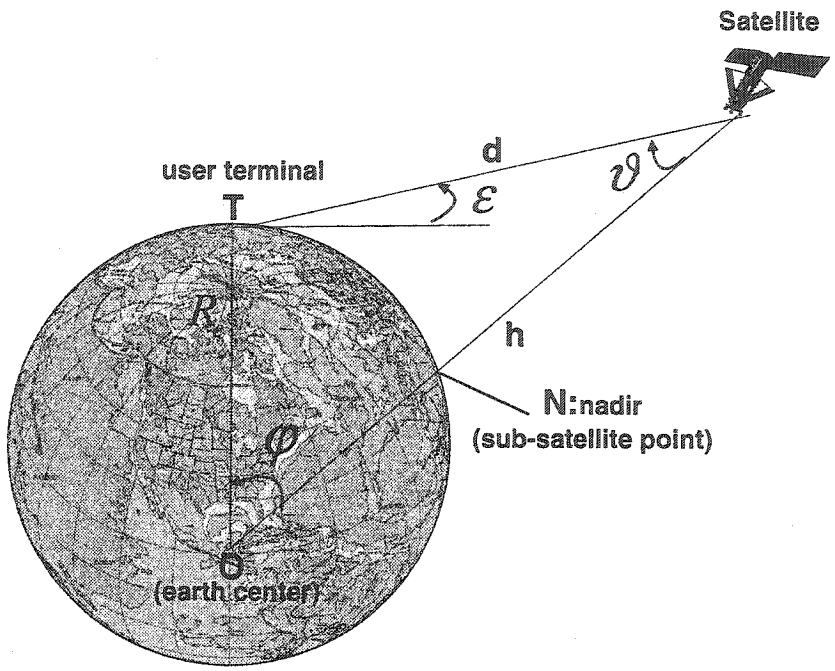

Figure 2-1 Geometric relations between satellite and mobile user on earth

We can state the important geometric parameters in the definition of a satellite communication system as follows:

- The elevation angle ε : Angle at which a user can see the satellite above the horizon,
- The nadir angle ϑ : Angle that gives the deflection of the user from nadir as seen from the satellite,
- The earth central angle φ : The angle between the sub-satellite point and user
- The slant range d : the distance between the satellite and user terminal
- The satellite altitude h : the distance between the satellite and the nadir point
- R_e : the radius of the earth

The coverage area or footprint of a satellite is defined as the area on the earth's surface where satellite is seen with an elevation angle ε, greater than a given minimum elevation angle $\varepsilon_{\min}$.

The threshold ε_{min} defines the border of the overall coverage area of the satellite. The minimum elevation ε_{min} is an important parameter to determine the satellite channel accessibility. The coverage area of a satellite as defined by geometry is a spherical cap on the earth's surface, whose contour is defined by minimum elevation angle. However, in this study, earth's curvature will be ignored and the coverage area will be determined relative to the antenna and cell cluster properties on a flat surface.

2.2 System Model and Signal Propagation

In this section we discuss the general signal propagation behavior in the satellite communication and the link definitions for mobile satellite networks. In view of the fact that system capacity calculation methods differ relative to the links considered, it is important to give explicit definitions of the links involved.

2.2.1 Radio Links in Satellite Communications

The radio links in satellite communications are illustrated in Figure 2-2.

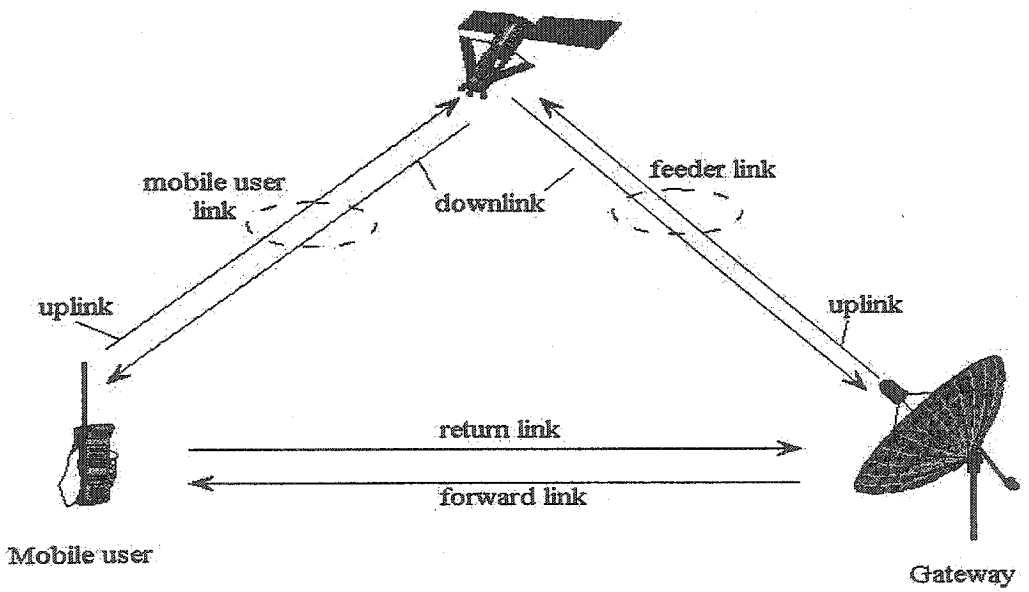

Figure 2-2 Link definitions for mobile satellite networks

The most critical link with regard to communication quality is the link between the mobile user and satellite. Because, handheld terminal antennas has lower gains than gateway stations and the visibility of gateways are usually better than the mobile users. Common names for this link are user link or service link. The link between the satellite and a fixed earth station is called the feeder link. The feeder links operate at higher frequencies (e.g. 14/12 GHz) where there is plenty of spectrum available. The mobile links typically operate in the L-band (e.g. 1.6 GHz).

Both links can be separated into an uplink and downlink. Finally, the series of one directional links from the fixed earth station to the user is called the forward link, and the links in the opposite direction constitute the return link.

In parametric performance evaluation and comparisons of satellite system, we will concentrate on the mobile user-satellite link and assume that the system is mobile-link limited. The contribution of the feeder link will be neglected.

In comparison of the mobile user uplink and downlink paths, we will concentrate on the system capacity calculations for uplink. That is because, in the mobile user downlink, perfect synchronization is possible when all users are synchronized at the gateway or satellite. One can reduce MAI that mobile users experience by using orthogonal codes through synchronization. Techniques for doing this include using Hadamard codes with perfectly synchronized users [Lyo97]. The limited number of orthogonal Hadamard codes, generally, implies orthogonality can be applied within a single beam but not between spot-beams. Therefore, in this case MAI in the mobile user downlink is coming from the satellite beams serving to the users in adjacent beams (inter-beam interference).

Contrary to the mobile user downlink, in the mobile user uplink, perfect synchronization of users scattered over a wide area is difficult. Therefore, we will assume asynchronous user uplink. It is no longer assumed that users are orthogonal within the considered beam. Consequently, MAI in the uplink is caused by the users in the other beams as well as the users in the wanted beam (intra-

beam interference). The addition of the intra-beam interference to the already existing inter-beam interference makes the system capacity mobile-user uplink limited.

2.2.2 Signal Propagation

In the capacity calculations of a CDMA system, received mobile user power levels have chief importance [Kud92]. When the signal propagates between a satellite and a user terminal, the signal attenuation due to free space loss is the main change observed on the received signal level. Since the attenuation increases with distance it is especially severe in the satellite scenario. Together with the antenna characteristics of the transmitter and receiver, we can calculate the received signal power level at satellite, which is a very important parameter for system capacity assessment.

Antennas are the interface between the radio link and the communications hardware. They are used as the start and end point of the radio link for transmission and reception. An isotropic antenna radiates uniformly in all directions, i.e., uniformly into 4π solid angle of the sphere. If an isotropic antenna operates with P_t transmit power, its power flux density produced at distance d can be found as:

$$\phi_{uni} = \frac{P_t}{4\pi d^2} \text{ in Watt / m}^2 \tag{2.1}$$

A directional antenna focuses the power radiation, by using the reflector, into a solid angle less than 4π. Accordingly, only a limited part of the sphere is illuminated with a specified power flux density, ϕ. The antenna gain is defined by the ratio of these flux densities.

$$G_t = \frac{\phi}{\phi_{uni}} \tag{2.2}$$

in linear form, where the index t refers to a transmit antenna. The same concept of antenna gain holds for directional receive antenna as well, which preferably receives power from a limited range of directions.

Antennas for handheld terminals typically limit the radiation and reception to the upper hemisphere, and thus exhibit antenna gains of G=1 to 3dB [Lut00]. Antennas with a higher directivity are required on board satellites which are shown in the following section.

The bore-sight of a directional antenna is the direction of maximum gain. The actual maximum gain is proportional to the antenna area and it can be given in linear units as:

$$G_{\max} = \eta\left(\frac{\pi D}{\lambda}\right)^2 \tag{2.3}$$

Here, D is the diameter of the antenna aperture, λ is the wavelength and η is the antenna efficiency typically in the range of 0.55-0.65 [Mar98].

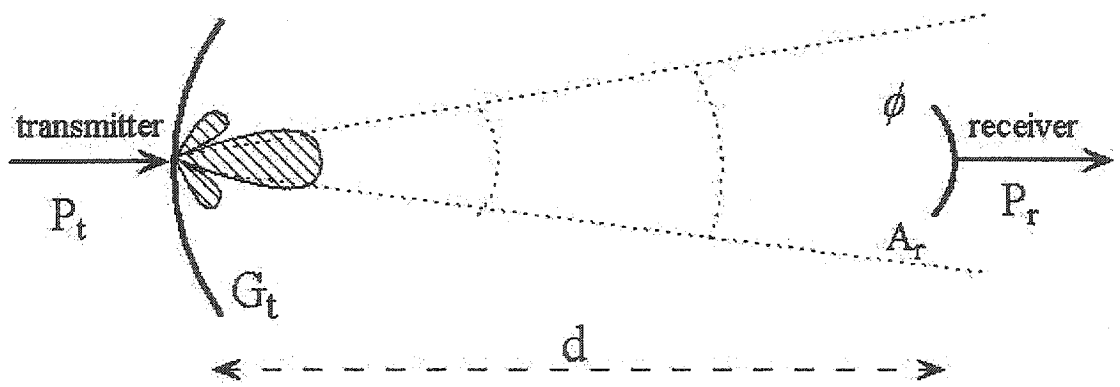

Figure 2-3 Radio link with directional antennas

Figure 2-3 shows a radio link with two directional antennas. From the power radiated by the transmit antenna, the receiver antenna picks up an amount that depends on the power flux density ϕ at the receive antenna, on the reflector area A_r and the efficiency η_r of the receive antenna. With these characteristics, we can write the received signal power as:

$$P_r = \eta_r A_r \phi = \eta_r A_r \frac{P_t G_t}{4\pi d^2} \tag{2.4}$$

Substituting the term $A_r = \pi D^2/4$ with equation (2.3) and taking the G_r as the gain of the receive antenna, we can find the received power as:

$$P_r = \frac{P_t G_t G_r}{(4\pi d/\lambda)^2} = \frac{P_t G_t G_r}{L_0} \tag{2.5}$$

The variable L_0 is called the free space loss [Ska88]. It describes the decrease of received power with increasing distance d between transmitter and receiver, due to the spatial dissipation of the radiated power. In our simulations and calculations we will concentrate on the received mobile user powers at the satellite in the mobile user uplink. It is assumed that power control is implemented in mobile user uplink for controlling the received power level. However, power-control is assumed to compensate only slowly-varying link variations such as those due to antenna roll-off and path length. The effect of power control error on the system capacity due to dynamic changes in the channel state is also considered.

2.3 Satellite Antennas

As we mentioned in the previous section, one of the key determinants of the satellite communication system performance is the satellite antenna and its gain characteristic. Spatial discrimination provided by satellite multi-beam antennas is very crucial in determining the capacity of mobile satellite system. In this section, details of satellite spot-beams, their number (cellular configuration) and the antenna gain characteristics are given for performance evaluation.

2.3.1 Spot-beam characteristics

A number of reasons can be given for using spot-beams in a satellite system. By using spot-beams, high satellite antenna gain can be obtained for the link budget, especially in GEO satellite systems, because spot-beams focus the transmitted power onto a much smaller area than the total viewing area of the satellite.

Another advantage of the spot-beam approach is that a frequency band can be reused in different beams to improve the bandwidth efficiency of the system. The frequency reuse factor depends on the multiple access scheme used.

However, there are some disadvantages of using multi-beam antennas. The increased complexity of satellite antenna, increased beam handovers (mainly for non-geostationary systems) and MAI arising between beams using the same frequency can be listed as major drawbacks.

The physical size of the antenna (diameter) is one of the most essential determinants of spot-beam gain pattern. It affects not only the power requirements for the satellite and the mobile terminal but also determines the minimum spot-beam size on earth, where by convention it is defined as 3 dB beam width.

In multi-beam satellite systems, the coverage area of the satellite is bigger than the illumination area of the spot-beam antenna; therefore the coverage area must be filled up with several spot-beams. From a technological point of view, spot-beams can be produced by multi-feed reflector antennas or phased-array antennas as indicated in [Lut00] and [Ven95]. In this thesis we will concentrate on the characteristics of spot-beams. The spot-beam generation techniques of satellite antennas are beyond of the scope of this thesis.

It will be assumed that satellite antennas are uniformly illuminated. The spot-beams in the cellular layout on the coverage area are arranged according to a gain-overlap criterion (3dB). The spot-beam gain is given by:

$$G_{spot}(\theta) = \left(\frac{J_1(u)}{u}\right)^2, \text{where u} = D\pi\left(\frac{\sin\theta}{\lambda}\right) \tag{2.6}$$

where, $J_1(.)$ is the Bessel function of the first kind and first order, D is the antenna diameter, λ is the carrier wavelength, and θ is the off-axis angle. The two-sided 3dB beam-width, $2\theta_{3dB}$ of uniformly illuminated spot-beam antennas is given by Maral [Mar98] as:

$$2\theta_{3dB} = (\lambda/D)x58^0 \tag{2.7}$$

and for non-uniformly illuminated antennas, tapered-aperture antenna, the two sided beam-width can be found by:

$$2\theta_{3dB} = (\lambda/D)x70^0 \tag{2.8}$$

A normalized[1] single spot-beam antenna gain pattern of a satellite operating at 1.6GHz and antenna diameter of 20 m is shown in the Figure 2-4.

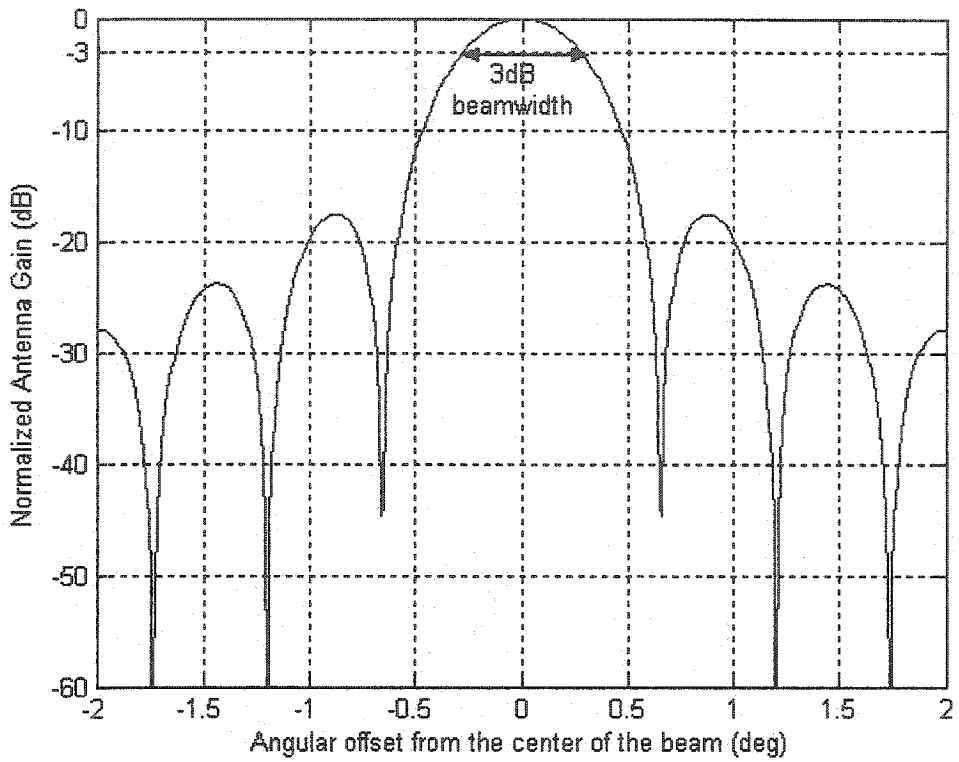

Figure 2-4 Gain characteristic of a spot-beam with antenna diameter of 20m operating at 1.6 GHz and the two-sided 3dB beam width is given by equation $(\lambda/D)x58^0$=0.54 deg

If we assume the antenna efficiency η=0.6, operational frequency f_0=1.6GHz and antenna diameter D=20m, the maximum gain at the bore-sight direction can be calculated with equation (2.3), G_{max}=48.3dB.

[1]Maximum value of the spot-beam antenna gain is set to 0dB.
3-D gain pattern of the same spot-beam antenna relative to angular offset is illustrated in Figure 2-5.

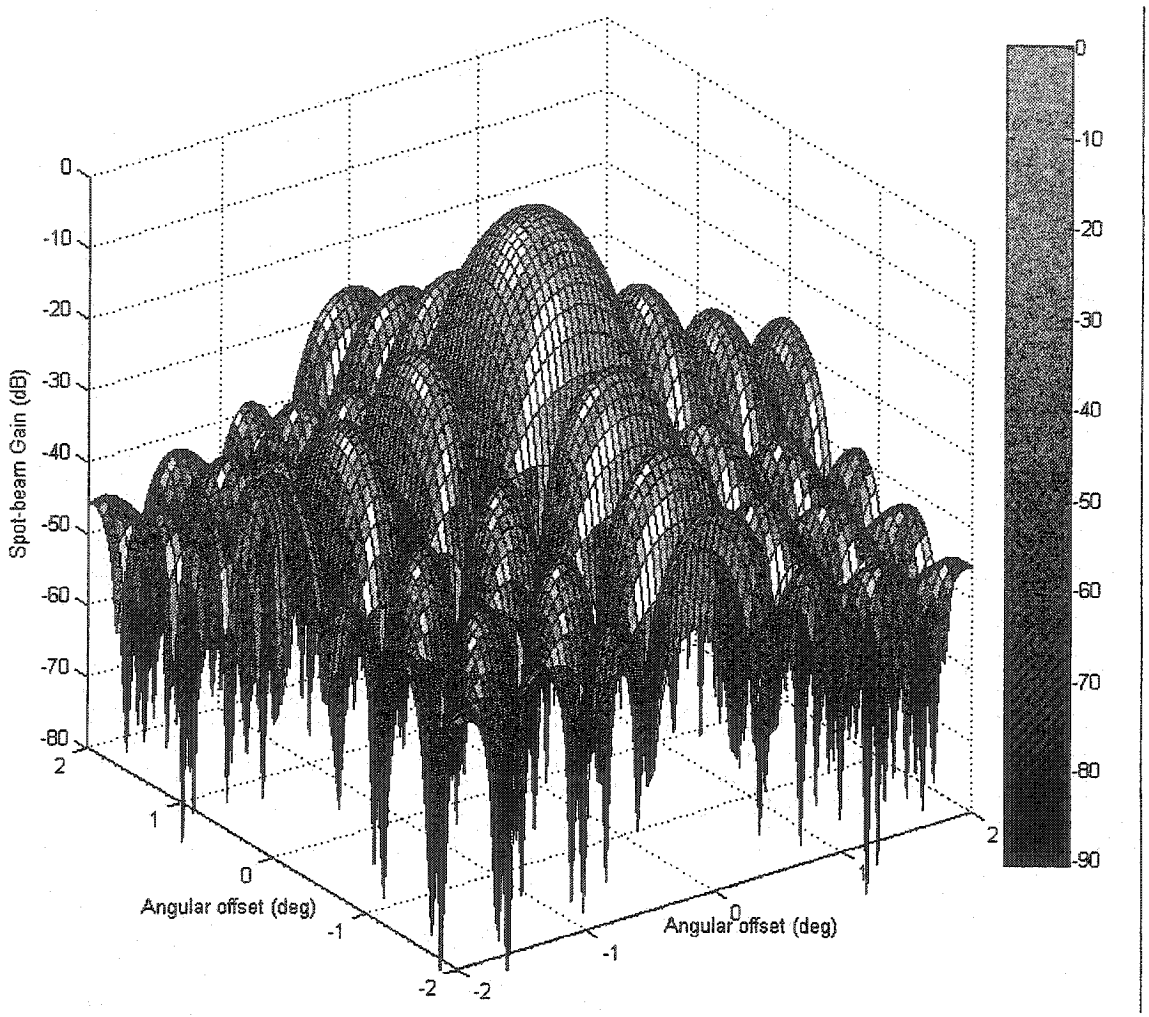

Figure 2-5 3-D Gain characteristic of a spot-beam with antenna diameter of 20m operating at 1.6 GHz and the two-sided 3dB beam width is 0.54 deg

The gain characteristic has a main lobe which falls off rapidly but it also has significant side lobes. In the gain overlap spot-beam configurations, the side lobes fall on the adjacent beams, which cause multiple access interference. In practice, antenna designers may taper the main lobe and/or side lobes to some extent but one can still expect the side lobes to be non-negligible.

Lutz [Lut97] uses another spot-beam antenna gain pattern, with non-uniform illumination, which leads to attenuation at the reflector boundaries:

$$G_{spot}(\theta) = \left(\frac{J_1(u)}{2u} + 36\left(\frac{J_3(u)}{u^3} \right) \right)^2 \tag{2.9}$$

where $u = 2.07123(\sin\theta/\sin\theta_{3dB})$, $J_1(u)$ and $J_3(u)$ are the Bessel functions of the first kind of order 1 and 3, θ is the angular offset from the center of the beam and θ_{3dB} is 3dB contour[2].

If we call the former spot-beam antenna gain pattern as *Gain1* and Lutz's spot-beam antenna gain pattern as *Gain2* and plot them in a same graph, the differences between two gains can be observed without difficulty as given in the Figure 2-6:

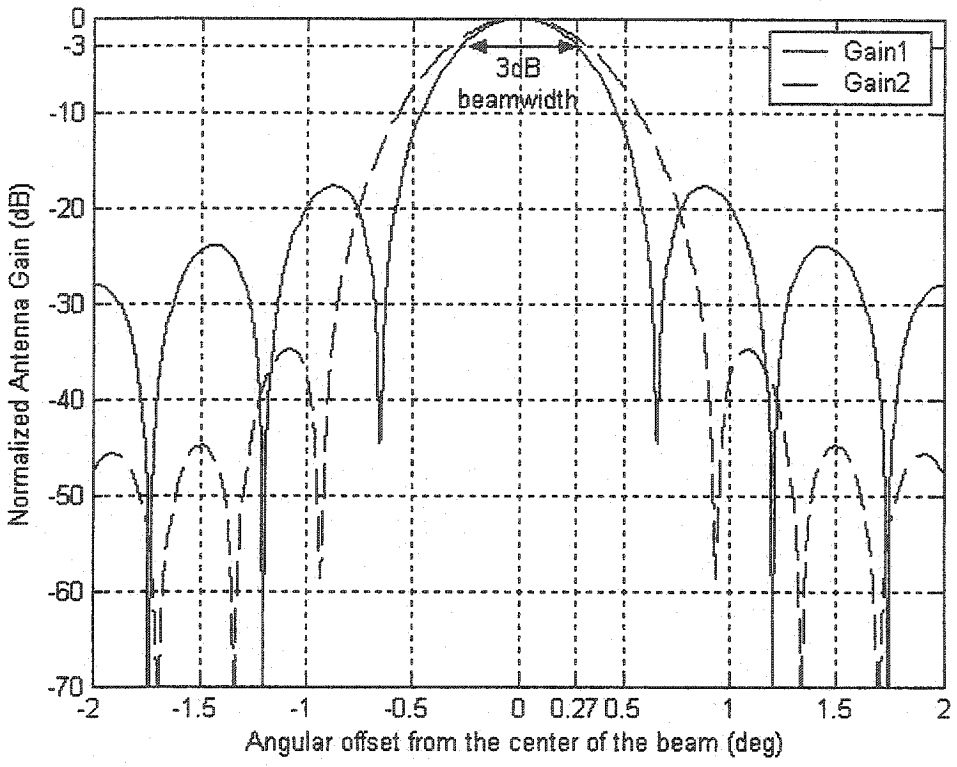

Figure 2-6 Two different spot-beam antenna gain patterns with antenna diameter of 20m, operating at 1.6 GHz. The two-sided 3dB beam width for Gain1 can be found by equation (2.6) and for Gain2 equation (2.9)

[2]3dB decrease of antenna gain compared to maximum spot-beam antenna gain at the beam center.

As can be noticed from the graph, the main lobe of Lutz's gain pattern is bigger, whereas its side lobes are significantly lower comparison to *Gain1*. In performance evaluation of a multi-cell satellite system, we will use the spot-beam gain pattern illustrated in Figure 2-4 and Figure 2-5.

2.4 The Cellular Concept

This thesis investigates a Geostationary (GEO) Satellite System using multi-beam antennas. That means the service area of the satellite (the satellite footprint) is covered by many beams. In the existing and planned satellite systems, the number of beams to cover the area equivalent to North America is between 200 to 300. For representation of the service area in our calculations and simulations, we utilized cellular (hexagonal) pattern that is used in the terrestrial systems. This section shows the model to represent the satellite multi-beam cellular layout. The satellite footprint model and approximations to the practical satellite system is particularly important for the proper calculation of the system capacity.

2.4.1 Concept of the Hexagonal Radio Cell Pattern

For the illustration of service area of a spot-beam, the hexagon is used as an idealized radio cell shape. In this section, 'spot-beam' and 'cell' terms denote the same concept, the area of a single beam. As shown in Figure 2-7, the hexagon can be used to fill out the whole satellite coverage area continuously without any overlapping of cells. Concerning the way in which to fill up a satellite footprint with cells, a typical approach is to surround a central cell (the nadir cell) with concentric rings of cells. In Figure 2-7, each ring of cells is illustrated with a different pattern.

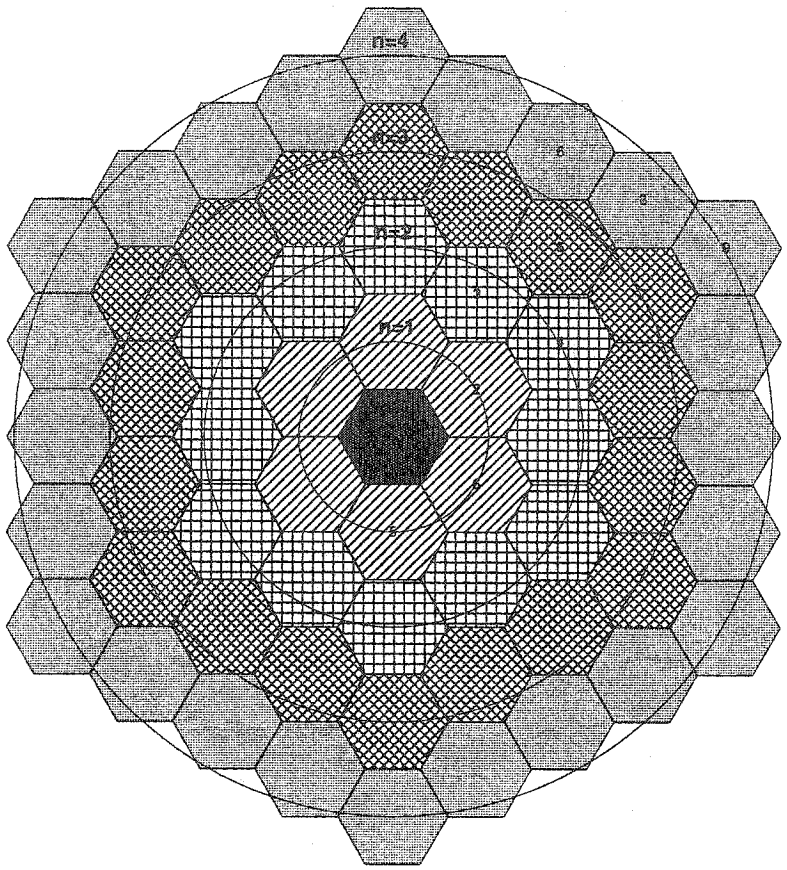

Figure 2-7 Satellite coverage area with rings of cells around the nadir cell

2.4.2 Cellular Layout, Frequency Reuse and MAI

In CDMA system, the same carrier frequency can be used in all spot-beams, since all signals are distinguished by nearly orthogonal code sequences [Vit94]. We will investigate the effect of MAI, i.e., interference caused by users using the same frequency, to the system capacity in the mobile user uplink. In this section we will present the calculation method of MAI. In the mobile user uplink, the interfering mobiles are those mobiles which radiate into the spot-beam of the desired mobile. Since, interference calculation only depends upon the beam of the desired mobile; it is transparent to the mobile's position within the beam[3].

[3]All the mobile users in the considered spot-beam experience the same interference.

Viterbi [Vit94] defined an approach to relate the interference powers caused by the users in the considered beam (intra-beam) and the interference power caused by the users in other beams (inter-beam) of satellite footprint in the mobile user uplink. He related the received inter-beam interference power to the intra-beam interference power and defined the Other-Cell-Interference (OCI) factor, f ,by taking the ratio of these interference powers. We will use the same methodology as Lutz's [Lut97], where OCI factor in satellite systems with CDMA power controlled uplink is calculated numerically for different orbits, clusters and antenna patterns.

In terrestrial CDMA systems the signal power decrease of the fourth power of distance is usually accepted [Vit94]. However, in multi-beam satellite systems the OCI factor can be calculated by considering the characteristic of the spot-beam antenna gain pattern, cellular layout of satellite footprint, frequency reuse method in the system and spot-beam gain overlap value. A spot-beam gain overlap value specifies the meeting points of the spot-beams in the footprint. For example, 3 dB gain overlap means, a spot-beam in the layout meets with its neighboring spot-beams at a point where the gain of each spot-beam is 3 dB less than their maximum gain (at the center of a spot-beam).

The OCI factor is a very important parameter in the evaluation of interference limited CDMA system capacity. In the calculation of the OCI factor, we will use the geometry of the user with respect to the satellite and the spot-beam antenna gain as given in Figure 2-8. This relative geometry is applied to each user in each spot-beam of the layout to calculate its interference to the wanted user in the mobile user uplink. Thet is because; the overall interference is the composition of a number of individual interferers.

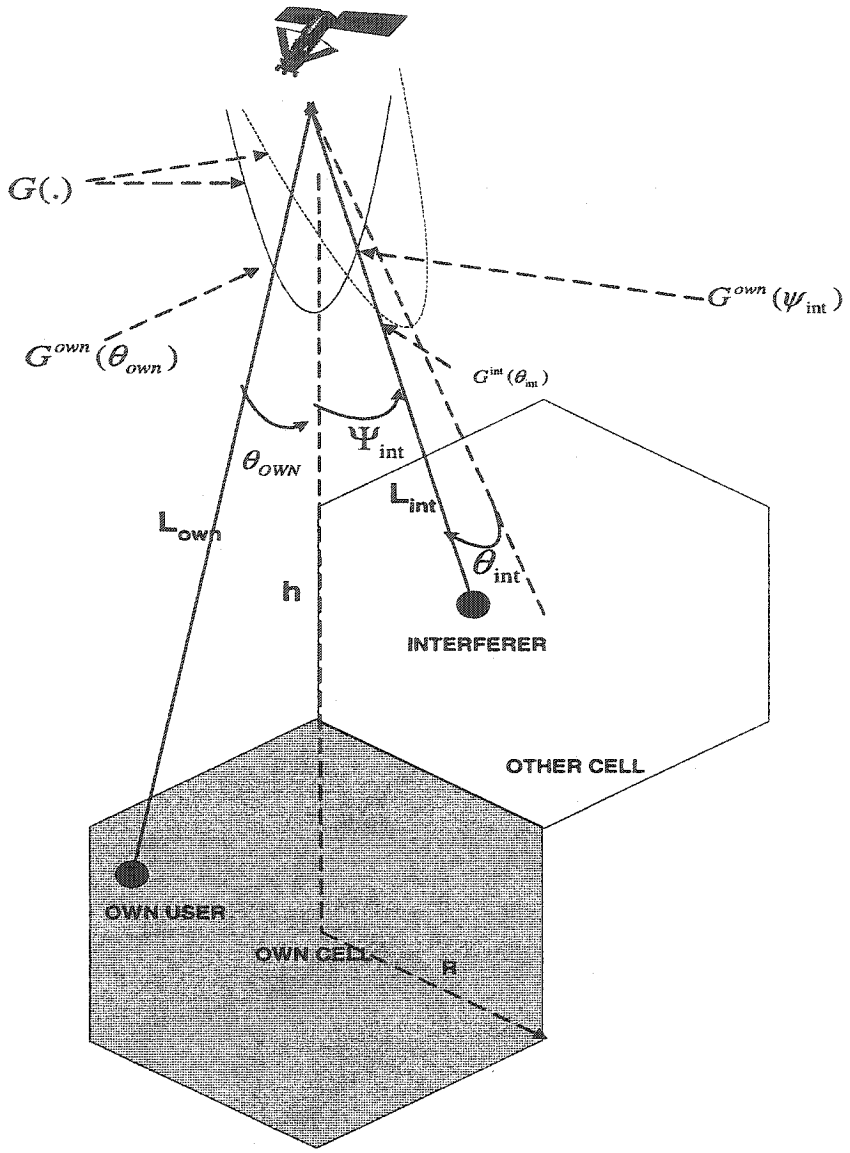

Figure 2-8 Own and other-cell interference scenario in a multi-beam system

In the calculation of the OCI factor, we assumed uniformly distributed users in the satellite coverage area. Although assuming uniform distribution of mobile users is not a realistic hypothesis, we will use this model for the first simulation approximation of the system. More realistic user distributions can be added for system performance evaluation in the future work. Uniform sampling of a spot-beam is illustrated in Figure 2-9. The locations of active mobile

users, whose numbers are less than the sampled positions, are randomly distributed over the uniformly sampled spot-beam.

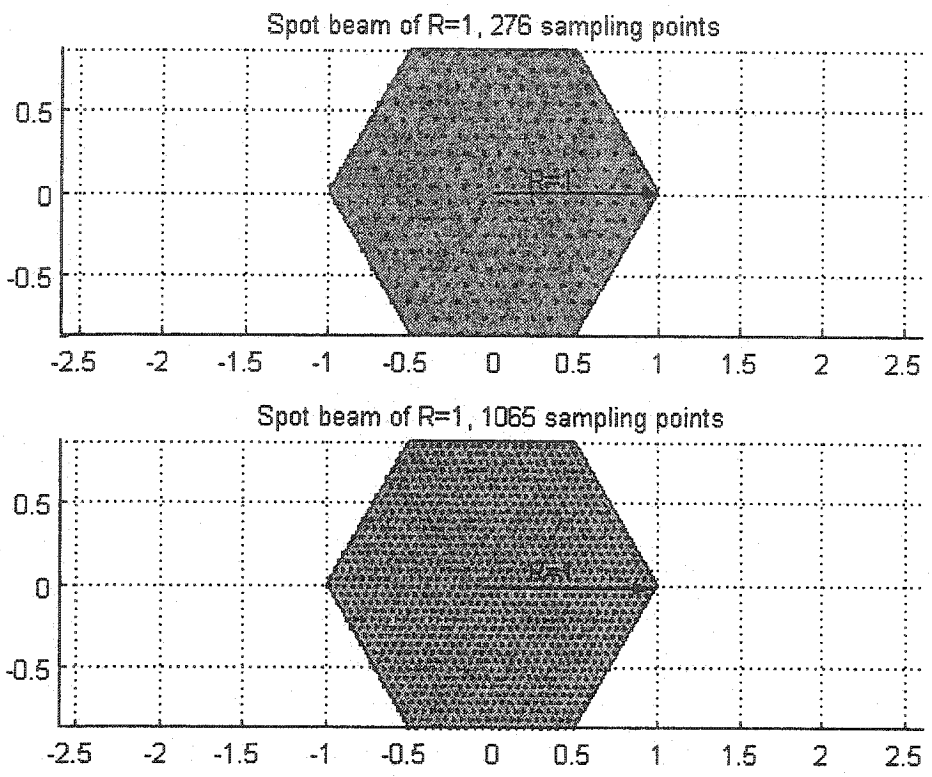

Figure 2-9 Illustration of the uniform sampling of a spot-beam. In the simulations conducted, spot-beams are sampled at 1065 different points for uniform distribution and the active mobile users are distributed randomly over the uniformly sampled points

By using the geometry illustrated in Figure 2-8, the OCI factor, *f*, can be estimated by calculating the total interference power received from all other-cell interferers *j* using the same frequency band, and dividing this estimate by the interference power received from interferers *i* within the own cell. Assuming all transmitter antenna gains are same and have unity gain ($G_t = 1$), the OCI factor can be found as:

$$f = \frac{\sum_{j \in \text{other cells}} \frac{P_j G(\Psi_j)}{L_j}}{\sum_{i \in \text{own cell}} \frac{P_i G(\theta_i)}{L_i}} \tag{2.10}$$

where G is the spot-beam antenna gain characteristic in the cellular layout, L_i and L_j are link-loss functions of user locations; θ_i, θ_j are the deflection angles of interfering user signals, relative to center of a particular spot-beam and Ψ_j is the receive angle of interfering signal from other spot-beam, relative to center of its own spot-beam. In the following calculations and computer simulations, the own spot-beam is considered as in the center of the cellular configuration which is in the nadir direction of the satellite. In the OCI factor calculations, the PPC of users relative to their own spot-beam[4] is assumed. N number of active users are randomly distributed over uniformly sampled spot-beam. The PPC mechanism for each spot-beam of the cellular layout is illustrated in Figure 2-10.

[4]The differences in signal attenuation and antenna gain are compensated, and received uplink power is maintained constant e.g., P_0 at satellite.

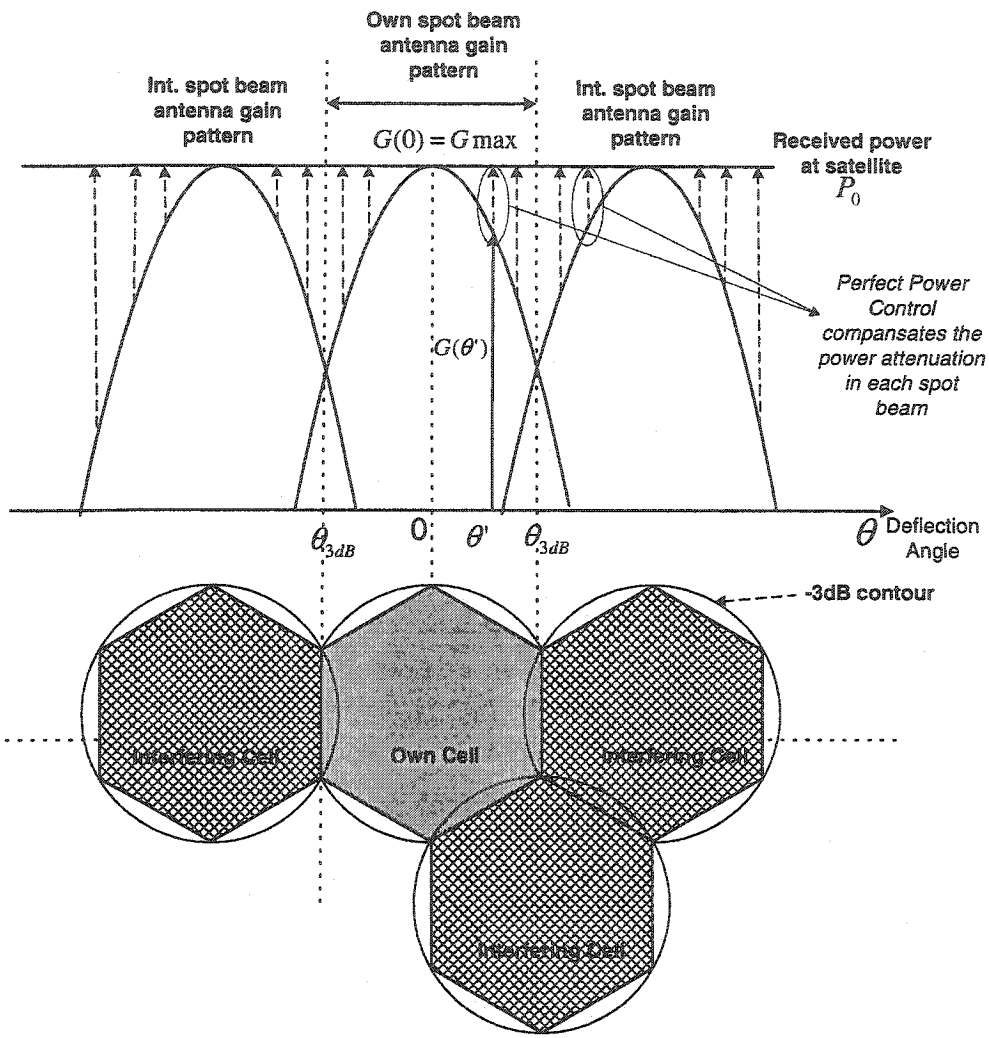

Figure 2-10 Perfect power control mechanism of each spot-beam in mobile user uplink

With these assumptions the OCI factor can be found as:

$$f = \frac{I_{\text{inter}}}{I_{\text{intra}}} = \frac{\sum_{j=1}^{other-cells} \sum_{k=1}^{N} \frac{G\left(\Psi_{j,k}\right)}{G\left(\theta_{j,k}\right)}}{(N-1)} \tag{2.11}$$

Among the system parameters affecting the OCI factor, we can count satellite footprint cellular layout, spot-beam overlap value, frequency reuse method between adjacent spot-beams and beam loadings in the satellite footprint.

Utmost importance should be given to the OCI factor and its calculation technique. That is because; the OCI factor is the only difference between single spot-beam and multi-beam satellite system capacity calculation methodology which will be defined and analyzed in Chapter 3.

In multi-beam satellite system performance simulations, we will calculate the OCI factor with different system parameters and subsequently evaluate the system capacity with the calculated OCI factor.

2.5 Mobile Fading Channel Characteristics

In a satellite system performance analysis, it is essential to have a solid knowledge of the specific characteristics of satellite mobile channels. At frequencies allocated to land mobile satellite systems, shadowing of the line of sight signal as well as multi-path propagation phenomenon can severely impair the link availability. In this section, we will investigate satellite mobile channel impairments and study satellite channel models used to simulate the satellite channel. The channel impairments result into power control error (PCE), which will decrease system performance as we will illustrate in chapter 4.

2.5.1 Satellite Mobile Channel Fadings

In satellite mobile radio systems, the received signal strength can generally be characterized according to three divisions. In the small-scale division, i.e. spatial movements of the order of one wavelength, the signal envelope typically has a Rayleigh or Rician distribution. In the medium-scale division, i.e. spatial movements of the order of tens of wavelengths; average power typically follows a lognormal distribution. In the large-scale division, i.e. spatial movements of the order of

miles, the median average power level typically varies in some power-law model with path length.

Large-scale signal variations can be characterized with idealized free-space model as we mentioned in section 2.2. This model ignores the effects of the environment in a mobile channel. In contrary to ideal free space model for most practical mobile channels, where signal propagation takes place in the atmosphere and near the ground, the free space propagation model is insufficient to describe the link characteristic. In mobile channels, we have to take into account the small-scale and medium-scale divisions as well. The medium-scale signal variation is caused by the fact that the transmitted signal might not reach the receiving antenna directly due to obstacles blocking the line-of-sight path, in other words, it might be shadowed. For the small-scale case, it is the superposition of signals coming from surroundings due to reflection, diffraction, and scattering caused by buildings, trees, and other obstacles on the receiver, which is known as multi-path propagation. A typical scenario for satellite mobile radio channel is shown in Figure 2-11.

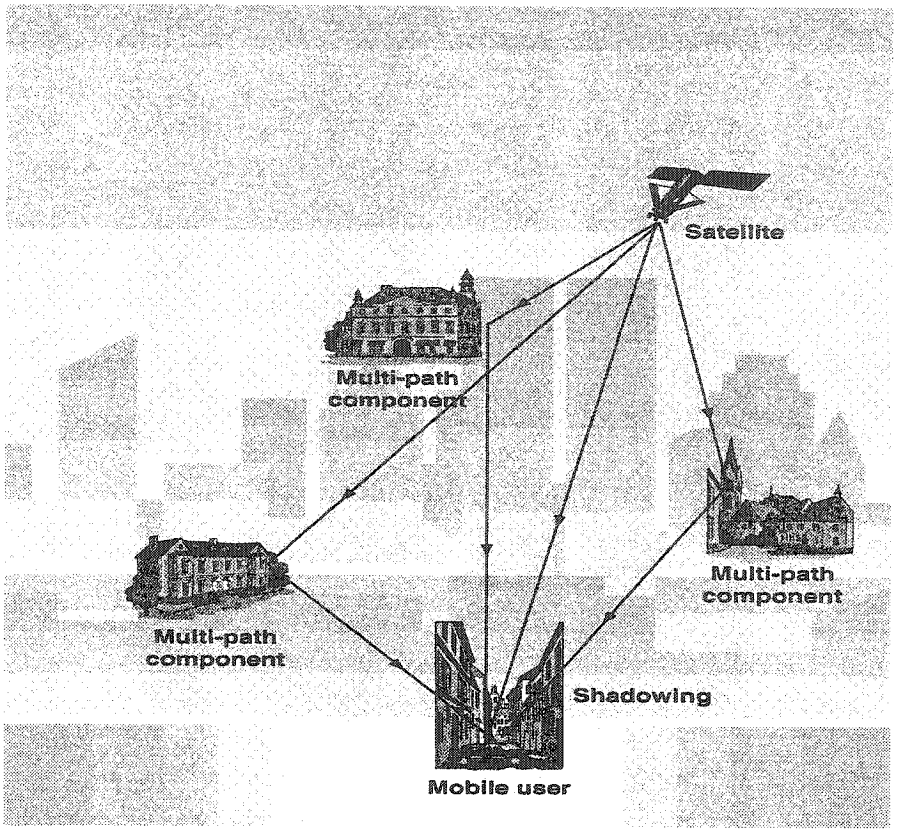

Figure 2-11 Signal propagation in satellite communications

In this section we will investigate the change of strength of the received signal in small-scale (fast fading) and medium-scale environment (slow fading). The reason for paying special attention to fading characteristics of the mobile channel is the fact that all the mobile satellite channel models are combination of slow and fast fadings. Therefore, the true representation of both fadings in a communication channel is particularly important.

2.5.1.1 Slow Fading (Shadowing)

In satellite communications, the particular structures (buildings, trees, etc.) along mobile to satellite path cause signal power variations. Variations of the shadowing around the mean and how severe the fading is depend on the environment. Some paths will suffer more; while others will be less obstructed and have increased signal strength. It is critical to account for this variation

in signal strength in order to predict the reliability and performance of any mobile satellite system.

In literature, measurements have shown that signal power variation is satellite communication can be represented by log-normal random variable, in other words normally distributed in dB [Loo85], [Lut91]. If we want to express the shadowing in dB, we can represent the shadowing component of the channel as

$$S(t) = 10^{\frac{\zeta(t)}{10}} \tag{2.12}$$

where ζ is a zero-mean normally distributed random variable (in dB) with standard deviation σ_ζ (also in dB).The standard deviation of the shadowing distribution (in decibels) is known as the location variability, σ_ζ. The location variability is a computed value from measurements and it depends on frequency and environment; it is greatest in urban areas and smallest in open areas.

2.5.1.2 Fast Fading (Multi-path Fading)

Even tough we correctly estimate path loss and shadowing for particular locations in a mobile satellite system, there is still significant variation in the received signal as the mobile moves over small distances comparison to the shadowing correlation distance. This event is fast fading and the signal variation is so rapid that it can only useful be predicted by statistical means.

We can count two types of fast fading. When the received signal is made up of multiple reflective rays with a significant line-of-sight (non-faded) component, the envelope amplitude due to multi-path fading has a Rician pdf, and is referred to as Rician fading or line-of-sight (LOS) propagation. The non-faded component is called the specular component. As the amplitude of the specular component approaches zero, the Rician pdf approaches a Rayleigh pdf and referred to as Rayleigh fading or non-line-of-sight (NLOS) propagation.

In NLOS situations the Rayleigh distribution is a proper model to measure fading amplitude statistics for mobile fading channels, which is called Rayleigh fading channels.

In the LOS situation, the received signal is composed of a both random multi-path component (e.g. Rayleigh case) and a coherent line-of-sight component which has essentially constant power. The power of LOS (specular) component needs to be greater than the total multi-path power to change the Rayleigh distribution to Rician distribution.

Until now we mentioned the signal distributions. Another important parameter in channel characterization is how fast the signal changes. It is especially important in power controlled systems where the PCE is mainly caused by the inability of power control algorithms tracking the changes in the channel. So far, the Rayleigh and Rice fading statistics didn't give any information about how rapidly the signal level changes between different time intervals (second-order fading statistics). Second-order statistics are concentrated on the distribution of the signal's rate of change, rather than with the signal itself.

Mobile user speed is one of the main factors that affect the accuracy of the power control performance and in order to see the effects of the user speed change we need to consider the correlation of the fast fading in satellite communication channel, which is a second-order statistic. The spectrum of the received signal gives valuable information about the second-order statistics of the channel. For example, the uncorrelated fast fading inspected so far, has a flat spectrum (independent values), whereas the correlated fading has a very specific spectral shape. In order to understand the shape of spectrum and how it comes out, we have to understand Doppler Effect concept.

The Doppler Effect causes a change of the actual frequency of the received signal, as observed by the mobile, by a factor proportional to the component of the mobile speed in the direction of the wave. We can define the Doppler shift f_d, as the change in the frequency and it can be found as follows:

$$f_d = \frac{v}{\lambda}\cos\alpha = f_0\frac{v}{c}\cos\alpha = f_m\cos\alpha \qquad (2.13)$$

where, v is the mobile user speed, f_0 is the operational frequency, c is the speed of light and α is the arrival angle of the incoming horizontal wave. In multi-path propagation example, waves arrive with numerous directions, each of which then has its own associated Doppler Frequency. The bandwidth of the received signal is therefore, spread compared to its transmitted bandwidth. This phenomenon is called Doppler spread. The relative amplitudes and directions of each of the incoming waves determine the exact shape of the resulting spectrum, which has a significant effect on the second-order fading statistics of the mobile signal. In order to analyze these effects, it is necessary to assume some realistic model of the statistics of the arrival angle of the multi-paths. The arriving waves at the mobile are assumed to be equally likely to come from any horizontal angle by Clark [Clr68]. This result is illustrated in the Figure 2-12 and called the classical Doppler Spectrum.

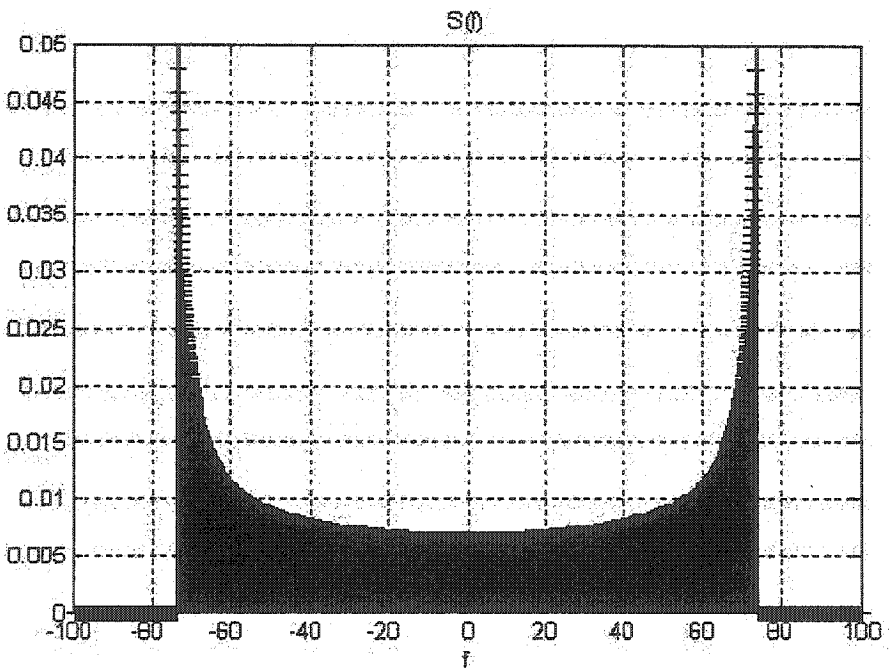

Figure 2-12 Doppler spectrum of a user with operational frequency f=1.6Ghz and user speed v=50km/h which has a maximum Doppler frequency fm=74Hz

The Doppler Spectrum illustrate in Figure 2-12 is used as a filter to correlate the independent Rayleigh random variables. Applicability of this spectrum in satellite communications, since Classical Doppler spectrum is normally used in terrestrial systems, is a major concern. It is stated in [Lut91] that Classical Doppler filter is appropriate to model the fading in city environment and a flat low-pass filter with a band-width of maximum Doppler frequency may be used for all types of environment. However, Loo [Loo91] used Classical Doppler spectrum for mobile satellite communication as a shaping low-pass filter for all environments

2.5.2 Satellite Mobile Fading Channel Models

After investigating general characteristics of fading components of mobile channels, we will concentrate on the satellite fading channel models in this section. Satellite communications systems include shadowing as dynamic process, along with the fast fading and they use statistical methods, for the physical descriptions of the channels.

In satellite communications, statistical models give an explicit representation of the channel statistics in terms of parametric distributions, which are a mixture of Rice, Rayleigh and lognormal components. These models utilize statistical theory to derive a reasonable analytical form for the distribution of the narrowband fading signal and then use measurements to find proper values of the parameters in the distribution. Assumption that the total narrowband fading signal in mobile satellite environments can be decomposed into two parts is common in all channel models. According to them narrowband channel is composed of a coherent part, usually associated with the direct path between the satellite and the mobile, and a diffuse part arising from a large number of multi-path components of differing phases. The magnitude of the diffuse part is accepted to have a Rayleigh distribution.

The most basic model is the Rice distribution which supposes that both components of the signal have stable mean power. Loo [Loo85], Corazza [Cor94] and Lutz [Lut91] have extended this model to account for the changing conditions associated with attenuation and shadowing of both

the coherent and diffuse components, which arise from mobile motion. A good fit to measured distributions over a wide range of environment and operating conditions can be provided with the condition of properly chosen parameters. In the following section we will concantrate on just one model (The Lutz model) for channel characterization.

2.5.2.1 The Lutz Model

In this model, the statistics of LOS and N-LOS states are represented by two distinct states and it is particularly appropriate for modeling channels in urban or suburban areas where there is a large difference between shadowed and un-shadowed statistics. The LOS condition is represented by a 'good' state, and the non-line-of-sight condition by a 'bad' state. In the good state, the signal amplitude is assumed to be Rice distributed, with a K factor which depends on the satellite elevation angle and carrier frequency. In the bad state, the fading statistics of the signal amplitude are assumed to be Rayleigh, but with a mean power which varies with a log-normal distribution in time. The mean and standard deviation of shadowing varies within the NLOS situation.

2.6 Summary

In this chapter, the basic definitions and elements of a geostationary satellite mobile communication system have been presented. The satellite and earth geometry, which characterizes the communication link and defines the coverage area, has been explained. One of the chief parameters of satellite communication that determines the system performance, satellite antenna, is given.

The hexagonal cellular pattern for the representation of the satellite footprint is introduced. The interference model and mobile user distribution in the hexagonal cellular layout relative to satellite that will be used in simulations are made clear.

Other Cell Interference, which is one of the key determinants in the capacity calculations of a CDMA satellite multi-beam systems and which significantly differs from terrestrial CDMA systems, is explained and the calculation method is stated.

General characteristics of mobile fading channels, different types of fadings (slow and fast fading) and finally land mobile satellite channel models are discussed. It is stated that in order to have a good representation of practical land mobile satellite link, time varying characteristics of the channel fadings should be considered.

Chapter 3

CDMA SATELLITE SYSTEM PERFORMANCE

This chapter examines the performance of satellite systems employing code division multiple access (CDMA). The carrier-to-total interference power ratios of mobile users and their probabilistic distributions are examined to assess the system capacity. Theoretical capacities of both single-beam and multi-beam satellite mobile systems are presented for mobile user uplink. An important problem in applying the CDMA scheme, unequal received power level at satellite stays still and its effect on system capacity is also analyzed.

The chapter is organized as follows. Theoretical capacity estimations of perfectly power controlled single beam and multi-beam systems are presented first. Application of theoretical capacity evaluation formulas to a satellite system with particular parameters (i.e. numeric values) is given for better concept clarity. Next, the effect of power control error on the system capacity is introduced. Finally, the outage probability calculation method is presented for imperfectly power controlled systems. The theoretical background of how to simulate the system with power control error is given in this chapter as well.

3.1 System Capacity with Perfect Power Control (PPC)

The calculation geometry of the interference model, mobile user locations in a spot-beam with respect to the satellite and the characteristics of the spot-beam antenna were shown in Chapter 2.

In satellite system performance calculations, the hexagonal cellular layout consists of three or four tiers[1] of surrounding spot-beams are considered and the mobile users in the cellular configuration are assumed to be uniformly distributed.

In this section, we explain the capacity calculation methods in a multi-beam satellite CDMA system with PPC, starting with the evaluation of a single beam capacity.

3.1.1 Single Beam Capacity

A system consisting of a single spot-beam with PPC means all mobile user uplink signals (mobile user-to-satellite) are received at the satellite at the same power level (e.g. P_0). If we assume N uniformly distributed users in the considered spot-beam, satellite spot-beam antenna demodulator processes a combination of received waveform containing the desired signal having power P_0 and $(N-1)$ interfering signals each has power P_0 as well. This assumption of the single beam and uniformly distributed mobile users are illustrated in Figure 3-1.

[1] 37-beam or 61-beam satellite footprint cellular layout.

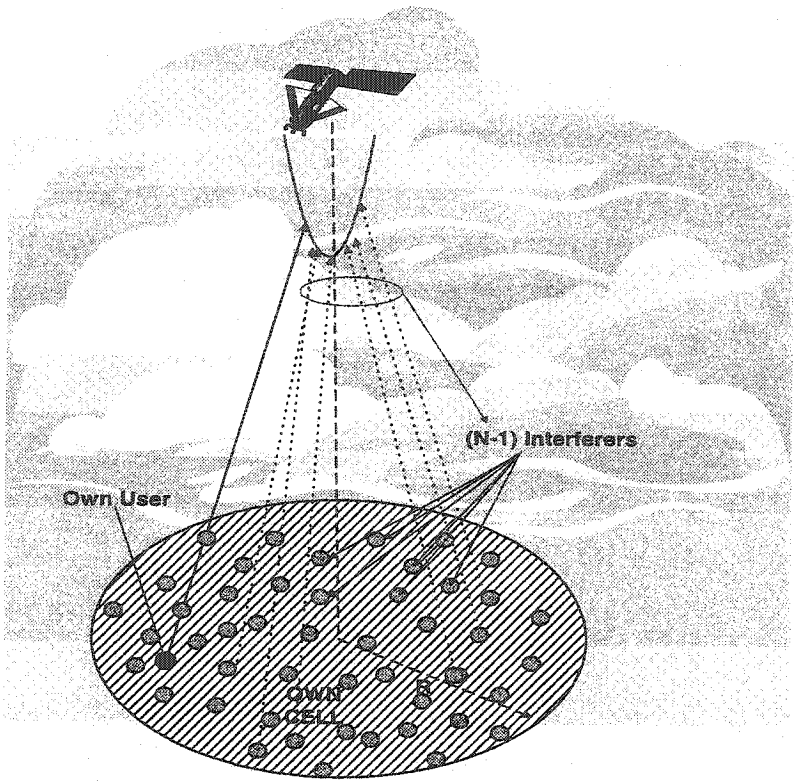

Figure 3-1 Mobile user and satellite geometry in a single-beam satellite system

With the assumption of N uniformly distributed mobile users in the considered beam, the desired signal power to interference power ratio (SIR) for perfectly power controlled single spot-beam system can be found as:

$$SIR = \frac{P_0}{(N-1)P_0} = \frac{1}{(N-1)} \tag{3.1}$$

Equation (3.1) ignores the background thermal noise power η. The background thermal noise power η in a channel operating in a bandwidth of W can be evaluated as follows:

$$\eta = N_0 W \tag{3.2}$$

where, N_0 is the one-sided thermal noise power spectral density. By combining equations (3.1) and (3.2), we can evaluate the SINR of the single beam system as:

$$SINR = \frac{P_0}{(N-1)P_0 + \eta} \tag{3.3}$$

The bit energy-to-interference power spectral density ratio is more important parameter for consistent system operation. Its numerator is obtained by dividing the desired signal power by the information bit rate R and the denominator by dividing the total interference power by the total bandwidth, W which can be calculated as:

$$\frac{E_b}{I_{tot}} = \frac{P_0/R}{\left[(N-1)P_0 + \eta\right]/W} = \frac{(P_0 W)/R}{(N-1)P_0 + \eta} = \frac{W/R}{(N-1) + \eta/P_0} \tag{3.4}$$

where, $PG = W/R$ is generally referred to as the processing gain E_b/I_{tot} is the bit energy-to-total interference density ratio of a mobile user within the considered spot-beam and N is the total number of mobile users in the spot-beam. Equation 3.4 assumes that considered system is synchronous and has flat spectrum. The processing gain is defined as the ratio of the chip rate to the bit rate $PG = R_c/R_b$. The chip pulse shape is assumed to be ideally band-limited according to the zero roll-off factor. Therefore, we can accept the the bandwidth of the CDMA carrier as $W = R_c$ and processing gain as $PG = W/R_b$. The calculation of processing gain as W/R_b is a reasonable assumption for asynchronous BPSK as long as it is a large value.

In a speech-oriented CDMA system, an important processing feature is stopping the transmission or at least reducing its rate and power when the voice activity is absent. This type of discontinuous transmission decreases the MAI received by each mobile user. Numerous measurements on two way telephone conversations have established that voice is active only about three-eighths of the time [Fra59]. Therefore, by using a voice activity detector to indicate active times and turning off the transmitter we can reduce the MAI as well as conserve the batteries of the hand held portable mobile terminals. We denote this factor as the voice activity factor V . Given that, CDMA capacity is interference limited [Vit93], any decrease in the interference converts itself directly into an increase in the system capacity.

If we take into account the voice activity factor V, we can modify equation (3.4) to

$$\frac{E_b}{I_{tot}} = \frac{W/R}{(N-1)V + \eta/P_0} \tag{3.5}$$

For a user communication link quality in a CDMA system, to satisfy the required standard, E_b/I_{tot} value of each mobile user should be greater than the required level of bit energy to interference power spectral density ratio, E_b/I_{req}, at the level of bit error performance required for digital voice transmission. In most voice oriented systems, this implies a BER of 10^{-3} or better [Gil91]. Among the factors to be considered in establishing the required E_b/I_{req} level, we can count the channel amplitude fading characteristics, i.e. in different fading environments we need different E_b/I_{req} values for the same BER performance, and the Forward Error Correcting (FEC) coding scheme used. As an example for a CDMA system using quadri-phase shift keying (QPSK) modulation with rate ½ constraint length K=9 convolutional code, it is E_b/I_{req} = 2.3 dB for AWGN channel, 5.0 dB for urban environment and 2.6 dB for highway [Moh97].

It is reasonable to think that in CDMA satellite communications, the traffic capacity of the mobile user uplink is maximized when all transmitted signals are received (e.g. at gateway or satellite) at the minimum power necessary to achieve the specified SINR (or E_b/I_{req}) level. That is because, if a mobile user transmits excessive power, it increases the total interference level other users experience. On the contrary, if a user transmits less power level than the system requires, its own channel performance would be degraded due to higher BER in signal transmission. Therefore, it is easy to see that with PPC, we can achieve the maximum user capacity for a single beam system. With PPC all mobile users located at different locations within the same cell have the same E_b/I_{tot}, which is almost equal to the required bit energy to interference power density ratio, $E_b/I_{tot} \cong E_b/I_{req}$.

With the help of this information, if we try to find the maximum number of active users in a single spot-beam with PPC, from equation (3.5), we end up with,

$$N_{\max} = 1 + \frac{W/R}{V}\left(\frac{I_{req}}{E_b} - \frac{\eta/W}{P_0/R}\right) = 1 + \frac{W/R}{V}\left(\left(\frac{E_b}{I_{req}}\right)^{-1} - \left(\frac{E_b}{N_0}\right)^{-1}\right) \tag{3.6}$$

where, E_b/N_0 is the per user bit energy to thermal noise power spectal density ratio and E_b/I_{req} is the required level of bit energy to interference power spectral density ratio at the level of bit error performance required for digital voice transmission.

In order to understand the system capacity calculation method, attention should be paid to the difference between the bit energy-to-thermal noise power spectral density, E_b/N_0 and the bit energy-to-total interference power spectral density E_b/I_{tot}. In a spread-spectrum system the total noise power is determined by the sum of the thermal noise power N_0 and the MAI. The desired bit error rate performance of the link is determined by $E_b/I_{tot} = E_b/(N_0 + I_0)$ or the ratio of the bit energy to the total noise spectral density ratio. E_b/N_0 takes into account just the thermal noise power spectral density in the denominator, whereas E_b/I_{tot} includes both interference and thermal noise power spectral density in the calculation.

From equation (3.6), we notice that the capacity of a spot-beam increases as we increase E_b/N_0 per user. In order to observe the behavior of this performance increase numerically, we have to specify the system parameters like E_b/I_{req} and the processing gain (W/R). We are assuming that a future mobile satellite system will be as compatible with a terrestrial system as possible. For that reason we choose the chip rate as 1.2288 Mc/s. In IS-95 the vocoder operates at 9.6 kbps. In a future system the bit rate may be lower such as 4 kbps. Hence the processing gain defined as *Rc/Rb* is 307. Figure 3-2, illustrates the change of the maximum simultaneous mobile user uplink capacity of a single spot-beam using asynchronous CDMA, relative to the per user bit energy to thermal noise spectral density ratio, E_b/N_0 with W/R=307 and the voice activity V=0.5.

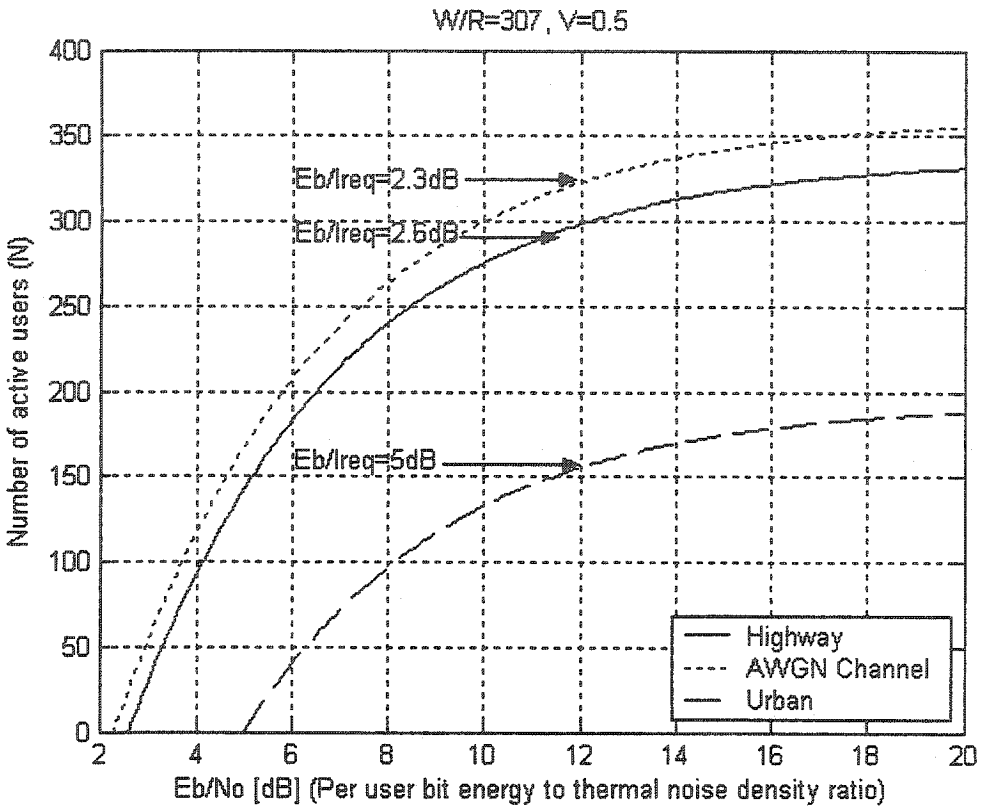

Figure 3-2 Maximum capacity of single beam satellite system using asynchronous CDMA relative to E_b/N_0 with E_b/I_{req} = 2.3dB, 2.6dB, 5dB W/R =307 and V=0.5

As we can see from Figure 3-2, the system capacity is highly dependent on E_b/I_{req}, which in turn, depends on channel coding, data modulation and FEC coding scheme used.

3.1.1 Multiple Spot-beam Capacity

The only difference of multiple spot-beam satellite system capacity calculation from single spot-beam calculation is taking into account the interference coming from other cells in the satellite footprint. In this section, we will calculate the capacity of a single beam (nadir beam) of the cellular layout, taking into account the other beams in the satellite footprint. The spot-beams are arranged according to a gain-overlap criterion. At this point, we have to recall the calculation of the MAI and the OCI factor in order to extend the equations (3.5) and (3.6) in a way to include the other cells in the cellular layout as well. Interference model and calculation technique were

described in Chapter 2. For convenience, we rewrite the OCI factor equation relating the intra and inter-cell interferences (I_{intra} & I_{inter}) already derived in Chapter 2.

$$f = \frac{I_{\text{inter}}}{I_{\text{intra}}} = \frac{\sum_{j=1}^{other-cells} \sum_{k=1}^{N} \frac{G(\Psi_{j,k})}{G(\theta_{j,k})}}{(N-1)} \tag{3.7}$$

In view of the fact that we consider N uniformly distributed mobile users per spot-beam and PPC, intra-cell interference power (I_{intra}, interference caused by the users in its own spot-beam) would be $P_0(N-1)$(all mobile users in the spot-beam, not including the wanted used). Inter-cell interference (I_{inter}) calculation method is given in Chapter 2, relative to the geometry and set-up considered for Geo-stationary satellite system.

By including the interference coming from the other spot-beams in the cellular layout, we can calculate the SINR for multiple spot-beam satellite as:

$$SINR = \frac{P_0}{I_{\text{intra}} + I_{\text{inter}} + \eta} = \frac{P_0}{(N-1)P_0 + I_{\text{inter}} + \eta} \tag{3.8}$$

From equation (3.7), it is shown that inter-cell interference affecting a user in the nadir (central) spot-beam of the cluster can be found by:

$$I_{\text{inter}} = \sum_{j=1}^{other-cells} \sum_{k=1}^{N} \frac{G(\Psi_{j,k})}{G(\theta_{j,k})} \tag{3.9}$$

If we combine equation (3.9) and equation (3.2) ($\eta = N_0 W$) in the general capacity equation (3.8), we have the overall signal power to interference power ratio as:

$$SINR = \frac{P_0}{V\left((N-1)P_0 + \sum_{i=1}^{Other-cells} \sum_{j=1}^{N} P_0 \frac{G(\psi_{\text{int}})}{G(\theta_{\text{int}})}\right) + N_0 W} \tag{3.10}$$

As we did in the single cell case, we can find the bit energy-to-interference power spectral density ratio (E_b/I_{tot}) of mobile users, whose numerator is obtained by dividing the desired signal power by the information bit rate R, and denominator by dividing the interference power by the total bandwidth W as follows:

$$\frac{E_b}{I_{tot}} = \frac{W/R}{V\left((N-1)+\sum_{i=1}^{Other-cells}\sum_{j=1}^{N}\frac{G(\psi_{\text{int}})}{G(\theta_{\text{int}})}\right)+\left(\frac{P_0}{\eta}\right)^{-1}} \tag{3.11}$$

Contrary to the single-beam satellite systems, despite having PPC, E_b/I_{tot} values of mobile users in the considered beam have time varying characteristics due to variations of the mobile users in the other beams in the cellular layout. The OCI factor calculation method illustrated in Chapter 2 is for the interfering users having particular locations in other spot-beams. However, the locations of the interfering mobile users in adjacent spot-beams have time varying characteristics as illustrated in Figure 3-3.

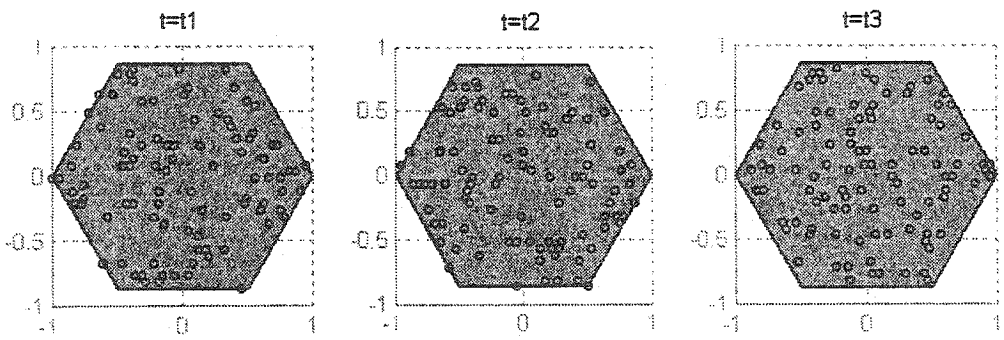

Figure 3-3 Illustration of time-varying locations of mobile interferers in beams

Therefore, the OCI factor, which is dependent on interferer locations, changes relative to time as well. The changing level of the interference coming from other beams in satellite footprint I_{inter}, causes variations on the total interference level a mobile user experiences; $I_{\text{tot}} = I_{\text{inter}} + I_{\text{intra}}$, which consequently changes the E_b/I_{tot} level of mobile users in the considered beam.

This time varying characteristic of the E_b/I_{tot} values of the mobile users is illustrated in Figure 3-4 with a certain system parameters. For the illustration, we consider the multi-beam satellite system with 37 beam cellular layout with 3 dB spot-beam overlap value with system parameters: E_b/N_0 =10dB, E_b/I_{req} =2.6 dB, W/R=307 and voice activity V=0.5.

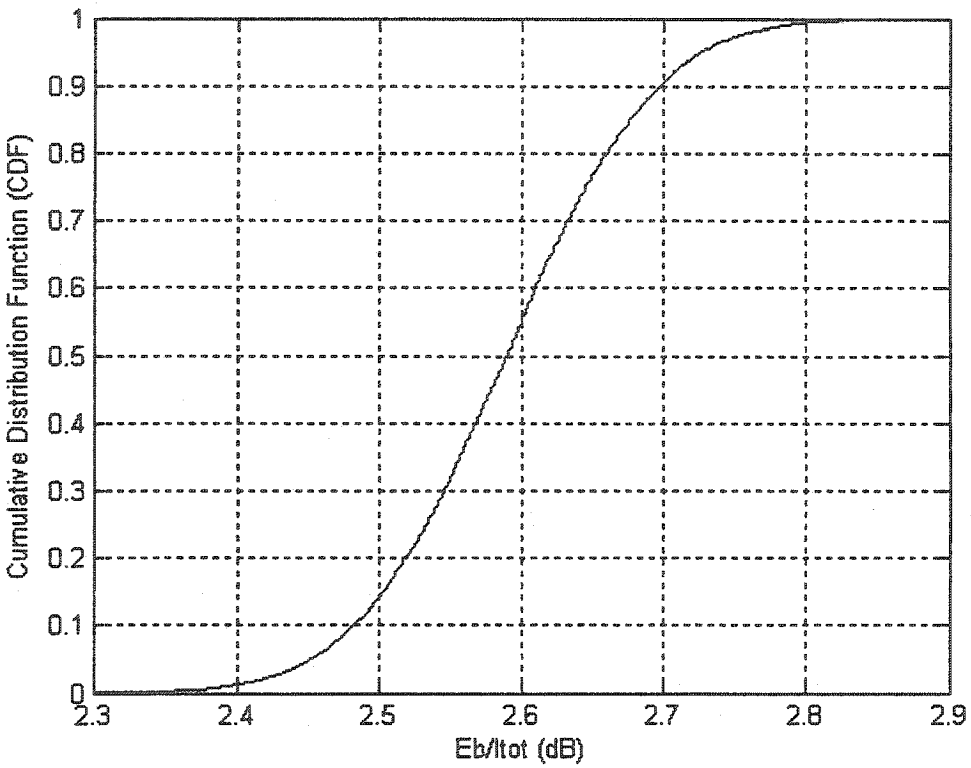

Figure 3-4 Time varying characteristic of mobile user E_b/I_{tot} values in the considered beam with the system parameters E_b/N_0 =10dB, E_b/I_{req} =2.6 dB, W/R=307 and V=0.5 in a 37 beam cellular layout

Time varying nature of the total interference and therefore the OCI factor affects the maximum active user capacity of the system. Figure 3-5 shows the time varying behavior of the OCI factor with the same system parameters.

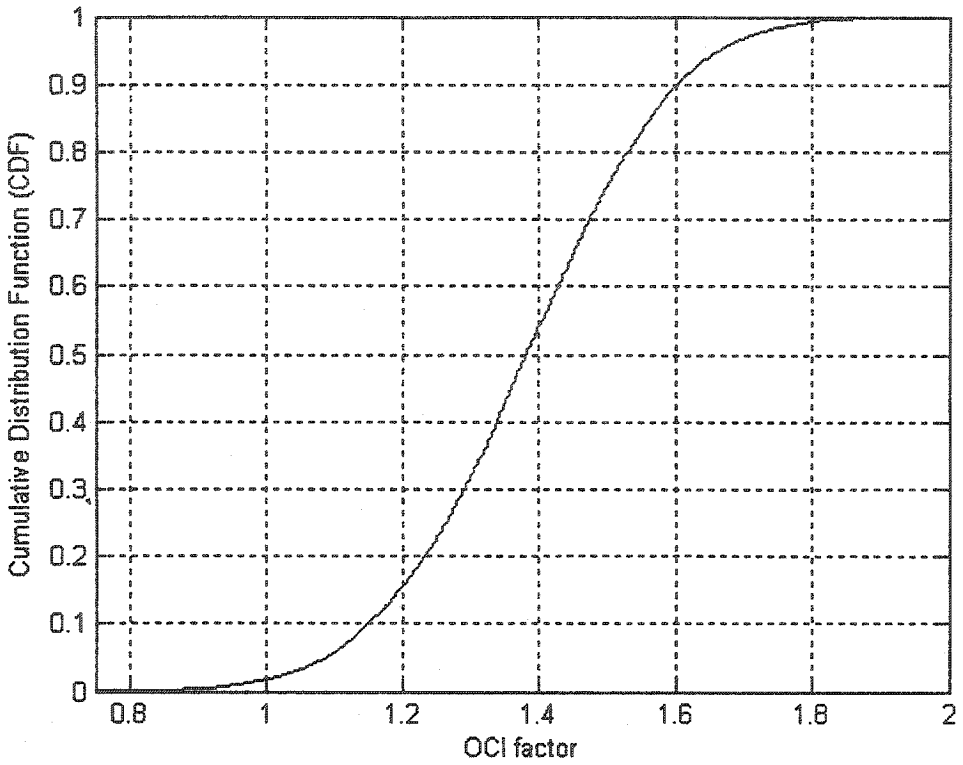

Figure 3-5 Time varying characteristic of the OCI factor with system parameters E_b/N_0 =10dB, E_b/I_{req} =2.6 dB, W/R=307 and voice activity V=0.5 in a 37 beam cellular layout

In the system capacity calculations, we will use the mean value[3] of the interference power. For the inter-cell interference calculation, this corresponds approximately to the median value of the OCI factor cdf. For multi-beam CDMA systems, we can find the expression relating the maximum number of active users in a spot-beam of the cluster to other system parameters from equation (3.11):

[3] Time average of the interference.

$$N_{\max} = 1 + \frac{W/R}{V(1+f)}\left(\frac{I_{req}}{E_b} - \frac{\eta/W}{P_0/R}\right) = 1 + \frac{W/R}{V(1+f)}\left(\frac{I_{req}}{E_b} - \left(\frac{P_0/R}{\eta/W}\right)^{-1}\right)$$
$$= 1 + \frac{W/R}{V(1+f)}\left(\left(\frac{E_b}{I_{req}}\right)^{-1} - \left(\frac{E_b}{N_0}\right)^{-1}\right) \quad (3.12)$$

As we see from equation (3.12), the maximum active user capacity of the system depends on the average OCI factor f. In order to compare the difference in the capacities of multi-beam and single beam systems and see the capacity reduction due to inter-cell interference, we show the capacity of the nadir cell in the satellite foot-print relative to the bit energy to thermal noise ratio, E_b/N_0 in Figure 3-6. In this figure, the average OCI factor is considered as $f = 1.36$, which can be verified from Figure 3-5.

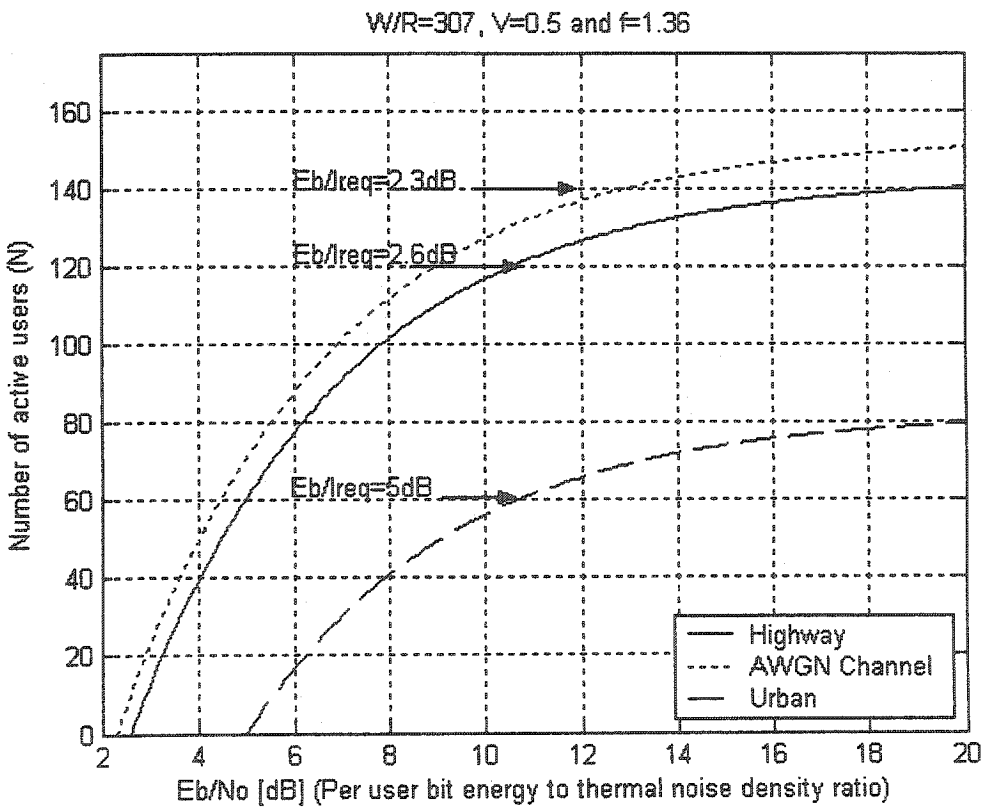

Figure 3-6 Maximum capacity of the nadir beam in multiple cell satellite system relative to E_b/N_0 with E_b/I_{req} = 2.3dB, 2.6dB, 5dB W/R =307, V=0.5 and the OCI factor=1.36

If we compare the multi-beam capacity curve with the single beam one, we can notice the capacity decrease of more than 50% percent due to inter-cell interference (e.g. f=1.36).

3.2 System Capacity with Power Control Error

CDMA communication systems are attractive from capacity point of view [Lee91], [Gil90]. However, CDMA communication systems suffer from unequal received power levels at satellite (or gateway) that degrades the capacity.

In a practical CDMA system, we cannot expect PPC. PCE is the result of power measurement error as well as not being able to compensate the instantaneous variations due to finite propagation delay in the power control process. An important feature of satellite communication channels is the excessive length of the round trip propagation delay, which reduces the effectiveness of the power control methods and makes PCE inevitable in capacity calculations for satellite systems.

3.2.1 Effect of Imperfect Power Control

The limitation of the IPC on the reverse link capacity of a CDMA system was studied in many papers e.g. [Kud93], [Pra93], [Tam97]. In addition to IPC, outage probability, defined as the predetermined value of probability that the received mobile user SINR is less than the required SINR [Koo00], is one of the most essential system parameters to be considered in system implementation. The reverse link capacity of a system is usually limited by a prescribed upper bound of outage probability. For the capacity calculations with PCE, we will investigate E_b/I_{tot} characteristics of the considered spot-beam mobile users, namely the probability distribution function (*pdf*) and the cumulative distribution function (*cdf*) of user E_b/I_{tot} s in the own spot beam.

In a communication link, when the power control is not perfect, the error is assumed to be log-normally distributed with standard deviation σ(in dB)[Gol94], which represents the PCE. The effect of the PCE in the mobile user uplink can be studied by multiplying the perfectly power controlled received user powers (e.g. P_o) by a log-normal random variable [Kud93], [Tam97]. Therefore, the received power for a mobile user $P_o^{'}$, becomes in this IPC case:

$$P_0^{'} = P_0 10^{\frac{\gamma}{10}} \tag{3.13}$$

where, P_o is the received power at satellite with PPC and γ is a zero-mean Gaussian random variable with a standard deviation σ_γ (in dB). When σ_γ=0 dB, the case corresponds to PPC. With the assumption that received power is log-normally distributed, the *pdf* of the power level at satellite can be expressed as:

$$f(P_r) = \frac{1}{\sqrt{2\pi}\sigma_\gamma} \exp\left\{ \frac{-\left[10\log_{10}(P_r) - 10\log_{10}(\overline{P}_r)\right]^2}{2\sigma_\gamma^{\,2}} \right\} \tag{3.14}$$

with the mean received power P_o for each mobile.

With this mobile user power level assumption, if we consider the reverse link with PCE and N uniformly distributed users, the total interference power received at the satellite for the j th mobile within the own spot-beam becomes:

$$I_j = V\left[\left(\sum_{i=0}^{All-cells} \sum_{j=1}^{N} P_0 10^{\frac{\gamma_{ij}}{10}} \frac{G(\psi_{ij})}{G(\theta_{ij})} \right) - P_0 10^{\frac{\gamma_{0j}}{10}} \right] \tag{3.15}$$

It should be noted that, in equation (3.15) the summation term includes all spot-beams, including the own spot-beam (indicated as 0th spot-beam). In order to find total interference affecting desired mobile user, we subtract the considered user's own received power from total interference summation on the right hand side of equation. Finally, this interference summation is scaled by voice activity V.

Therefore, SINR of each user in the own spot-beam can be found by dividing transmitted signal power of the user by the total interference power affecting the link as shown below:

$$SINR = \frac{P_0 10^{\frac{\gamma_{0j}}{10}}}{V\left[\left(\sum_{i=0}^{All-cells}\sum_{j=1}^{N} P_0 10^{\frac{\gamma_{ij}}{10}} \frac{G(\psi_{ij})}{G(\theta_{ij})}\right) - P_0 10^{\frac{\gamma_{0j}}{10}}\right] + \eta} \tag{3.16}$$

Since, both the transmit power of each user and the total interference affecting the transmit channel are different, unlike the PPC case, *SINR* value of each user in the considered beam is different.

Similar to the PPC case, we can define this ratio in terms of bit energy to total interference power spectral density ratio as:

$$\frac{E_b}{I_{tot}} = \frac{(W/R)10^{\frac{\gamma_{0j}}{10}}}{\left[\left(\sum_{i=0}^{All-cells}\sum_{j=1}^{N} 10^{\frac{\gamma_{ij}}{10}} \frac{G(\psi_{ij})}{G(\theta_{ij})}\right) - 10^{\frac{\gamma_{0j}}{10}}\right] + N_0} \tag{3.17}$$

As it can be seen in equation (3.17), similar to $SINR$, E_b/I_{tot} value of each user in its own spot-beam is different from other users. In order for a mobile user to have a sufficient communication link quality (e.g. $BER \leq 10^{-3}$), its E_b/I_{tot} value has to satisfy the condition $E_b/I_{tot} \geq E_b/I_{req}$, which we will focus on in the next section as outage probability.

3.2.2 Outage Probability Calculation

For any multi-user communication system, the measure of its economic value is not the maximum number of users that can be served simultaneously, but the peak load that can be supported with a given quality and service availability. In our system, we assume that a new user is denied service, if its E_b/I_{tot} value cannot satisfy the required bit energy to interference power spectral density ratio E_b/I_{req}. Therefore, we can define the outage probability as:

$$p_{out} = \Pr\left((E_b/I_{tot}) < (E_b/I)_{req}\right) \tag{3.18}$$

In order to compute the outage probability of the users in the system, one has to approximate the distribution of interference, which is the sum of lognormal random variables. If k number of mobile users are transmitting simultaneously in a spot-beam and if the power of each mobile is controlled individually, then the total received interference power is the summation of k independent, identical and log-normally distributed random variables each denoted by P_i:

$$P_I = \sum_{i=1}^{k} P_i \tag{3.19}$$

Fenton showed that [Fen60] the pdf of P_I for k users is approximately log-normal with the following logarithmic mean $m_I(k)$ and variance $\sigma_I^2(k)$:

$$m_I(k) = \ln(k) + m + \frac{\sigma^2}{2} - \frac{1}{2}\ln\left(\frac{1}{k}e^{\sigma^2} + \frac{k-1}{k}\right) \tag{3.20}$$

$$\sigma_I^2(k) = \ln\left(\frac{1}{k}e^{\sigma^2} + \frac{k-1}{k}\right) \tag{3.21}$$

Therefore, we can conclude that pdf of user SIR in a spot-beam would be the ratio of two log-normal random variables, which is another log-normally distributed random variable:

$$SIR = 10^{\frac{\gamma}{10}} / 10^{\frac{\zeta}{10}} = 10^{\frac{\gamma-\zeta}{10}} \text{ with } I_{tot} = 10^{\frac{\zeta}{10}} \tag{3.22}$$

where ζ and $\gamma - \zeta$ have Gaussian distributions.

From the system and interference model given in Chapter 2, the outage probability of the considered spot-beam can be simulated by first generating a large set of points uniformly distributed in the spot-beam and for each location of mobile, simulation is repeated to check if its E_b/I_{tot} falls below E_b/I_{req}. The outage probability can be derived numerically for the different locations using the equation

$$p_{out} = \lim_{K\to\infty} \frac{1}{K}\sum_{k=1}^{K} \Delta_k \tag{3.23}$$

where Δ_k is an indicator function for each user in the spot-beam (for each k) Δ_k=1, if the condition $E_b/I_{tot} \le E_b/I_{req}$ is satisfied, else Δ_k=0.

3.4 Summary

In this chapter, capacity calculations of the satellite multi-beam CDMA systems with PPC and capacity reductions with PCE are explained theoretically.

Theoretical formulas for capacity calculation of perfectly power controlled single-beam satellite CDMA system are derived first. With the introduction of the inter-cell interference and the OCI factor, the capacity calculation formula is extended to multi-beam satellite case. The un-availability of equal user power levels at satellite is considered next and PCE is introduced to the capacity calculation formula. The considered spot-beam user's E_b/I_{tot} pdf is chosen to illustrate the capacity reduction due to IPC and finally the calculation method of outage probability is explained.

Chapter 4

SIMULATION RESULTS

In this Chapter, the performance of multi-beam satellite CDMA system described in Chapter 2 and Chapter 3 is analyzed with simulations. Mobile user uplink capacity, which limits the multi-beam mobile satellite systems, is evaluated with different system parameters. In the simulations, the geometrical relations with mobile users on earth and satellite, spot antenna characteristics of the satellite and cellular layout properties of satellite footprint described in Chapter 2 are utilized. Theoretical capacity formulas for different systems (e.g., single beam system, multi-beam system, capacity with PCE), which are derived in Chapter 3, are employed for concluding results of system performance.

The structure of this chapter is as follows: Initially, satellite system descriptions and reference system parameters used in the simulations are given. Capacity assessment of the CDMA satellite systems is presented for perfectly power controlled systems first and the consequence of PCE is analyzed considered after. In perfectly power controlled satellite system section, we start evaluating the capacity of single cell system in the beginning. The consideration of multiple beams will introduce the OCI factor. We will concentrate on multiple beam systems and investigate the effects of cellular layout, beam overlap value, spot-beam loading and frequency reuse policy of the systems on the OCI factor, consequently to the system capacity. With the intention of having practical results, we will investigate the capacity performance of the system with constant serving area. Power limitation on the satellite is considered next, and we conclude section by calculating extra power required at satellite for PPC of the mobile users in the considered spot-beam.

The effect of PCE and capacity reduction in the system due to IPC relative to PPC case is considered subsequently. Evaluation of outage probability through simulation is presented in this

section as well. Finally, we close the chapter by calculating the link margin of the systems considered.

4.1 System Model and Parameters

In order to relate the theoretical capacity formulas obtained and geometrical relations presented in the previous chapters to practical systems, a reference GEO satellite system is introduced here.

Table 4-1 Reference multi-beam satellite system for capacity calculations

Antenna diameter	**D=20m**
Voice activity	**V=0.5**
Signal bit energy to thermal noise power spectral density ratio	**Eb/N_0= 10 dB**
Required bit energy to interference power spectral density ratio	**Eb/I_{req}=2.6 dB**
Processing gain	**W/R=307**
Satellite type	**Multi-beam GEO**
Operational frequency	**f_o=1.6GHz**

In our system, required bit energy to interference power spectral density ratio is assumed to be $E_b/I_{req} = 2.6\text{dB}$, which is sufficient for satisfactory channel quality for a user in highway with QPSK modulation and rate ½ constraint length 9 convolutional coding strategy [Moh97].

The reference scenario assumes a uniform mobile user distribution on the coverage area, 50% voice activity factor, frequency reuse in every spot-beam, 61 spot-beam cellular layout and 3 dB beam overlap in satellite footprint. In the following sections, the parametric capacity comparisons are made.

An important point worth mentioning is, in parametric capacity calculations the mean value of the interference power is used. The time varying nature of the user signals is employed in order to calculate the link margin of the system and system availability.

4.2 Perfectly Power Controlled Systems

In PPC systems, all mobile users' signals in the considered spot-beam are assumed to be received at the same power levels at the satellite. That means, all the attenuation loss difference, channel power variations are assumed to be compensated without errors.

4.2.1 Single Beam Satellite Systems

We start the perfectly power controlled mobile user uplink system capacity calculations with considering a single-beam satellite system. We will assume uniformly distributed users in the considered beam. In PPC systems, each user bit energy-to-total interference power spectral density ratio in the spot-beam is the same and it can be calculated as:

$$\frac{E_b}{I_{tot}} = \frac{W/R}{(N-1)V + \eta/P_0} \tag{4.1}$$

An equation giving an explicit relation between the number of mobile users served and the system parameters might be more useful for the system capacity calculations and the simulation result comparisons with the theoretical outcomes. If we solve the equation (4.1) for capacity (N), we have the following equation for theoretical uplink capacity of a spot-beam for asynchronous CDMA system:

$$N_{\max} = 1 + \frac{W/R}{V}\left(\frac{I_{req}}{E_b} - \frac{\eta/W}{P_0/R}\right) = 1 + \frac{W/R}{V}\left(\left(\frac{E_b}{I_{req}}\right)^{-1} - \left(\frac{E_b}{N_0}\right)^{-1}\right) \tag{4.2}$$

As stated in Chapter 3, for the system communication link quality of a mobile user to satisfy the necessary standard, E_b/I_{tot} value of each mobile user should be greater than E_b/I_{req}, which is the required level of bit energy to interference power spectral density ratio at the level of bit error performance required for digital voice transmission. Our simulation technique depends on the fact that if this requirement is satisfied for each mobile user or not.

In order to prove the accuracy of our simulation technique, we compare the capacity results of our simulation with the theoretical results. The capacity calculation simulation steps for PPC case are given as follows:

- ✓ Set the satellite system parameters (e.g. E_b/I_{req}=2.6dB, V=0.5, E_b/N_0=10dB and W/R=307).
- ✓ Uniformly sample each cell (e.g. 1000 samples per cell to represent uniform sampling).
- ✓ Randomly assign the first mobile user in one of the locations of the spot-beam, N=1.
- ✓ Calculate E_b/I_{tot} of the mobile user with equation (4.1) and compare it with E_b/I_{req} .
- ✓ If ($E_b/I_{tot} \geq E_b/I_{req}$) =>
  - Increase the number of users in the considered beam by one (e.g.,N=N+1),
  - randomly assign the location of the new user
  - return to step 4

  Else => Assign the spot-beam capacity as N and exit the loop.

4.2.2 Multi-Beam Satellite Systems

The OCI factor is the only difference between the capacity assessments of single beam and multi-beam satellite systems. The calculation method of the OCI factor was explained in detail in Chapter 2 and the system capacity calculation method with the OCI factor was given in Chapter 3. In the simulation of multi-beam systems we calculate the capacity of the nadir beam with considering other beams in the cellular lay-out. The overall system capacity can be calculated by multiplication of the nadir beam capacity by the number of the spot-beams in the satellite footprint.

As we saw in Chapter 3, the capacity of a single beam of the multi-beam system with uniformly distributed mobile users in the cellular layout can be found by calculating the bit energy-to-total interference power spectral density ratio (E_b/I_{tot}) as follows:

$$\frac{E_b}{I_{tot}} = \frac{W/R}{V\left((N-1)+\sum_{i=1}^{Other-cells}\sum_{j=1}^{N}\frac{G(\psi_{int})}{G(\theta_{int})}\right)+\left(\frac{P_0}{\eta}\right)^{-1}} = \ldots$$

$$= \frac{W/R}{V\left(1+\left[\frac{\sum_{i=1}^{Other-cells}\sum_{j=1}^{N}\frac{G(\psi_{int})}{G(\theta_{int})}}{(N-1)}\right]\right)+\left(\frac{P_0}{\eta}\right)^{-1}} = \frac{W/R}{V(N-1)(1+f)+\left(\frac{P_0}{\eta}\right)^{-1}} \tag{4.3}$$

where we denote the OCI factor as:

$$f = \frac{I_{inter}}{I_{intra}} = \frac{\sum_{j=1}^{other-cells}\sum_{k=1}^{N}\frac{G(\Psi_{j,k})}{G(\theta_{j,k})}}{(N-1)} \tag{4.4}$$

As we did in the single spot-beam system, if we solve equation (4.3) for the number of active mobile users supported simultaneously, we have the capacity ***per spot-beam*** for asynchronous CDMA as follows:

$$N_{max} = 1+\frac{W/R}{V(1+f)}\left(\frac{I_{req}}{E_b}-\frac{\eta/W}{P_0/R}\right) = 1+\frac{W/R}{V(1+f)}\left(\left(\frac{E_b}{I_{req}}\right)^{-1}-\left(\frac{E_b}{N_0}\right)^{-1}\right) \tag{4.5}$$

In the simulation of the multi-beam satellite CDMA system, except for the minor changes, we will use the same steps described for the single beam case. We can state the minor changes as:

- ✓ Considering the overall cellular layout instead of a single beam for user distributions.
- ✓ Increasing the number of users in each beam of the cellular layout in simulation step number 3, instead of increasing just in the considered spot-beam.
- ✓ Utilizing equation (4.3) in step number 4 for the comparison of E_b/I_{tot} with E_b/I_{req}.

The OCI factor has the utmost importance in satellite multi-beam CDMA capacity calculations. Therefore, in the following sections we will investigate the change of the OCI factor relative to system parameters, which shows itself in capacity variations of the system. In order to observe the performance difference of the systems with different parameters and to obtain a fair comparison, we evaluated the satellite CDMA multi-beam system capacities for constant

coverage area. It will be shown that, the OCI factor in satellite systems is bigger than the typical terrestrial CDMA systems, which is 0.44, with the power decrease of fourth power of distance. [Vit94] For the parametric capacity comparisons, the effect of satellite cellular configuration, spot-beam overlap value, frequency reuse in the satellite footprint and spot-beam loadings on the OCI factor, are considered.

4.2.2.1 Effect of Cellular Layout on the Performance of Multi-Beam Satellite CDMA System

In the interference model, we considered 7, 19, 37 and 61 spot-beam layouts with uniformly distributed mobile users in the satellite footprint. We calculated the OCI factor with 3 dB spot-beam gain overlap value. Figure 4-1, illustrates the cellular layout structure which is composed of rings of cells around the nadir cell. Spot-beams in each ring are illustrated with different pattern for clarity. For the simulation efficiency, we calculated the interferences of darker cells in Figure 4-1 and utilized the symmetry between the cells in the same ring relative to the nadir cell.

The number of adjacent spot-beams in the cellular layout included in the interference estimation is an important parameter. It is altering the OCI factor and consequently the system capacity. If we increase the number of the other spot-beams (rings of cells) included in the calculation, the OCI factor affecting the nadir beam will increase as well. From the geometrical point of view, in the mobile user uplink, the further the interfering spot-beam from the considered spot-beam, the less its effect will be, due to larger offset angles of the interfering mobile signals at wanted user's spot-beam, therefore causing less interference. As an example, the effect of an interfering mobile in the spot-beam of the first ring is higher than the one in the second ring. We calculated the OCI factor up to the spot-beams of 4^{th} ring (e.g. 61 spot-beams satellite foot-print).

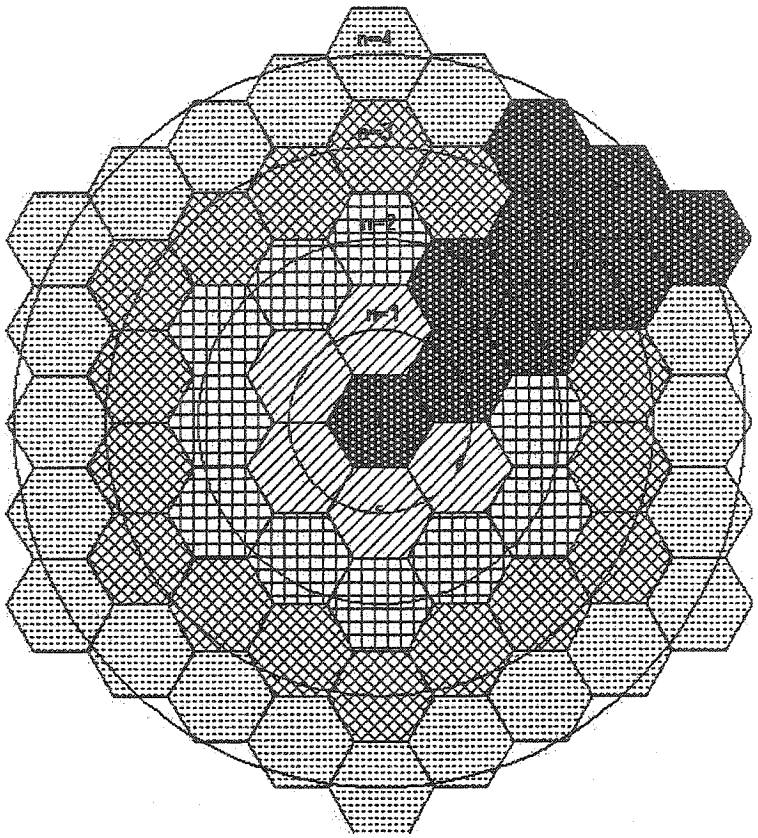

Figure 4-1 Satellite footprint with ring of spot-beams

Intuitively, one expects the effect of increasing the number of beams to be more significant when the number of beams is small, e.g., when increasing from four to seven beams. However, with a large number of beams, one expects to asymptotically reach some limiting behavior. It appears clear from the results presented in Table 4-2 that the 61-beam case is close to this limit. That is, for more than 61 beams, the number of beams does not significantly affect the OCI factor and therefore capacity per beam. However, the overall system capacity is the product of the number of beams in the cellular layout and the capacity per beam calculated.

The change of the OCI factor, capacity per spot-beam and the overall capacity of satellite footprint, relative to the ring of cells considered, are illustrated in Table 4-2.

Table 4-2 The effect of the number of beams included in the estimation of the OCI factor with satellite antenna diameter D=20m, operational frequency f_o=1.6 GHz , satellite altitude h=36000km , 3dB spot-beam overlap value and full frequency reuse

# of rings of spot-beams included in estimation	Capacity per Spot-beam	Capacity of satellite footprint	OCI factor, f
n=1 (7 beams)	*133*	*931*	*1.097*
n=1+2 (19 beams)	*123*	*2337*	*1.260*
n=1+2+3 (37 beams)	*120*	*4440*	*1.321*
n=1+2+3+4 (61 beams)	*118*	*7198*	*1.355*

As seen in the table, the effect of the outer spot-beams is minimal on the 4th ring.

One might find it more suitable to show the contribution percentages of the rings of spot-beams in the OCI factor value. Figure 4-2 illustrates the contributions of cell rings in a pie chart.

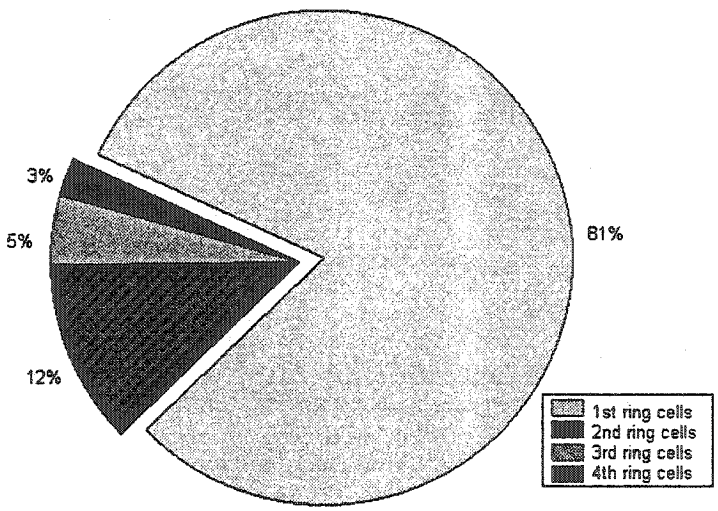

Figure 4-2 Contribution illustration of spot-beam rings in the OCI factor

In the parametric evaluations of the OCI factor (e.g., spot-beam overlap value, frequency reuse policy) in the following sections, all the 61 spot-beams (4 rings of cells) of the satellite footprint are considered in the simulations.

4.2.2.2 Effect of Beam Overlap Value on the Performance of Multi-Beam Satellite CDMA System

Another system parameter influencing the OCI factor is the spot-beam contour. In order to investigate the influence of spot-beam isolation, the gain decrease at spot-beam contour is considered as variable. The variation of the spot-beam contour changes the shape of the antenna gain of a spot-beam and therefore alters the amount of the OCI. This is different from the terrestrial case, where the signal attenuation is usually described a power law of distance.

In order to investigate the change of the OCI factor for different spot-beam contours (e.g. -2dB, -3dB,-4dB), we have to recall the antenna spot-beam gain characteristic and the meaning of the spot-beam overlap value. The phrase of "Spot-beams in a cellular layout having 3dB gain overlap" means that each spot-beam in the layout touches its neighbor spot-beams (at the edge of spot-beam coverage) at a gain value which is 3 dB less than the gain value at the spot-beam center. The spot-beam overlap concept is illustrated in 37 beam layout in Figure 4-3.

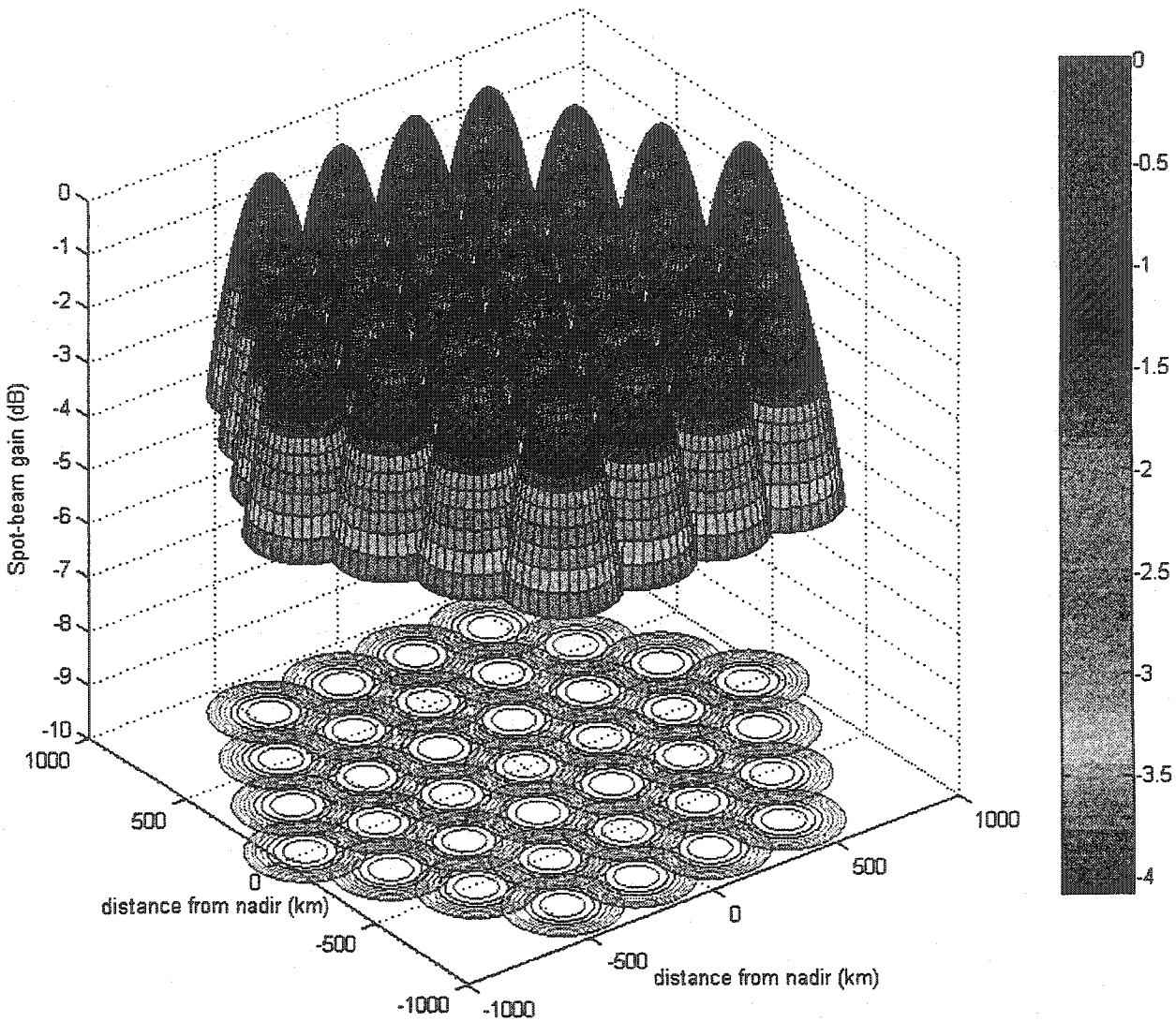

Figure 4-3 Spot-beam overlap value illustration in a 37 beams cellular layout

For the simulation of the system, we have to investigate the spot-beam gain pattern given in Chapter 2 in Figure 2-4 and find the angular offset of the received signal from the center of the spot-beam that corresponds to these (-2dB, -3dB,-4dB) spot-beam overlaps. Here, we give the spot-beam gain characteristic for convenience in Figure 4-4.

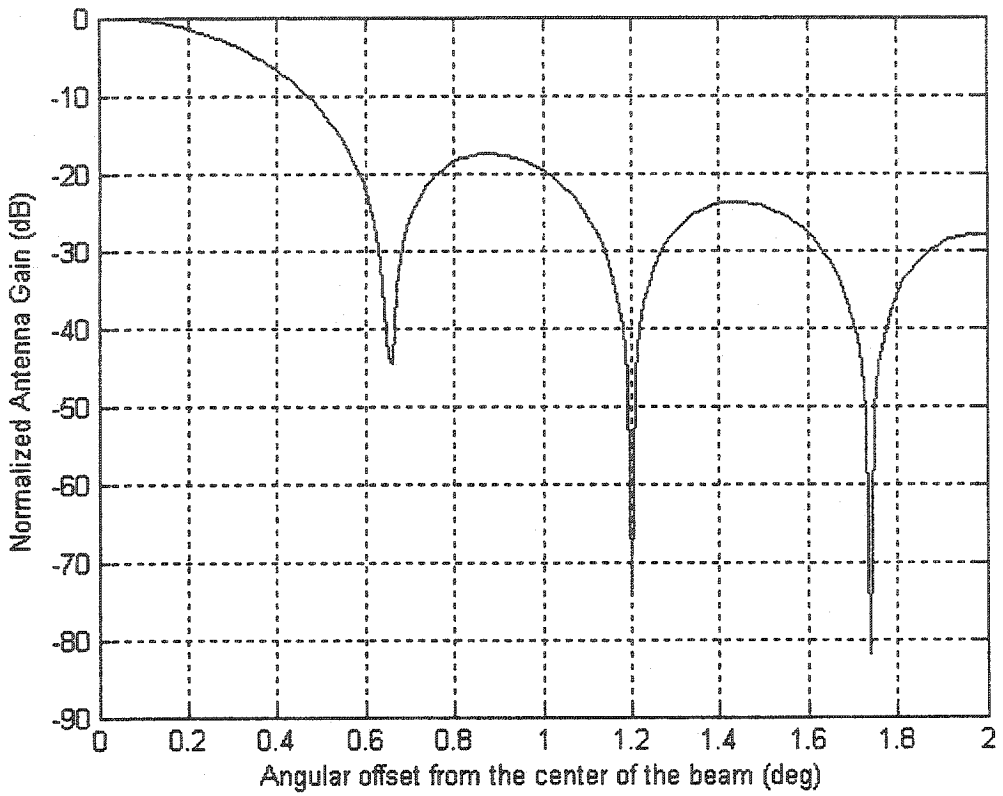

Figure 4-4 Satellite antenna spot-beam gain pattern with satellite antenna diameter D=20m and operational frequency *fo*=1.6 GHz

If we magnify the upper-left part of Figure 4-4, we can easily see the angle values corresponding to the wanted gain overlaps. Figure 4-5 shows the angular offset values clearly for certain antenna gain values. These angular offset values will be used with the geometrical relations of the satellite and earth to evaluate the coverage area of the spot-beam.

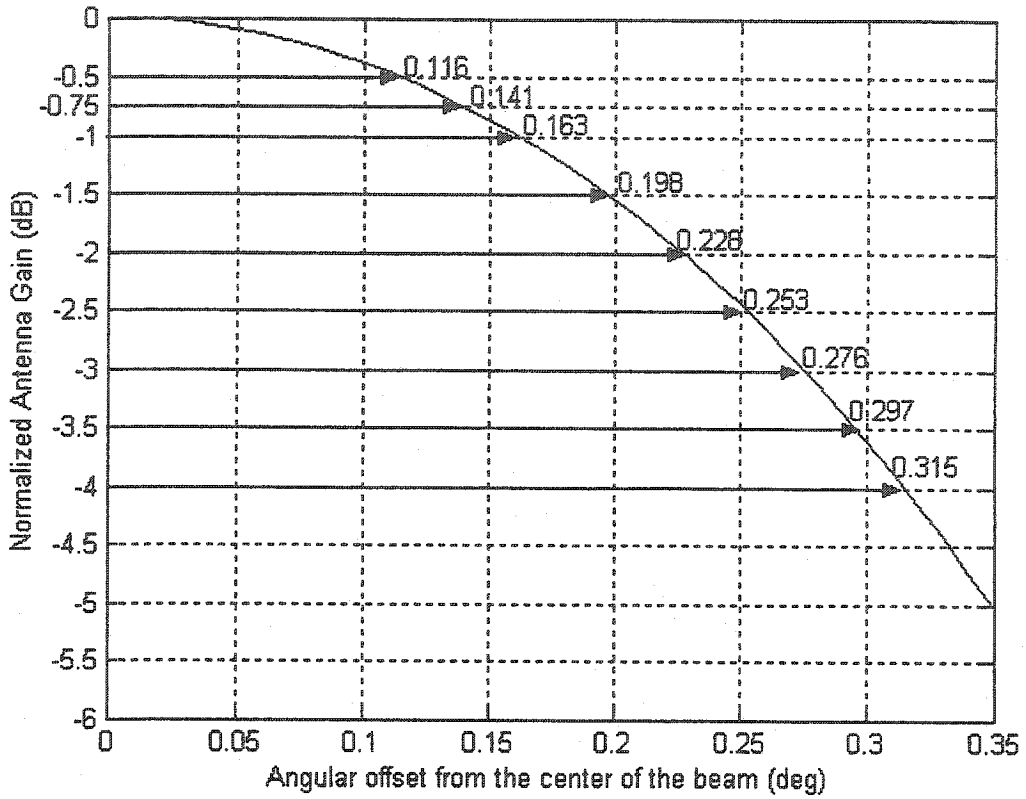

Figure 4-5 Magnified angular offset values for different spot beam gain overlaps with antenna diameter D=20m and operational frequency *fo*=1.6 GHz

By choosing a larger gain decrease at the spot-beam overlap contour, one can decrease the power spilling out from a spot-beam, which causes less inter-cell interference to other beams. To accomplish this, satellite antenna diameter has to be increased, or the number of spot beams must be reduced for a constant service area, which affects the overall system capacity. Table 4-3 illustrates the change of the OCI factor and the spot-beam radius on earth relative to the spot-beam overlap value.

Table 4-3 The OCI factors for different spot-beam gain overlaps, with 61 cell layout and full frequency reuse

Gain overlap value (dB)	Cell radius (Rcell, km)	The OCI factor
-0.25dB	51.5 km	16.9775
-0.5dB	73km	8.4364
-0.75dB	89km	5.8489
-1.0dB	102km	4.3411
-1.25dB	114 km	3.4497
-1.5dB	124km	2.8420
-1.75dB	134 km	2.4335
-2.0dB	143km	2.0979
-2.25dB	151 km	1.8502
-2.5dB	159km	1.6538
-2.75dB	166.5 km	1.4868
-3.0dB	173km	1.3564
-3.25dB	180 km	1.2439
-3.5dB	187km	1.1541
-3.75dB	192 km	1.0817
-4.0dB	198km	1.0167

Figure 4-6 illustrates the effects of two concepts, the contribution of spot-beam rings in the cellular layout and spot-beam overlap value, on the OCI factor together. As it can be seen from the figure, as we increase the spot-beam isolation (i.e. higher gain decrease on spot-beam contour) the OCI factor affecting the nadir beam decreases and the spot-beams on the first ring of cells dominate the OCI factor.

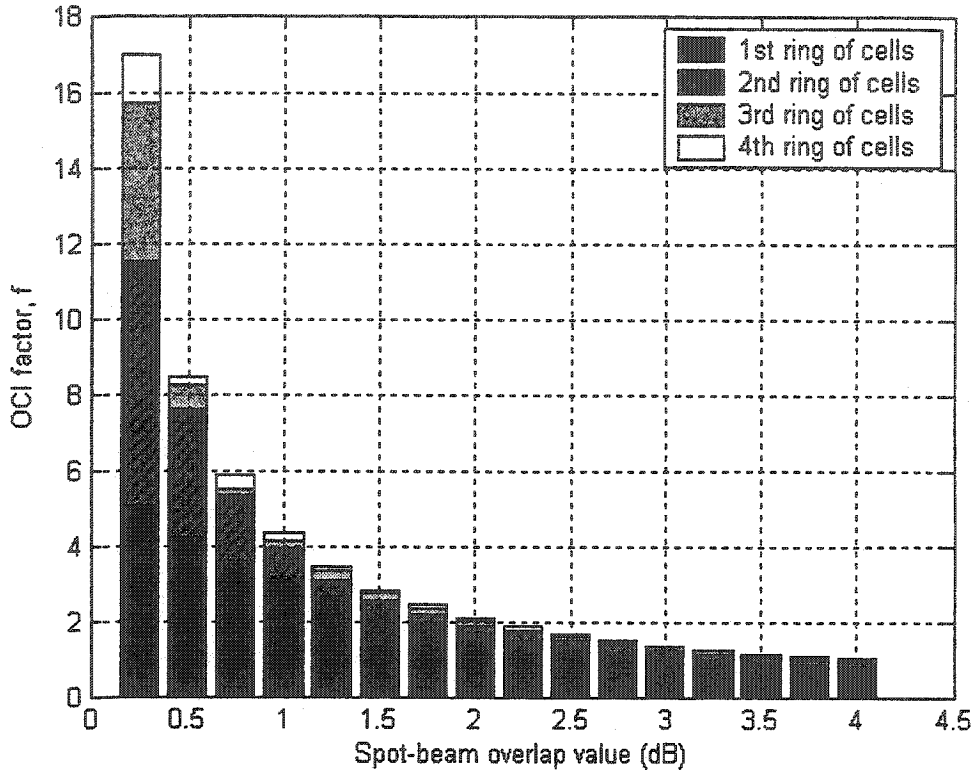

Figure 4-6 The effect of the spot-beam isolation and the number of spot-beams in the cellular layout on the OCI factor in a system of 61 cell layout and full frequency reuse

As illustrated in Table 4-3, with the assumption of the constant cellular layout (e.g., 61 spot-beams), as we increase the spot-beam isolation (decrease of antenna gain on spot-beam contour), the radius of the spot-beam increases which ends up increased coverage area of the satellite. This increasing area concept might cause wrong interpretations of the system performance.

The increase of a spot-beam area along with the lower gain overlap value between spot-beams is illustrated in Figure 4-7 with the system of antenna diameter D=20m, transmission frequency f=1.6GHz and GEO satellite at altitude h=36000km.

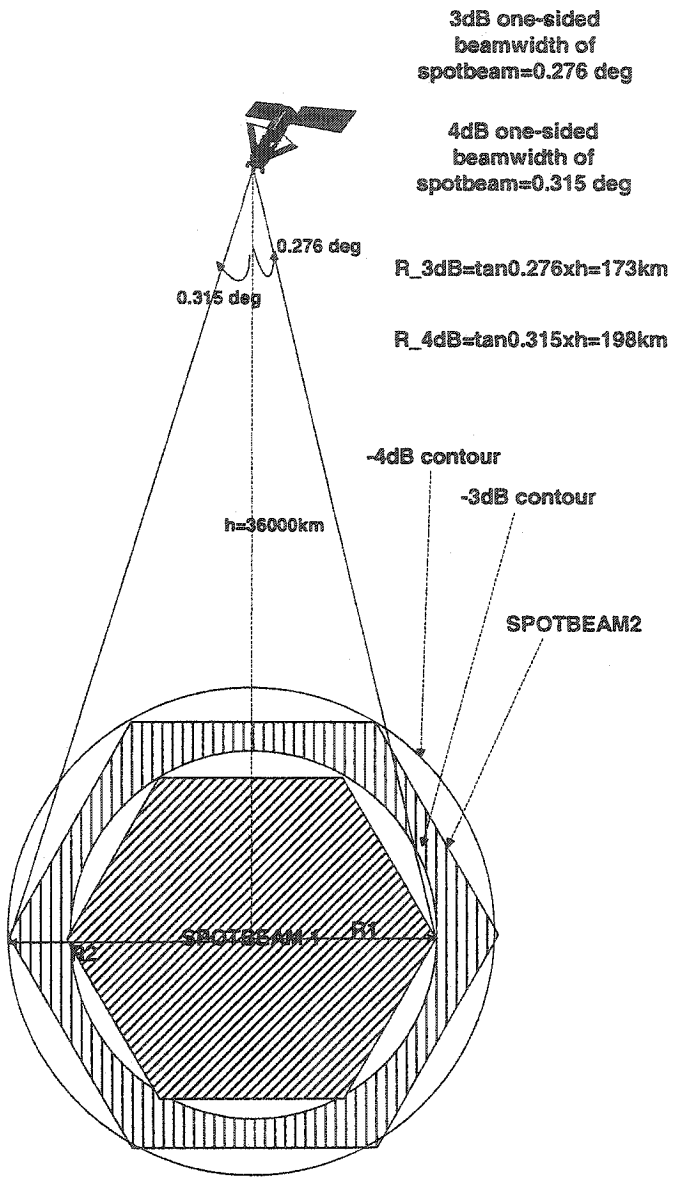

Figure 4-7 Area (or radius) increase of a spot-beam along with lower spot-beam overlap. -4dB and -3dB spot-beam overlaps are shown with GEO satellite (h=36000km). One-sided 3dB and 4dB beam-widths are read from spot-beam antenna pattern

In order to have a meaningful result from system performance simulations, we have to consider a constant coverage area for the satellite system. With the aim of representing the constant area, we are going to consider a coverage area consisting of 100 spot-beams overlapping on 3dB contour, which is the most common overlap value in satellite systems [Lut97]. Therefore, we will

normalize our calculation results relative to 3dB gain overlap. Consequently, the total area to be covered can be represented as:

$$Area \approx 100\left(\pi R_{3dB}^2\right) \tag{4.6}$$

Number of spot-beams of different overlap values can be calculated easily by equating the constant coverage area. The number of spot-beams having an overlap value X dB is illustrated as follows:

$$Area \approx 100\left(\pi R_{3dB}^2\right) \approx \#_{XdB}\left(\pi R_{XdB}^2\right) \Rightarrow \#_{XdB} \approx round\left(100\left(\frac{R_{3dB}}{R_{XdB}}\right)^2\right) \tag{4.7}$$

In our capacity calculations for different spot-beam overlap values and constant coverage area we will take the reference system parameters W/R=307, V=0.5, E_b/I_{req}=2.6dB and E_b/N_0=10dB, repeated here for convenience. The effect of f will be analyzed in the overall capacity. With assumption of reference system parameters in equation (4.5), the capacity ***per spot-beam*** can be shown to be inversely proportional to the OCI factor:

$$N_{\max} = 1 + \frac{276.3}{(1+f)} \tag{4.8}$$

Table 4-4 illustrates the change of the spot-beam capacity and satellite footprint overall capacity due to the altered OCI factor. As we see from Table 4-4, by using a larger overlap values, we represent the constant area with less beams. Even though, increasing beam isolation is leading to less OCI factor and increased capacity ***per spot-beam***, the overall system capacity for constant serving area decreasing due to representation of coverage area with fewer spot-beams.

Table 4-4 The OCI factor and capacity calculation for a constant serving area for different spot-beam overlap values

Gain overlap value (dB)	Cell radius (Rcell, km)	# of users per spot-beam	# of spot-beams for the constant area	# of users for the constant area	The OCI factor
-0.25dB	51.5 km	16	1128	18048	16.9775
-0.5dB	73km	30	562	16860	8.4364
-0.75dB	89km	41	378	15498	5.8489
-1.0dB	102km	52	288	14976	4.3411
-1.25dB	114 km	63	230	14490	3.4497
-1.5dB	124km	73	195	14235	2.8420
-1.75dB	134 km	81	167	13527	2.4335
-2.0dB	143km	90	146	13140	2.0979
-2.25dB	151 km	98	131	12838	1.8502
-2.5dB	159km	105	118	12390	1.6538
-2.75dB	166.5 km	112	108	12096	1.4868
-3.0dB	173km	118	100	11800	1.3564
-3.25dB	180 km	124	92	11408	1.2439
-3.5dB	187km	129	86	11094	1.1541
-3.75dB	192 km	134	81	10854	1.0817
-4.0dB	198km	138	76	10488	1.0167

4.2.2.3 Effect of Frequency Reuse on the Performance of Multi-Beam Satellite CDMA System

By keeping in mind the fact that the MAI in a multi-beam system is caused by all the spot-beams in the satellite footprint, one might think that instead of using the same frequency in all the spot-beams, introducing 3-Cell, 4-Cell or 7-Cell frequency reuse clusters may substantially reduce the OCI factor and increase capacity. However, the capacity increase due to interference reduction might not exceed the capacity loss due to reduced spectral efficiency. This is the question behind our motivation to simulate different frequency reuse strategies for the satellite footprint.

In order to illustrate the OCI decrease in different frequency reuse schemes, we numerically calculated the OCI factor in 3-Cell, 4-Cell and 7-Cell frequency reuse clusters with 61 spot-beams satellite footprint and 3 dB spot-beam overlap.

Figure 4-8 represents frequency reuse pattern of the 3-cell frequency reuse cluster used to calculate the OCI factor. Each pattern shows the different operational frequencies used in spot-beams.

We expect a dramatic decrease of the OCI factor in the transition from full frequency reuse to 3-Cell frequency reuse cluster. That is because, Table 4-2 shows that the first ring of the cells has the biggest effect on the OCI factor, which is not included in the OCI factor calculation in 3-Cell frequency reuse cluster.

In the 3-Cell frequency reuse system capacity evaluation, we have to take into account the reduced spectral efficiency and the new numerically calculated OCI factor. The calculated values for per spot-beam and constant coverage area are illustrated in Table 4-5.

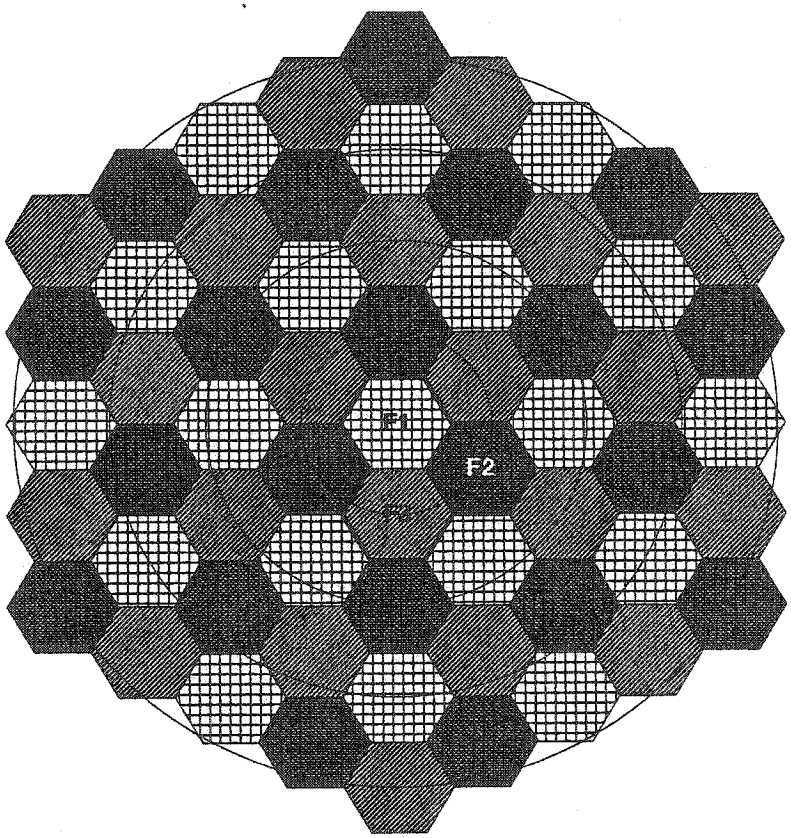

Figure 4-8 3-Cell frequency re-use pattern on a 61 cell satellite footprint

Table 4-5 The OCI factor and capacity of 3-Cell frequency reuse for constant coverage area

Gain overlap value (dB)	# of users per spot-beam	# of spot-beams for the constant area	# of users for the constant area	The OCI factor
-0.25dB	16	1128	18048	5.0048
-0.5dB	30	562	16860	2.1127
-0.75dB	41	378	15498	1.2814
-1.0dB	52	288	14976	0.7851
-1.25dB	63	230	14490	0.4691
-1.5dB	73	195	14235	0.2700
-1.75dB	79	167	13193	0.1749
-2.0dB	82	146	11972	0.1342
-2.25dB	83	131	10873	0.1229
-2.5dB	83	118	9794	0.1201
-2.75dB	83	108	8964	0.1185
-3.0dB	83	100	8300	0.1162
-3.25dB	83	92	7636	0.1128
-3.5dB	84	86	7224	0.1090
-3.75dB	84	81	6804	0.1053
-4.0dB	84	76	6384	0.1016

For 4-Cell frequency reuse cluster used in the satellite footprint is given in Figure 4-9. In the comparison of the results of 3-Cell cluster and 4-Cell cluster frequency reuse, we do not expect spectacular decrease in the OCI factor. Because, the OCI factor decrease in 4-Cell cluster relative to 3-Cell cluster comes from 2nd and 3rd ring of beams which have less influence in the OCI factor. Similar to the 3-Cell frequency reuse system we will calculate the capacity together with the decreased OCI factor and spectral efficiency. The calculated values for a constant coverage area are illustrated in Table 4-6.

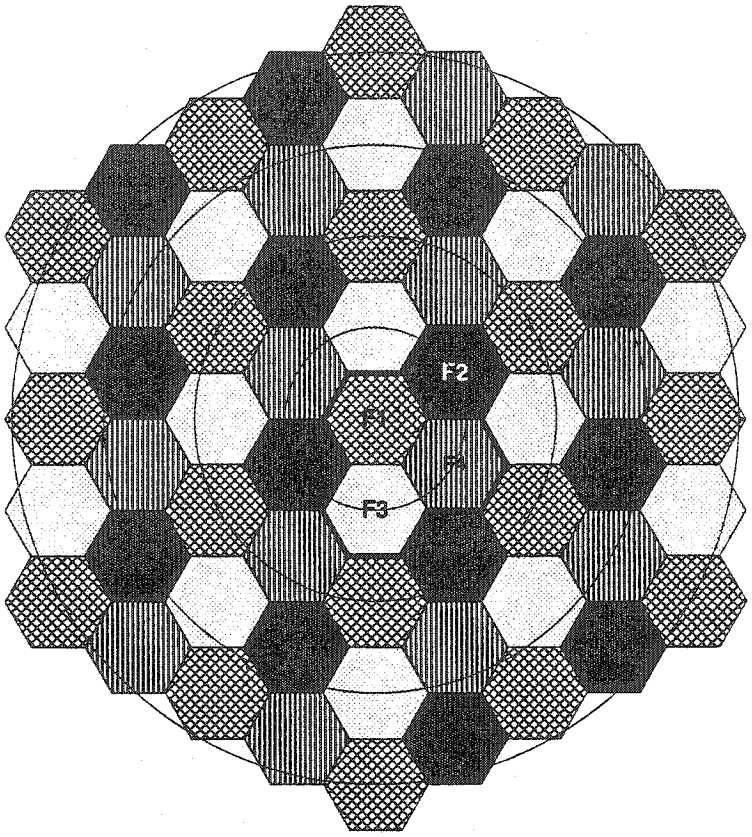

Figure 4-9 4-Cell frequency re-use pattern on a 61 cell satellite footprint

Table 4-6 The OCI factor and capacity of 4-Cell frequency reuse for constant coverage area

Gain overlap value (dB)	# of users per spot-beam	# of spot-beams for the constant area	# of users for the constant area	The OCI factor
-0.25dB	*16*	*1128*	*18048*	*3.5131*
-0.5dB	*29*	*562*	*16298*	*1.4318*
-0.75dB	*40*	*378*	*15120*	*0.7462*
-1.0dB	*52*	*288*	*14976*	*0.3233*
-1.25dB	*61*	*230*	*14030*	*0.1494*
-1.5dB	*63*	*195*	*12285*	*0.1016*
-1.75dB	*63*	*167*	*10521*	*0.1030*
-2.0dB	*63*	*146*	*9198*	*0.1113*
-2.25dB	*63*	*131*	*8253*	*0.1137*
-2.5dB	*63*	*118*	*7434*	*0.1112*
-2.75dB	*63*	*108*	*6804*	*0.1052*
-3.0dB	*63*	*100*	*6300*	*0.0979*
-3.25dB	*64*	*92*	*5888*	*0.0898*
-3.5dB	*64*	*86*	*5504*	*0.0825*
-3.75dB	*65*	*81*	*5265*	*0.0764*
-4.0dB	*65*	*76*	*4940*	*0.0710*

The system for 7-Cell frequency reuse is almost the same as 3-Cell and 4-Cell cluster systems. Nevertheless, the performance of 7-Cell system is poorer due to almost the same OCI factor compared to 3 and 4-Cell systems and highly reduced spectral efficiency. 61-cell cellular layout with 7-Cell frequency reuse is illustrated in Figure 4-10 and the values obtained from the simulation are given in Table 4-7.

Table 4-7 The OCI factor and capacity of 7-cell frequency reuse for constant coverage area

Gain overlap value	# of users per spot-beam	# of spot-beams for the constant area	# of users for the constant area	The OCI factor
-0.25dB	*16*	*1128*	*18048*	*1.5877*
-0.5dB	*31*	*562*	*17422*	*0.2910*
-0.75dB	*38*	*378*	*14364*	*0.0466*
-1.0dB	*38*	*288*	*10944*	*0.0567*
-1.25dB	*37*	*230*	*8510*	*0.0866*
-1.5dB	*37*	*195*	*7215*	*0.0911*
-1.75dB	*37*	*167*	*6179*	*0.0763*
-2.0dB	*38*	*146*	*5548*	*0.0549*
-2.25dB	*39*	*131*	*5109*	*0.0385*
-2.5dB	*39*	*118*	*4602*	*0.0282*
-2.75dB	*39*	*108*	*4212*	*0.0226*
-3.0dB	*39*	*100*	*3900*	*0.0205*
-3.25dB	*39*	*92*	*3588*	*0.0199*
-3.5dB	*39*	*86*	*3354*	*0.0198*
-3.75dB	*39*	*81*	*3159*	*0.0196*
-4.0dB	*39*	*76*	*2964*	*0.0193*

From Tables 4-5, 4-6 and 4-7 we see that in low beam isolations, where we have high OCI factor, introducing 3-Cell or more frequency reuse reduces the interference in such a degree that it can compensate the capacity loss due to using one-third or less spectral efficiency compared to spectral efficiency of full frequency reuse. But, as we increase the beam isolation, it begins not to be sufficient enough to compensate.

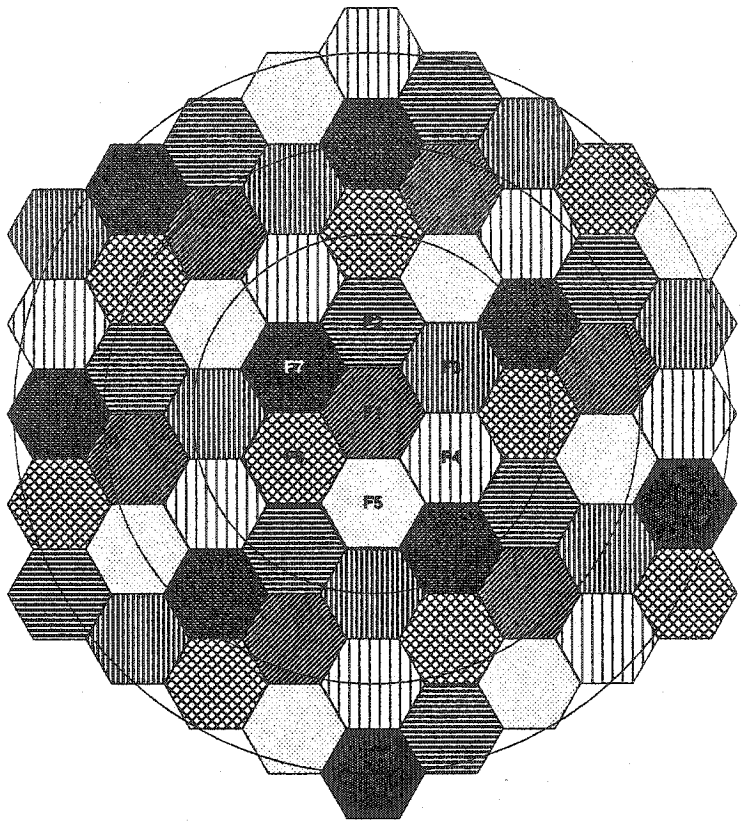

Figure 4-10 7-Cell frequency re-use pattern on a 61 cell satellite footprint

We can show the trend of capacity loss of 3, 4 and 7-Cell frequency reuse relative to full frequency reuse in graph. We know that with the PPC of user terminals, the uplink capacity for asynchronous CDMA system can be approximated as described in equation (4.5). With specified system parameters, e.g. V=0.5, E_b/I_{req}=2.6 dB and E_b/N_0=10dB, the capacity of the system can be calculated by just two variables like processing gain W/R and OCI factor f. Therefore, for CDMA with full frequency reuse, the capacity per beam can be represented as:

$$N_{1-\text{Cell}} \approx \frac{W/R}{(1+f_{1-\text{Cell}})} \tag{4.9}$$

In 3-Cell frequency reuse cluster, equation would be:

$$N_{3-\text{Cell}} \approx \frac{1}{3}\left\{\frac{W/R}{(1+f_{3-\text{Cell}})}\right\} \tag{4.10}$$

and in 4-Cell frequency reuse cluster, we have the equation as follows:

$$N_{4\text{-Cell}} \approx \frac{1}{4}\left\{\frac{W/R}{(1+f_{3-\text{Cell}})}\right\} \tag{4.11}$$

and finally in 7-Cell frequency reuse cluster it is:

$$N_{7\text{-Cell}} \approx \frac{1}{7}\left\{\frac{W/R}{(1+f_{3-\text{Cell}})}\right\} \tag{4.12}$$

The OCI factors for different systems (e.g., $f_{3\text{-Cell}}, f_{4\text{-Cell}}, f_{7\text{-Cell}}$) are calculated and presented in Table 4-5, 4-6 and 4-7. If we plot the ratio of other system capacities (e.g., $N_{3\text{-Cell}}, N_{4\text{-Cell}}, N_{7\text{-Cell}}$) to cluster one system capacity ($N_{1\text{-Cell}}$) relative to the spot-beam overlap values, we can see the point where the decrease of the OCI factor in 3,4 and 7-Cell cluster frequency reuse systems can compensate the decrease of spectral efficiency caused by utilizing adjacent frequency reuse clusters.

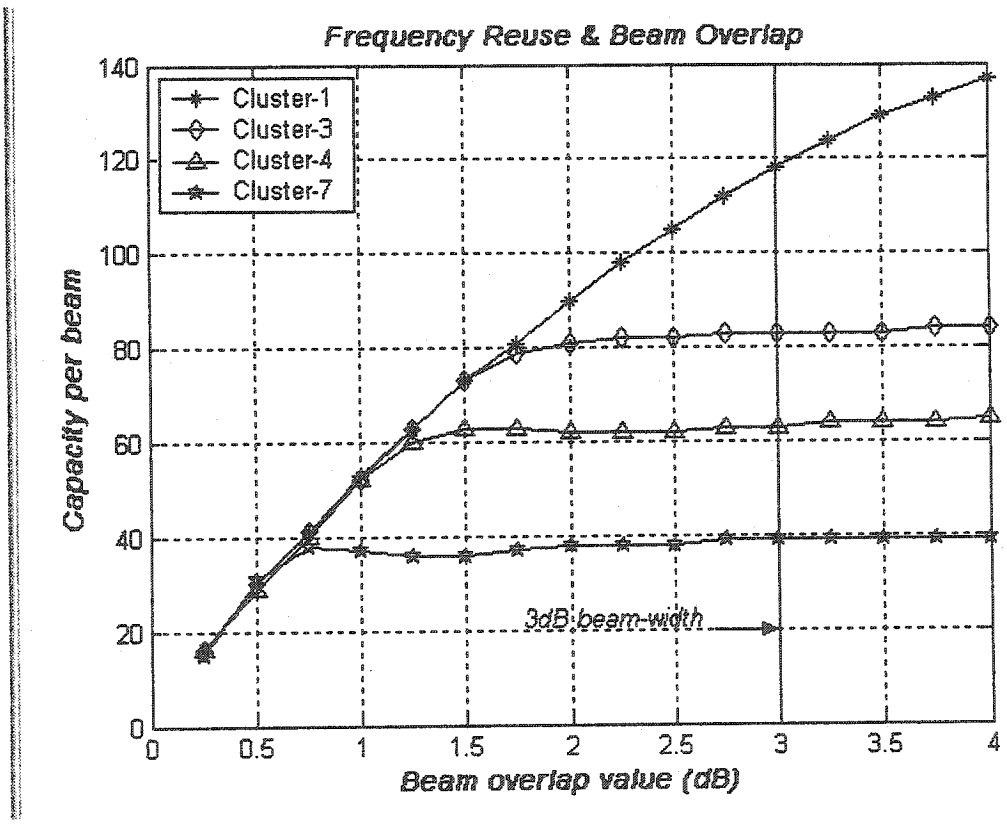

Figure 4-11 Capacity ratios of the different systems relative to spot-beam overlap values with V=0.5, E_b/I_{req}=2.6 dB and E_b/N_0=10dB

As seen in the figure, Cluster-1 (full frequency reuse) system is superior at spot beam overlap values of 1.50 dB and higher. If we plot the OCI factors of different frequency reuse schemes, we can easily see the major factor affecting the capacity change. Figure 4-12 illustrates the change of the OCI factor of systems relative the spot-beam overlap values. If we want to compare different frequency reuse policies, it is obvious from graph that, at lower beam overlap values the decrease in the OCI factor due to changing the frequency reuse (e.g., from full frequency reuse to 3-Cell cluster frequency reuse) can compensate the spectral efficiency loss.

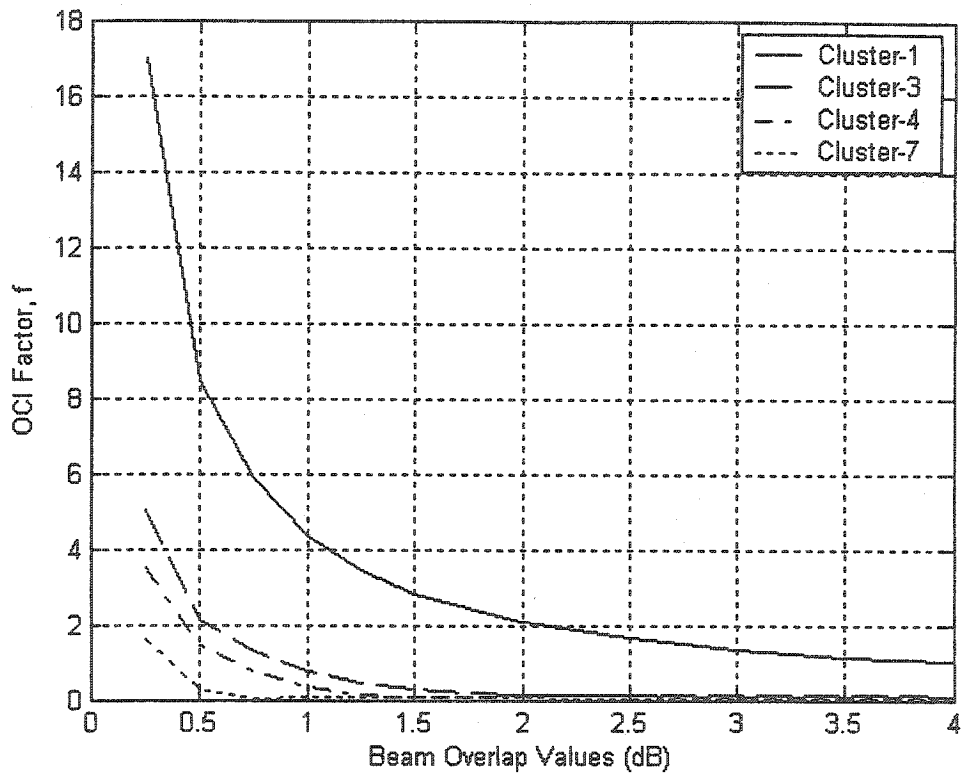

Figure 4-12 The OCI factor of different frequency reuse systems relative to beam overlap values

However, at higher beam overlap values, the change in OCI factor is relatively small and can not pay off for the spectral efficiency loss. At beam overlap values higher than 1.5 dB, the OCI factors of all frequency reuse systems having more than cluster 1, are almost equal. So, it is

reasonable to use 3-Cell cluster frequency reuse in order prevent further capacity loss due to diminished spectral efficiency.

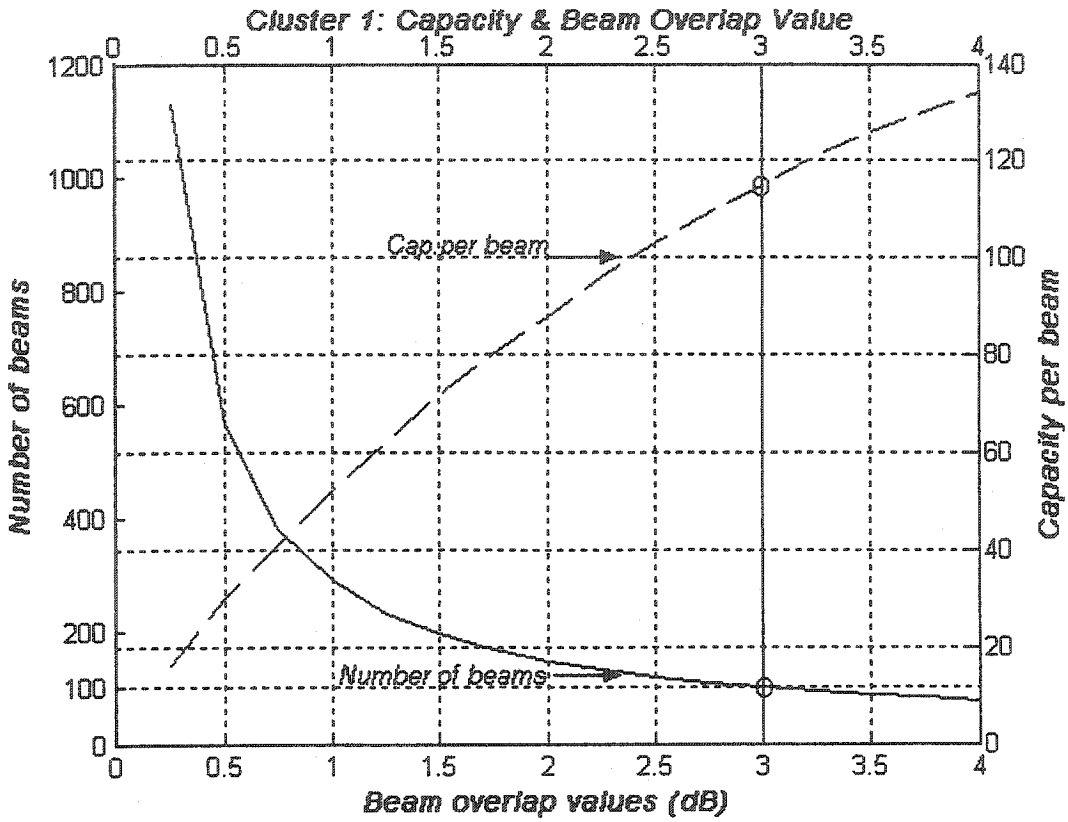

Figure 4-13 Capacity per beam and number of beams for a constant coverage area

Figure 4-13 illustrates both the capacity of the single beam with full frequency reuse and the number of beams for constant serving area. For constant area representation we chose 100 beams with 3dB beam contour. As we can see from the graph as we decrease the spot-beam contours the number of the beams is increasesing exponentially. Thefore, even though the capacity per beam is decreasing as we decrease the spot-beam contor, the capacity of the overall system is increasing. The capacity of the overall system can be easily found by multiplying the capacity per beam and the number of the beams in the constant coverage area.

4.2.2.4 Effect of Loading on the Performance of Multi-Beam Satellite CDMA Systems

In this section, we will investigate the effect of the beam loading on the system performance. Until this section, we considered that all the spot-beams in the cellular layout were fully loaded, in other words they were being operated on the maximum capacity that they can supply. In this section, we change the loadings of surrounding spot-beams (other beams) and investigate its effect on the performance of the nadir beam. It will be shown that with low loading values in other spot-beams, one can obtain higher capacity in the considered beam due to reduced interference coming from surrounding cells. In the simulations, we considered 75%, 50% and 25% loadings of other cells.

Table 4-8 The OCI factor and the capacity calculations of the reference system for a constant serving area with different spot-beam loadings

Gain overlap value	The OCI factor 100% loading	User # with 100% loading	The OCI factor 75% loading	User # with 75% loading	The OCI factor 50% loading	User # with 50% loading	The OCI factor 25% loading	User # with 25% loading
-0.25dB	16.9775	16	12.7331	21	8.4888	30	4.2444	53
-0.5dB	8.4364	30	6.3273	38	4.2182	53	2.1091	89
-0.75dB	5.8489	41	4.3867	52	2.9245	71	1.4622	113
-1.0dB	4.3411	52	3.2559	65	2.1706	88	1.0853	133
-1.25dB	3.4497	63	2.5872	78	1.7248	102	0.8624	149
-1.5dB	2.8420	73	2.1315	89	1.4210	115	0.7105	162
-1.75dB	2.4335	81	1.8251	98	1.2168	125	0.6084	172
-2.0dB	2.0979	90	1.5735	108	1.0490	135	0.5245	182
-2.25dB	1.8502	98	1.3876	116	0.9251	144	0.4625	189
-2.5dB	1.6538	105	1.2403	124	0.8269	152	0.4134	196
-2.75dB	1.4868	112	1.1151	131	0.7434	159	0.3717	202
-3.0dB	1.3564	118	1.0173	137	0.6782	165	0.3391	207
-3.25dB	1.2439	124	0.9329	143	0.6220	171	0.3110	211
-3.5dB	1.1541	129	0.8656	149	0.5770	176	0.2885	215
-3.75dB	1.0817	134	0.8113	153	0.5409	180	0.2704	218
-4.0dB	1.0167	138	0.7625	157	0.5083	184	0.2542	221

If we compare the new capacity values calculated with the maximum capacity estimated when all the spot-beams in cellular configuration are fully loaded, we can see from Table 4-8 that, 40% capacity increases in the considered beam can be observed with the condition of 50% loading of

other spot-beams and 3 dB overlap. This capacity increase can reach to 80% with 25% loading case. The loading of spot-beams has superior importance in the link-margin and system reliability calculations which will be analyzed in the following sections thoroughly.

4.2.3 Satellite Power Requirement for PPC

Until now we concentrated on the mobile user uplink capacity of the CDMA system, which limits the overall system capacity. Unlike terrestrial cellular networks, in a mobile-satellite network, transmissions are constrained by available satellite power. With PPC assumption, we presumed that power variations in the user's spot-beam are compensated with power control on both uplink and downlinks. Here in this section, we will touch another critical issue in satellite communication and we will calculate the extra power needed at satellite to be supplied to uniformly distributed mobile users in a spot-beam area for perfectly power controlled systems.

In the calculation we are going to utilize satellite spot-beam gain equation, which determines the power variation on the spot-beam coverage area:

$$G(\theta)=\left(\frac{J_1(u)}{u}\right)^2, \text{with u} = D\pi\left(\frac{\sin\theta}{\lambda}\right) \tag{4.13}$$

We know that received power of the mobile user is decreasing as the mobile moves away from the spot-beam center. The power decrease is given in equation (4.13), which varies relative to off-axis angle,θ (angular separation of received mobile signal from cell-center direction). If we modify the equation (4.13) and change the variable from off-axis angle θ to distance from spot-beam center in *km*, *r*, utilizing the geometrical relations between these parameters from Figure 4-7, we have the following equation.

$$G(r)=\left(\frac{J_1(u)}{u}\right)^2, \text{with u} = D\pi\left(\frac{\sin\{a\tan[r/h]\}}{\lambda}\right) \tag{4.14}$$

where r is the distance from the spot-beam center and h=36000 km is the satellite altitude.$G(r)$ gives the power degradation caused by the spot-beam antenna pattern for a mobile user who is r

distance away from spot-beam center. In other words, the mobile user at a distance r km from spot-beam center receives $G(r)$ less power than a user at spot-beam center.

In order to calculate the extra power required at satellite for a spot-beam to keep all the users' power same as if they are at the spot-beam center, we have to specify the power increase in the mobile users' signal relative to spot-beam gain decrease.

For the PPC case, the power required for a single user at a distance r km from the spot-beam center can be found as:

$$P_{user} = \frac{1}{G(r)} \tag{4.15}$$

However, if we want to calculate the total power required for all users in the spot-beam, we have to consider all of the users in the spot-beam area. Different types of user distributions can be considered in the spot-beam area, but we will assume that mobile users are uniformly distributed in the spot-beam coverage area. The total power required for a spot-beam of gain X dB decrease on its contour can be evaluated by the integral given in equation (4.16)

$$P_{spot} = \int_0^{R_{XdB}} \frac{1}{G(r)} 2\pi r dr = \int_0^{R_{XdB}} \left\{ \frac{D\pi\left(\frac{\sin\{a\tan[r/h]\}}{\lambda}\right)}{J_1\left[D\pi\left(\frac{\sin\{a\tan[r/h]\}}{\lambda}\right)\right]} \right\}^2 2\pi r dr \tag{4.16}$$

In order to have a meaningful representation and to find the extra power required for the PPC, we have to normalize the value we calculated in equation (4.16). If there were not any power degradations due to spot-beam antenna, the transmitted power levels for all users would be the same regardless of their position. If we consider each user's transmitted power as P_0=1watt, the power required for the users uniformly distributed on the spot-beam area can be calculated as:

$$P_{\text{no-deg}} = \int_0^{R_{XdB}} (1watt)(2\pi r) dr = \pi R_{XdB}^2 \tag{4.17}$$

If we name this power level as power with no-degradation, the extra power supplied from the satellite for compensating the spot-beam antenna gain roll-off relative to no-degradation power would be found by taking the ratio of this power levels as shown in equation (4.18):

$$P_{ext} = \frac{P_{\text{no-deg}}}{P_{spot}} = \frac{1}{\pi R_{XdB}^2} \int_0^{R_{XdB}} \left\{ \frac{D\pi \left(\frac{\sin\{a\tan[r/h]\}}{\lambda} \right)}{J_1\left[D\pi \left(\frac{\sin\{a\tan[r/h]\}}{\lambda} \right) \right]} \right\}^2 2\pi r dr \qquad (4.18)$$

Figure 4-14 illustrates the required power calculation method in a satellite spot-beam. Satellite spot-beam gain pattern is demonstrated by the graph in the upper part of the Figure 4-14. The shadowed part of the spot-beam shown at the bottom part of Figure 4-14 illustrates the gain decrease in the spot-beam area. As one moves away from the center of the beam, he will experience more power degradation. The distance from the beam center is assumed to be positive as we go to positive *X* axis and negative as we go to negative *X* axis.

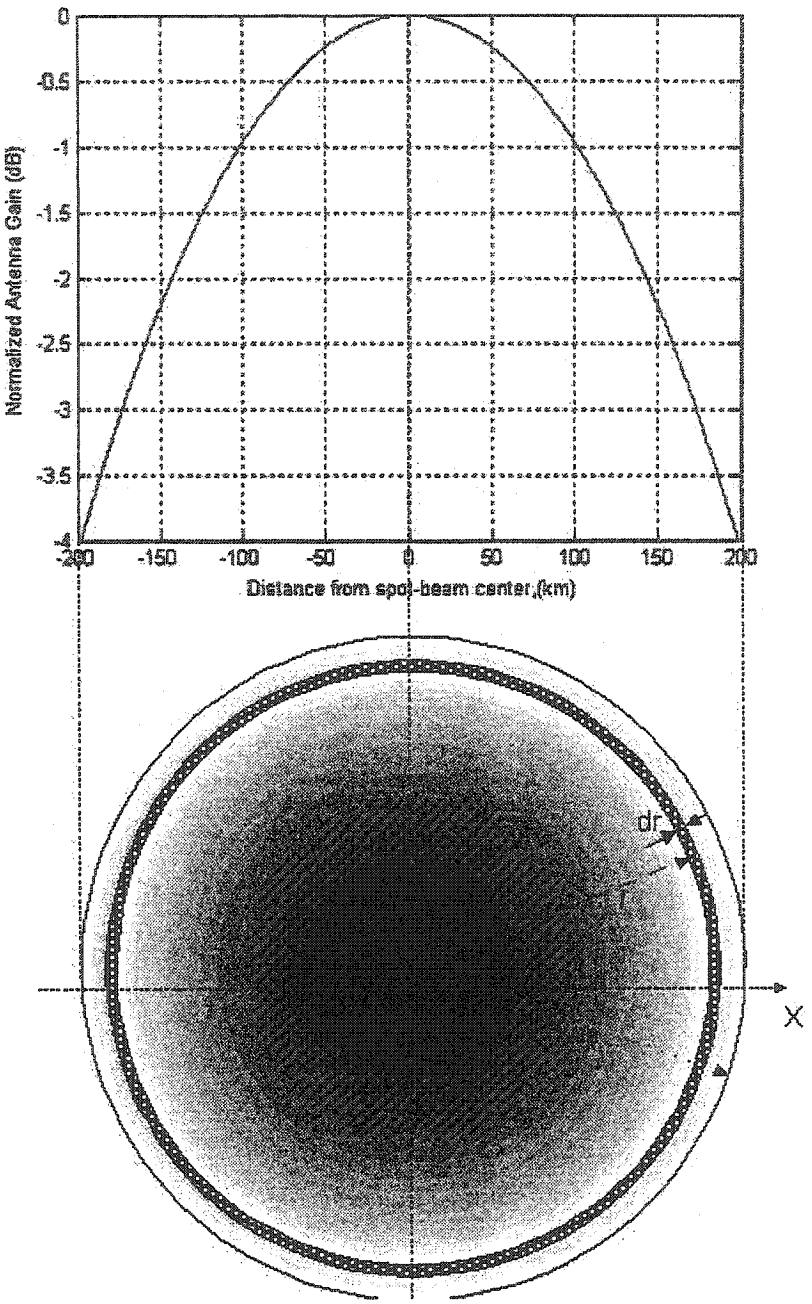

Figure 4-14 Calculation method of extra power required in PPC with satellite antenna diameter D=20m, operational frequency *fo*=1.6 GHz and GEO satellite at h=36000 km altitude

We can observe the extra power required for a single spot-beam together with the user capacity per spot-beam and the capacity of whole satellite footprint in Table 4-9. As we expected, the

power required to keep all the uniformly distributed users at the same power level is increasing as we increase the spot-beam isolation. The increase of the required power is slow due to the slow gain decrease illustrated in the gain pattern in Figure 4-14.

Table 4-9 OCI factors of different spot-beam gain overlaps along with power requirements for PPC

Gain overlap value	Cell radius (Rcell)	# of users per spot-beam	# of spot-beams for constant area	# of users for constant area	Average Extra Power required for PPC in a spot-beam	The OCI factor
-0.25dB	51.5 km	16	1128	18048	0.126dB	16.965
-0.5dB	73km	30	562	16860	0.255dB	8.428
-0.75dB	89km	41	378	15498	0.382dB	5.842
-1.0dB	102km	53	288	15264	0.506dB	4.335
-1.25dB	114 km	63	230	14490	0.637dB	3.444
-1.5dB	124km	73	195	14235	0.759dB	2.838
-1.75dB	134 km	82	167	13694	0.894dB	2.429
-2.0dB	143km	90	146	13140	1.026dB	2.094
-2.25dB	151 km	98	131	12838	1.153dB	1.847
-2.5dB	159km	105	118	12390	1.288dB	1.651
-2.75dB	166 km	112	108	12096	1.424dB	1.485
-3.0dB	173km	118	100	11800	1.549dB	1.355
-3.25dB	180 km	124	92	11408	1.691dB	1.243
-3.5dB	187km	129	86	11094	1.841dB	1.154
-3.75dB	192 km	134	81	10854	1.954dB	1.082
-4.0dB	198km	138	76	10488	2.095dB	1.017

4.3 Imperfectly Power Controlled Systems

The limitation of the IPC on the mobile user uplink capacity of a CDMA system and representation of the mobile user powers at satellite with PCE is mentioned in Chapter 3. In this section, we will investigate the effect of PCE on multi-beam satellite CDMA system performance with simulations. In order to observe the effect of IPC, we will first assume that the users are perfectly power controlled and find the maximum capacity of the nadir beam. This maximum capacity is calculated when all the spot-beams in the cellular layout are fully loaded. After finding the maximum user capacity of the nadir beam in satellite cellular configuration, in order to investigate IPC of user powers in the spot-beam, we multiply the perfectly power controlled

user powers (P_0), with predetermined PCE values, which are log-normally distributed random variables with changing standard deviations, σ_γ. The magnitude of PCE standard deviation depends on the accuracy of power control process. We will indicate the capacity degradation due to PCE, relative to the PPC capacity or maximum capacity. We will investigate the considered spot-beam user's E_b/I_{tot} pdf and cdf's to assess the capacity of system and to see the percentage of the users satisfying the required communication link quality (e.g., $E_b/I_{tot} \geq E_b/I_{req}$)

We can analyze the effect of the PCE on the reference system capacity in Figure 4-15. It shows the cdf of 118 simultaneously active mobile users' E_b/I_{tot} values in the considered spot-beam. An expected result of PPC is obvious as shown in the figure. That is, all transmitted signal powers of mobile users in the spot-beam are the same and received at satellite at the minimum power needed to achieve the specified $E_b/I_{tot} = E_b/I_{req} = 2.6\,\text{dB}$. Therefore, cdf of all mobile user E_b/I_{tot} s in the considered spot-beam is just a unit step function at $E_b/I_{tot} = 2.6\,\text{dB}$.

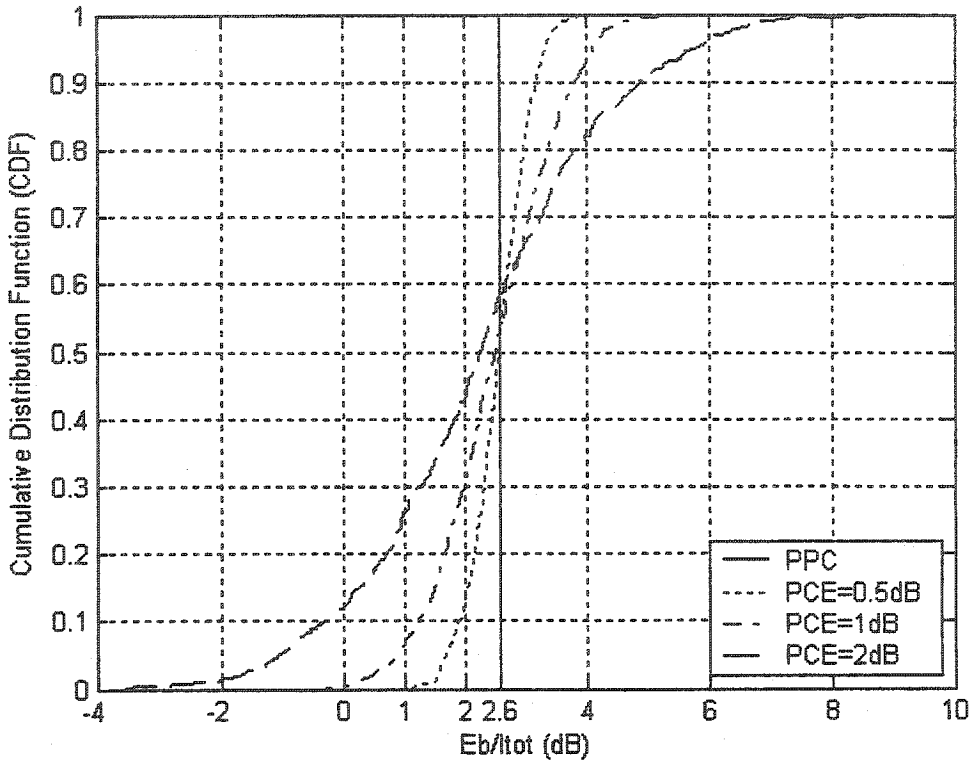

Figure 4-15 Effects of different PCE standard deviation values on user Eb/Itot cdf with system of $E_b/N_0 = 10$dB, V=0.5, W/R=307, $E_b/I_{req} = 2.6$dB

If we consider PCE, E_b/I_{tot} values of each user in the spot-beam would be different (Equation 3.17 of Chapter 3). Consequently, the users within a spot-beam have a continuous cdf distribution rather than just a unit step function for their E_b/I_{tot} cdf. Taking into account the PCE, we observe that almost half of the users' performance is degraded comparison to PPC, in other words $E_b/I_{tot} \leq E_b/I_{req}$. Increasing PCE standard deviation will cause further dispersion around the optimum E_b/I_{tot} value (2.6 dB with PPC), which means that some user's performance is degraded significantly.

As mentioned in Chapter 3 in equation (3.22) we can theoretically approximate the pdf of *SINR* (or E_b/I_{tot}) of users in the considered spot-beam. In Figure 4-16, we show both analytically obtained and simulated values of user E_b/I_{tot} pdfs. As seen in Figure 4-16, simulated pdf values

give good correlation with the analytical ones. Figure 4-15 and Figure 4-16 demonstrate that even with small PCE, almost half of the user's E_b/I_{tot} is lower than the required value, E_b/I_{req}.

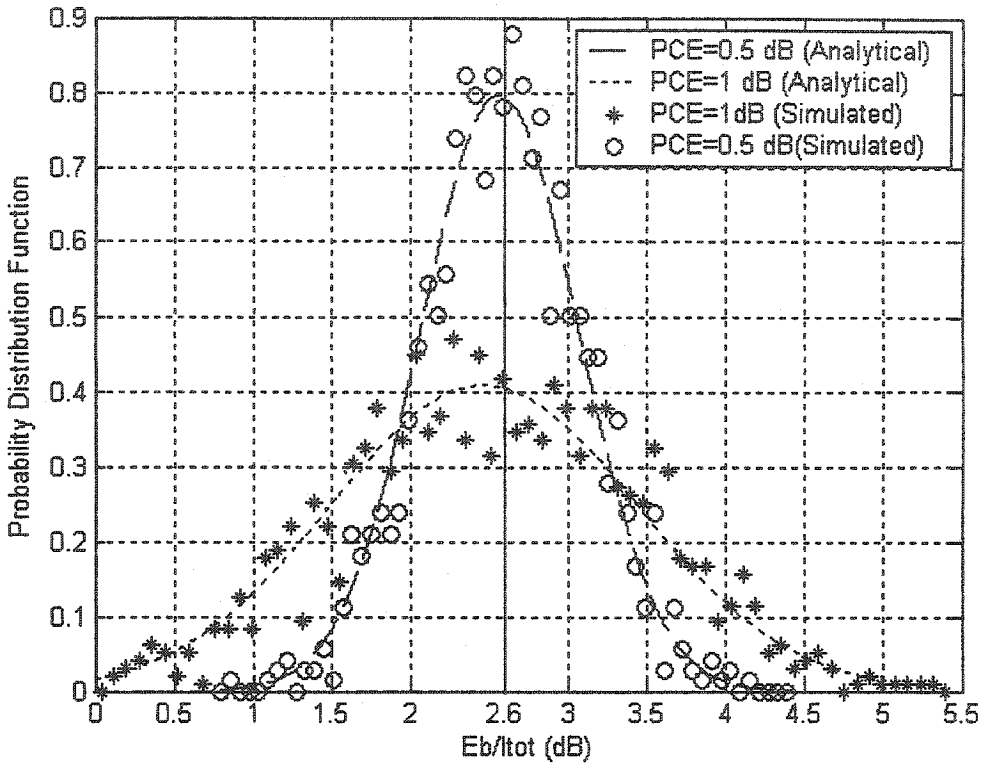

Figure 4-16 Effects of different PCE standard deviation values on own spot-beam user Eb/Itot pdf with the system of $E_b/N_0 = 10$dB, V=0.5, W/R=307, $E_b/I_{req} = 2.6$dB

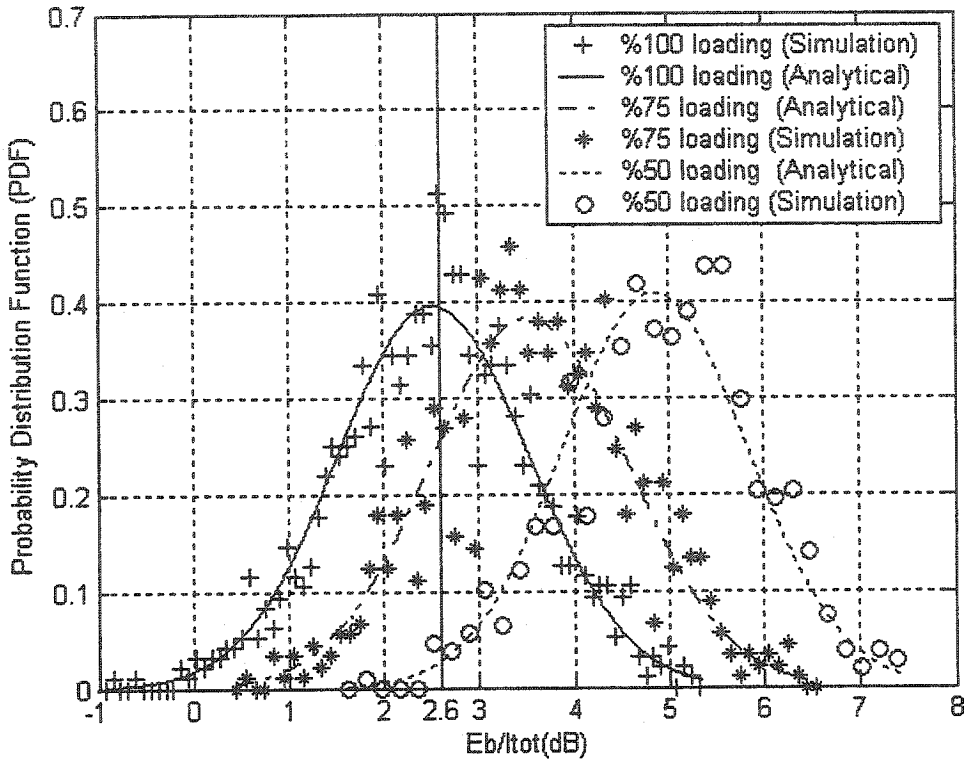

Figure 4-17 Comparisons of different loadings with PCE=1dB with system of $E_b/N_0 = 10\text{dB}$, V=0.5, W/R=307, $E_b/I_{req} = 2.6\text{dB}$

In Figure 4-15 and Figure 4-16, initially we considered that the spot beams were fully loaded, then, PCE applied to disperse user powers relative to predetermined PCE and finally the performance of the system is observed. However, in real time systems, normally spot beams are not used with the maximum capacity. Figure 4-17 investigates the effect of beam loading on the performance of multi-beam system. From Figure 4-17, we observe that, plots of pdf's of user's E_b/I_{tot} s in the nadir beam shift to right as we decrease the loading. That is because as we decrease the number of users in a spot-beam, the interference power coming from all users of the considered spot-beam as well as neighboring beams will decrease while keeping the same transmission power for the wanted user. Therefore, the probability of active mobile users having a satisfactory communication link is increasing with the decreasing value of spot-beam loading. For

example, with a certain PCE, the system can supply a good communication link 9 out of 10 users (90% percent) instead of 10 out of 20 (50% percent). One thing worth mentioning is that, in the spot-beam loading analysis on the OCI factor, we calculated the maximum attainable capacity of the own spot-beam while lowering the loading in the adjacent spot-beams, but not in the considered beam. However, in the capacity analysis with PCE, we decreased the loading in all the spot-beams (including the nadir beam) and estimated the number of the users satisfying the required system performance condition with PCE. The calculation of outage probability, defined as the failing probability to achieve E_b/I_{req}, is done over the number of users already reduced relative to full loading.

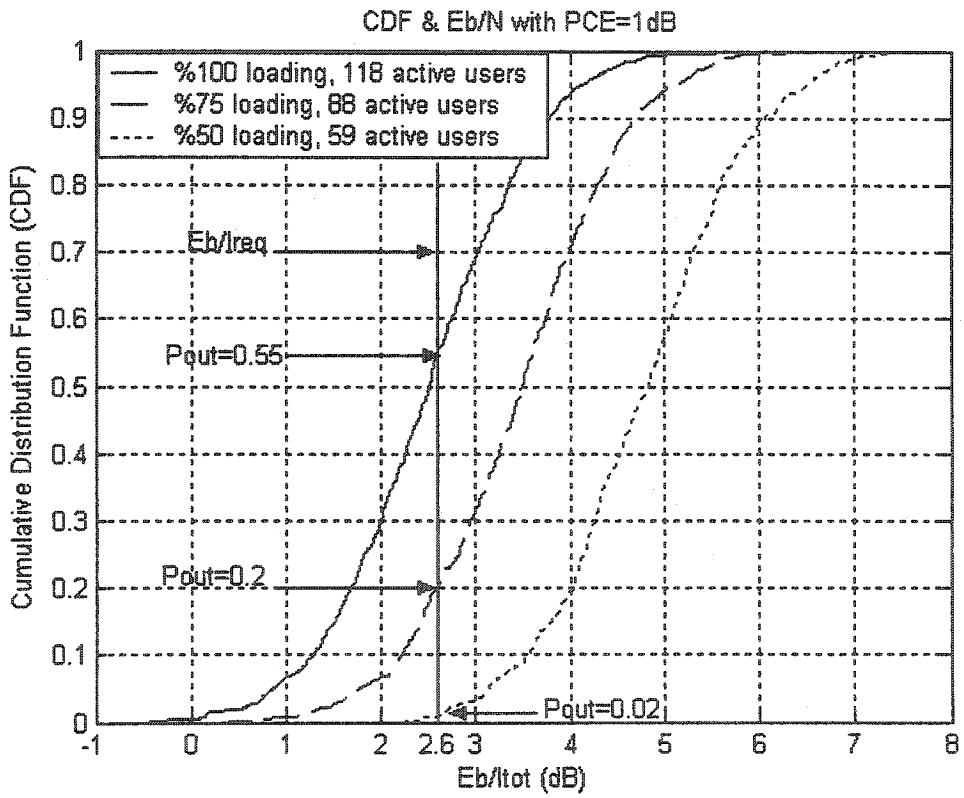

Figure 4-18 Comparisons of different loadings with PCE=1dB with system of $E_b/N_0 = 10$ dB, V=0.5, W/R =307, $E_b/I_{req} = 2.6$ dB

It is easier to see the outage probability of the system by analyzing the cdf curves instead of pdfs. We show the cdf values of the reference system with different loadings. We can see from Fig.4-19 that with the same system specifications, we can serve 82% of active mobile users (18% outage probability) with 75% loading (approximately 88 active users) or support half of the maximum capacity (59 active users, 50% loading) with outage probability 2%.

In order to see the effect of the thermal noise on the system capacity with PCE, we plotted the system performances with constant PCE and varying SNR.

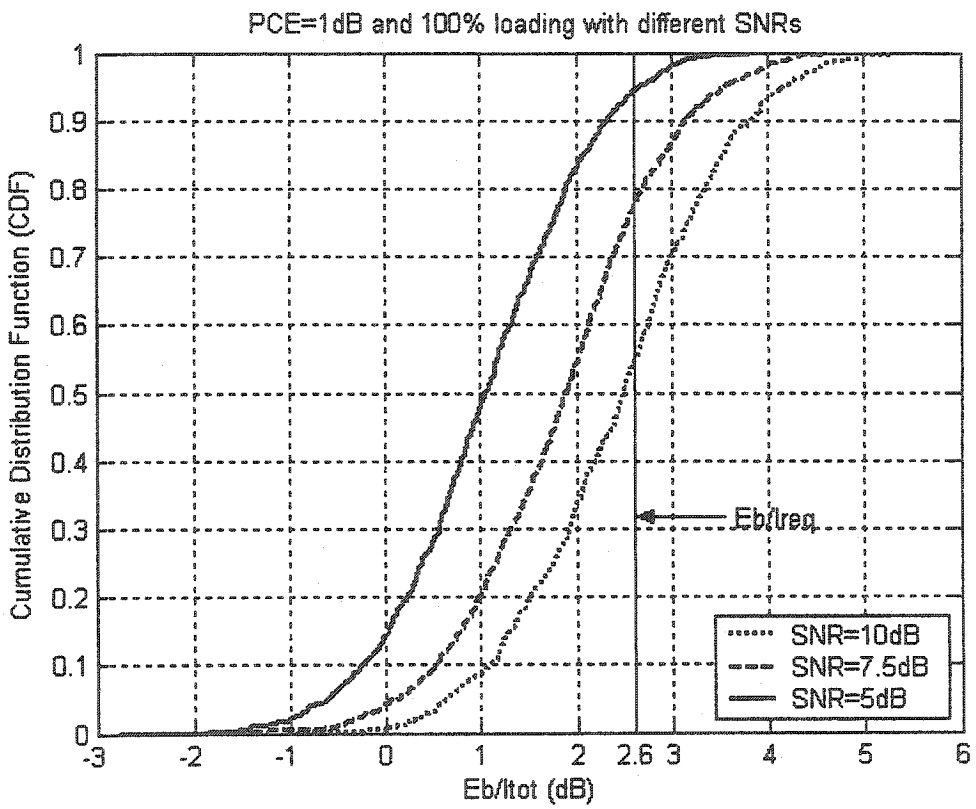

Figure 4-19 Comparison of systems with different SNRs with full loading and PCE=1dB

Figure 4-19 shows that in satellite systems the capacity depends on the thermal noise. It shows the performance of the same reference system with 100% beam loading and PCE=1dB. If system operates with SNR=10dB, P_{out}=55%, but if you decrease the user SNR to 7.5dB P_{out}=80% and if

you continue decreasing user SNR to 5 dB, P_{out} reaches to 95%. So, we can conclude that system performance is highly dependent on SNR.

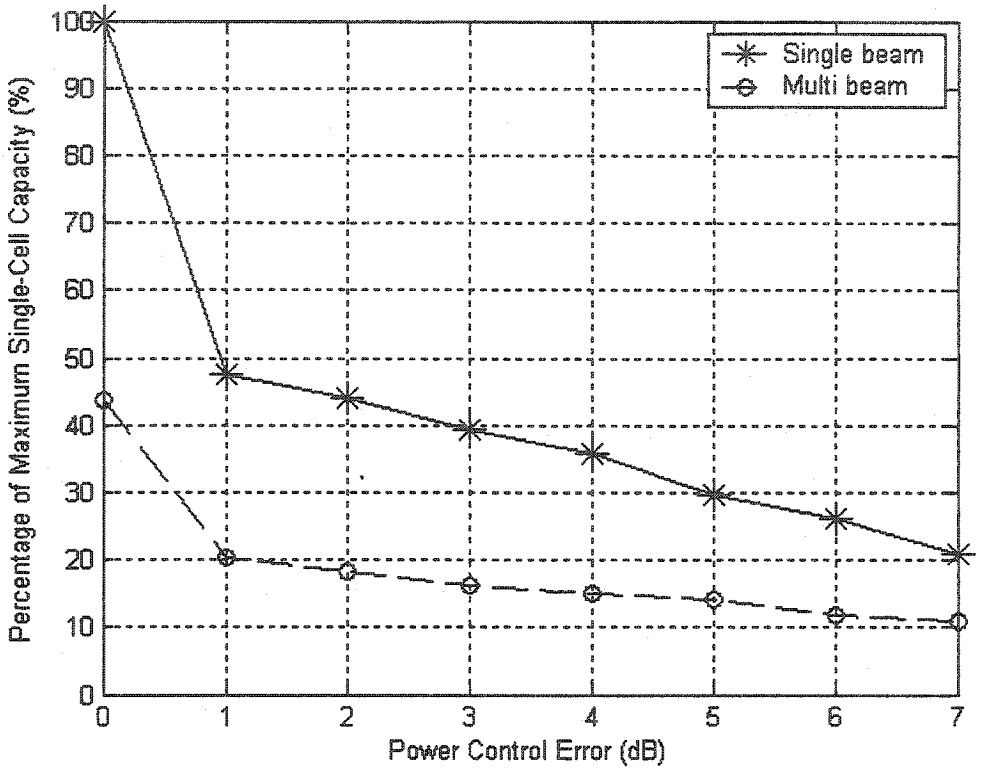

Figure 4-20 Effects of PCE and multiple cell interference on satellite system capacity

Figure 4-20 illustrates the effect of PCE on the system capacity as defined by outage probability. It shows the capacity reduction in percentages, due to the PCE for both single-beam and multi-beam system. In Figure 4-20, the effect of the inter-beam interference is obvious (i.e,the effect of OCI factor). As an example, in the PPC case (e.g. $PCE = 0\,\text{dB}$), the maximum capacity decreased more than 50% when considering multiple beams instead of a single beam, which is expected with the calculated OCI factor $f = 1.36$.

4.4 Link Budget

A link budget analysis forms the corner stone of the system design. Link budget analysis is performed in order to analyze the effect of system parameters such as transmission power, spot-beam loading and so on, in order to ensure that a given target Quality of Service (QoS) can be achieved.

The mission specifies a value of mobile user's E_b/I_{tot} greater than or equal to E_b/I_{req} during a given percentage of the time. For example, 99% of the time means that the system guarantees the 99% service availability. As implied, in order to calculate the link budget of the system we have to investigate the time variant behavior of the mobile user performance. We can define the excess link margin (ELM) as the difference between the mobile user E_b/I_{tot} value and the required E_b/I_{req} value for acceptable link performance:

$$LM_{excess}(dB) = E_b/I_{tot}(dB) - E_b/I_{req}(dB) \tag{4.19}$$

In this section we calculate the link margin of the multi-beam satellite CDMA system with different loadings. Through link budget analysis, we will estimate the system capacity as well as system availability defined as the percentage of time that the system can supply satisfactory communication link quality. In the simulations, we used the reference satellite system parameters with E_b/I_{req} =2.6 dB. In the calculations we considered the users in the nadir beam. The capacity values and loadings given are for the nadir beam. We used the *cdf* curves as a tool to investigate the system availability. The *cdf* curves derived indicates that the user E_b/I_{tot} value changes in time in the considered beam.

First we will concentrate on perfectly power controlled systems. In a multi-beam satellite system with PPC the E_b/I_{tot} value variations of a mobile user in the considered beam in time with different spot-beam loadings are given in Figure 4-21:

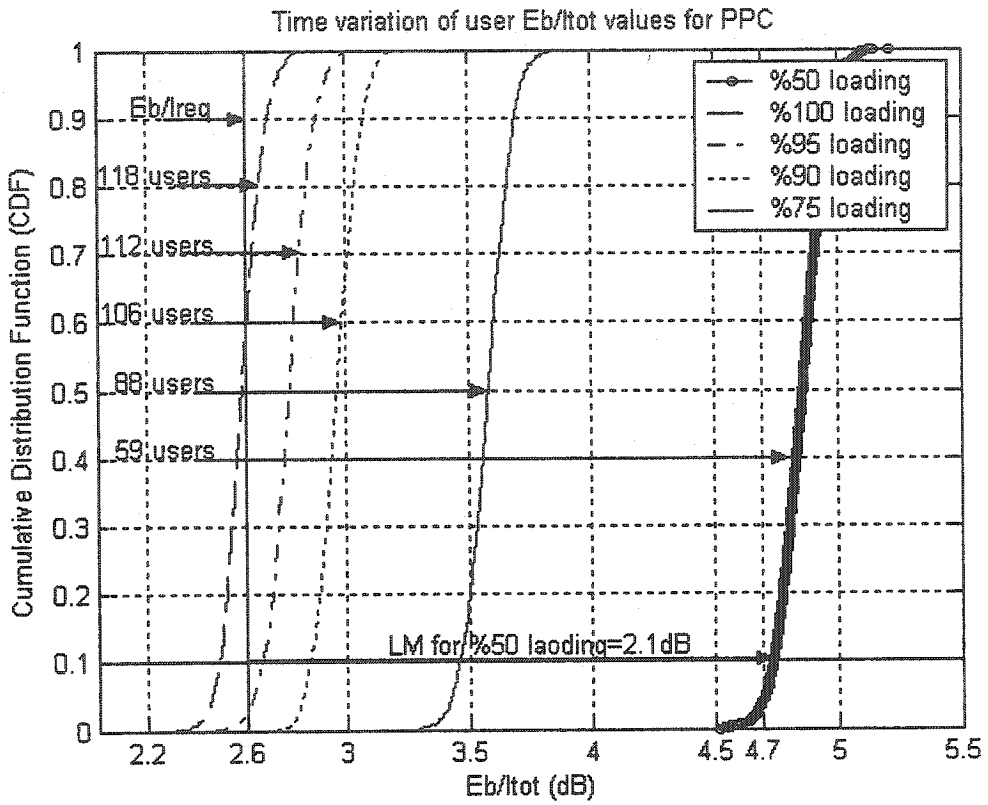

Figure 4-21 User Eb/Itot cdf with different spot-beam loadings in PPC

As it can be seen from Figure 4-21, if we operate the satellite system with 100% loading (maximum capacity, 118 active mobile users in the considered beam) in each spot beam, 60% of the time, mobile user's E_b/I_{tot} values would be less than E_b/I_{req} =2.6 dB, which does not satisfy the required BER=10^{-3}. However, if we decrease the loading to 95% (112 active mobile users), in PPC case, the system can supply a good communication link quality 95% of the time. System with 106 active users (90% loading) can serve all of its active mobile users all the time. From Figure 4-21 we can calculate the ELM for the systems with different loadings and system availabilities. For example, we want to calculate the ELM for 90% system availability (e.g.,

system supplies an adequate service quality to its mobile users 90% of the time). Figure 4-21 shows that with 50% loading, 90% percent of the time user E_b/I_{tot} value is bigger than 4.7dB. This value decreases in 75% loading to 3.4dB. Therefore, with 50% loading (59 active mobile users) we have, 4.7dB-2.6dB=2.1dB ELM, where as this value decreases to, 3.4dB-2.6dB=0.8dB in 75% loading (88 active mobile users).

If we consider the PCE, the variations of user E_b/I_{tot} values increases. Figure 4-22 illustrates the system operating with 0.5dB PCE.

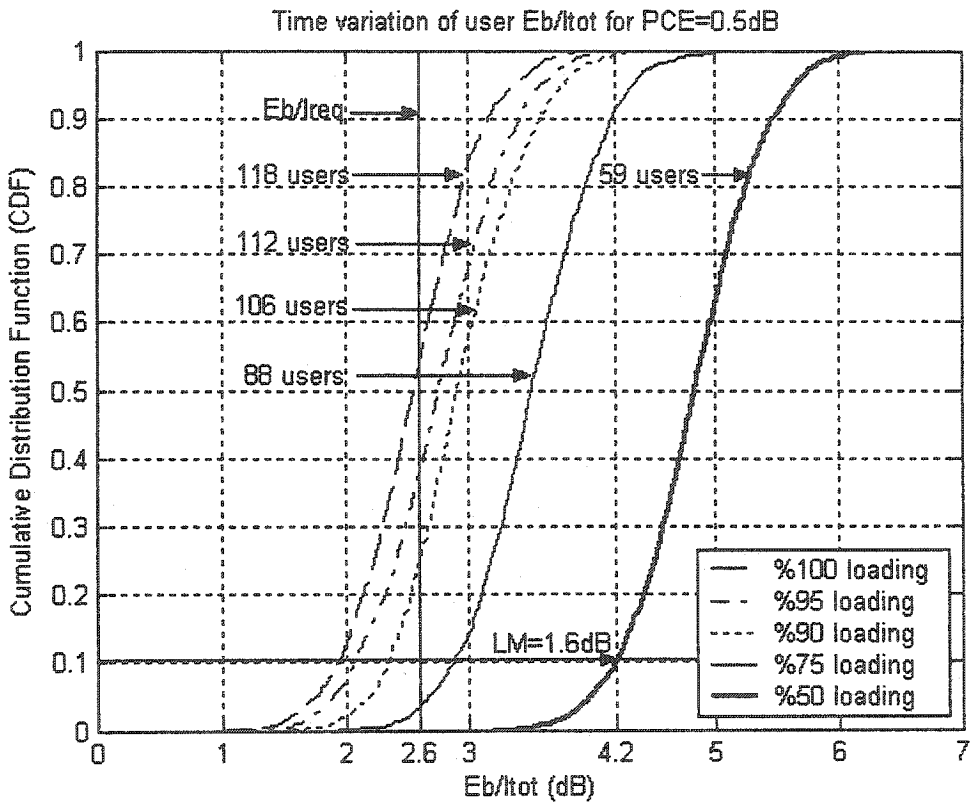

Figure 4-22 User Eb/Itot cdf with different spot-beam loadings in PCE=0.5dB

If we want to calculate the ELM for PCE=0.5 dB case with 50% system loading and 90% system availability we have, 4.2dB-2.6dB=1.6dB ELM instead of 2.1dB ELM of PPC case. The increase of signal power variations due to system PCE causes to a decrease in the ELM of the system.

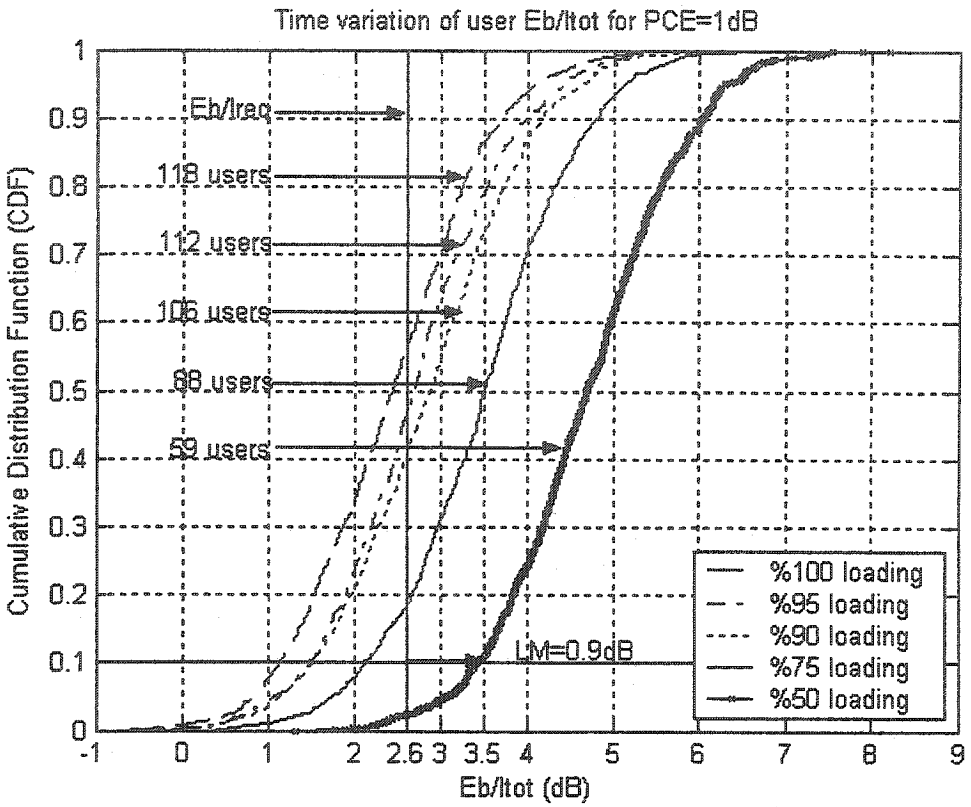

Figure 4-23 User Eb/Itot cdf with different spot-beam loadings in PCE=1dB

If we calculate the ELM again for PCE=1 dB case with 50% system loading and 90% system availability we have, 3.5dB-2.6dB=0.9dB ELM.

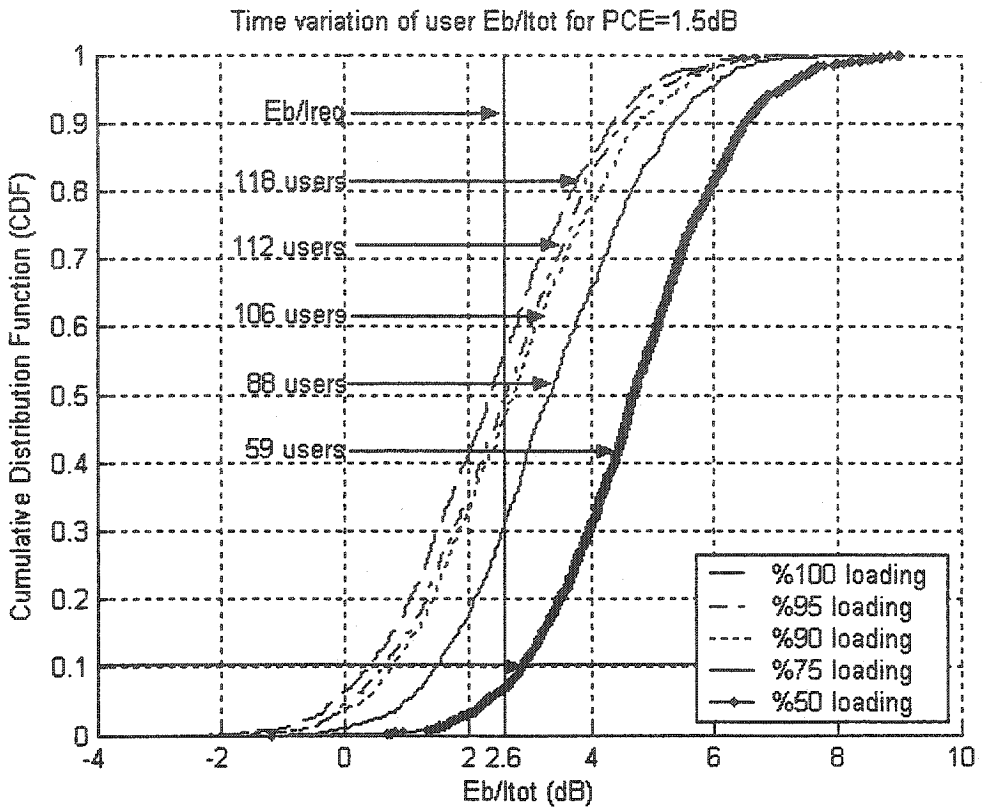

Figure 4-24 User Eb/Itot cdf with different spot-beam loadings in PCE=1.5dB

If we consider the system with PCE=1.5 dB, we do not have any ELM as illustrated in Figure 4-24. That is to say, the system barely handles the 59 active mobile users (50% loading) with 90% system availability and PCE=1.5dB.

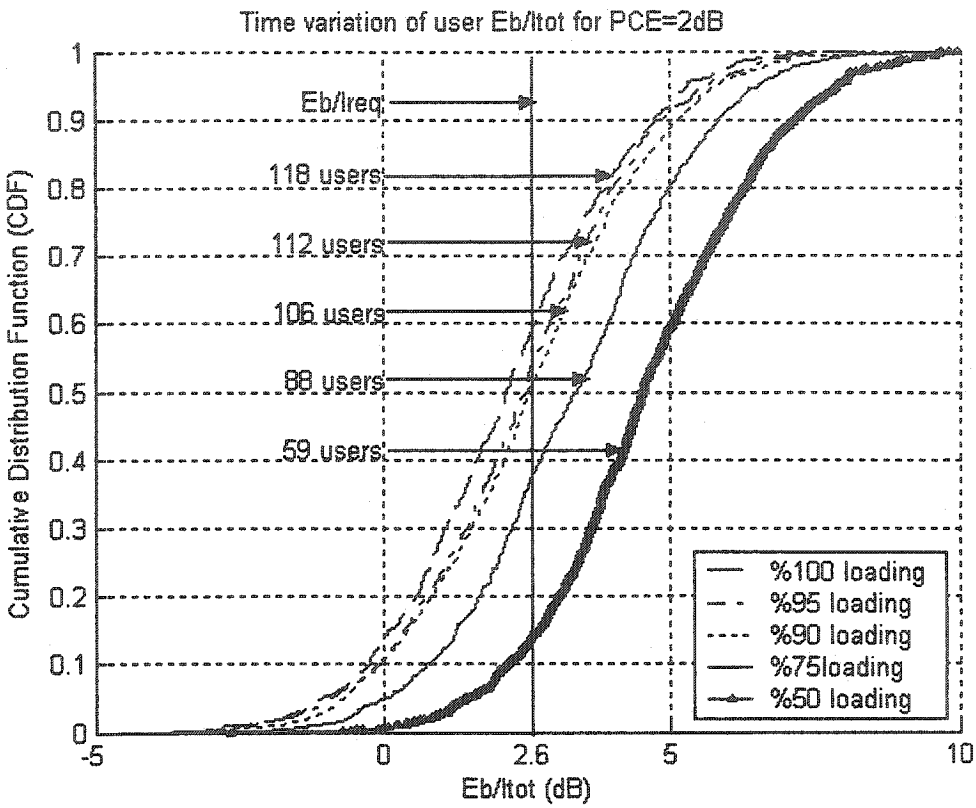

Figure 4-25 User Eb/Itot cdf with different spot-beam loadings in PCE=2dB

If we consider the system with PCE=2 dB, we see from Figure 4-25 that the system is not able to support 59 active mobile users with 90% system availability. Figure 4-25 shows that in order to serve 59 mobile users PCE=2dB, we have to decrease the system availability to 85% of time.

Finally, we consider the system with the same loading and different PCE values. Figure 4-26 illustrates the decrease in the ELM of the system relative to PCE and shows the ELM for 50% loading.

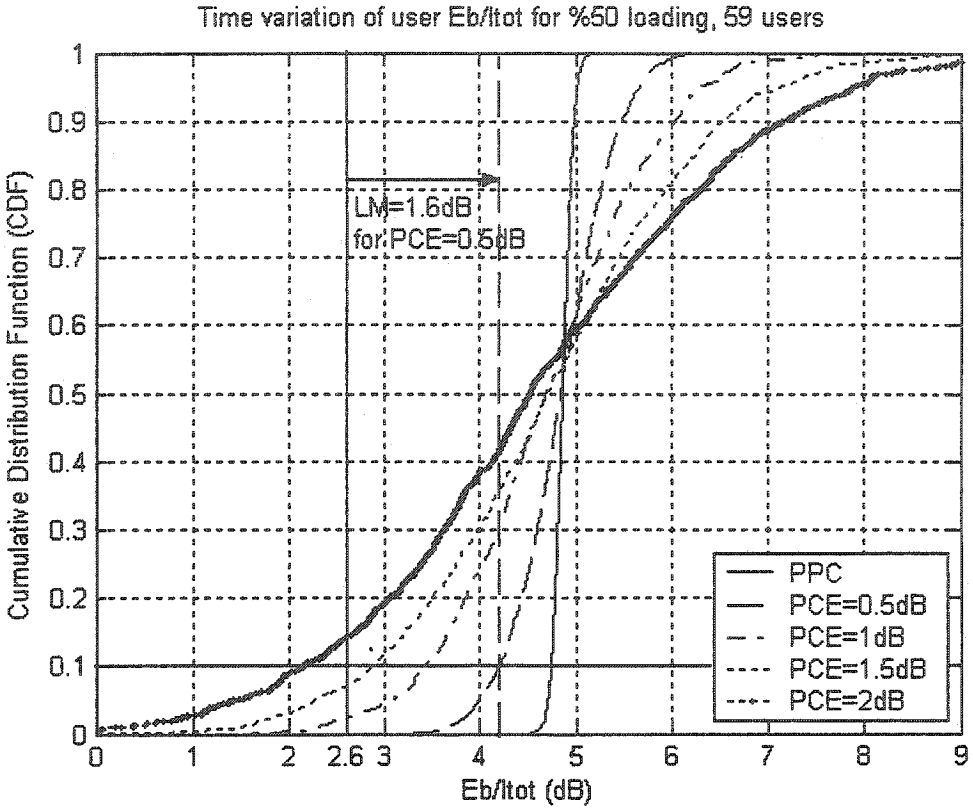

Figure 4-26 User Eb/Itot cdf with different PCEs and %50 loading

4.4 Summary

In this section we compare the performances of the satellite systems in a number of scenarios. These scenarios include varying the number of spot-beams, spot-beam loadings, spot-beam overlap values and different frequency reuse clusters. Change of the OCI factor of the system considered and its consequence on the overall system capacity are presented in Tables. The cdf and pdf curves of active mobile users' E_b/I_{tot} in the considered spot-beams are derived and compared to find both the capacity and the ELM of the satellite system. All the simulations are performed with MATLAB.

Chapter 5

SUMMARY, CONCLUSIONS, CONTRIBUTIONS AND RECOMMENDATIONS FOR FUTURE WORK

5.1 Summary

The main idea of this thesis has been to understand the interaction between the system design parameters that are used in CDMA multi-beam GEO satellite systems. The background information about satellite communications and satellite system parameters that affect the performance have been given in Chapter 2. Satellite-earth geometry, satellite radio links, the hexagonal spot beam layout and frequency re-use concept between spot-beams have been defined. The mobile user-satellite geometry for uplink MAI calculations has been introduced.

In Chapter 3, the details of the capacity calculations and theoretical formulas for different types of systems (e.g., single beam, multi-beam, system with PCE) have been presented.

System simulation descriptions and comparisons of simulation results to theoretical ones have been given in Chapter 4. Satellite systems having different spot-beam overlap values, cellular layouts, frequency reuse policies and spot-beam loadings have been considered in performance evaluations. In addition, the outage probability calculations and link margin calculations have been performed for practical satellite systems.

5.2 Conclusions

In this thesis we have mainly dealt with two major design issues of multi-beam satellite systems. One of these is the evaluation of the MAI for CDMA multi-beam satellite systems. We have concentrated on the effects of the system design parameters on the OCI factor, since the OCI factor perfectly represents the MAI characteristics of the multi-beam systems.

The effect of cellular layout on the OCI factor has been analyzed first. As we take into account more spot-beams in the satellite footprint, the OCI factor increases. From the geometrical point of view, in the mobile user uplink, the further the interfering spot-beam from the considered spot-beam, the less its effect will be, due to larger offset angles of the interfering mobile signals at wanted user's spot-beam, therefore causing less interference. The OCI factor has been calculated up to the 4th ring of spot-beams, because the consideration of further spot-beams barely affects the OCI factor.

It has been shown that introducing a 3-Cell cluster frequency reuse scheme substantially reduces the OCI factor and improves the system capacity. Nevertheless, further increasing the frequency reuse scheme (e.g., 4-Cell frequency reuse, 7-Cell frequency reuse etc.) does not decrease the OCI as much as it does in the transition of full frequency reuse to 3-Cell frequency reuse scheme and it causes system capacity loss due to reduced spectral efficiency.

Additionally, it has been demonstrated that the spot-beam contour is another key system parameter that affects the OCI factor. Usually, the spot-beam contour is defined by a 3dB decrease of spot-beam antenna gain. Higher beam isolation leading to less interference can be achieved by choosing a larger gain decrease at spot-beam contour. Even though, superior spot-beam isolation supplies an increased capacity ***per spot-beam***, the overall system capacity for constant serving area decreases due to representation of coverage area with fewer spot-beams (less spectral efficiency).

The power requirement at satellite in PPC case for each cell has been evaluated and it has been shown that more power is needed for highly isolated spot-beams (i.e., higher power decrease at spot-beam contour).

The effect of adjacent beam loading on the OCI factor has also been investigated. It has been shown that with low loading in other spot-beams in the cellular layout, one can obtain higher capacity in the considered beam due to reduced inter-cell interference. We can see from Table 4-8 that, 40% capacity increases in the considered beam can be observed with the condition of 50%

loading of other spot-beams with 3 dB overlap. This capacity increase can reach to 80% with 25% loading.

The second design issue considered in this thesis is the consequence of the PCE on system capacity. We have assessed the system capacity by evaluating the number of users satisfying the required bit energy to total interference density ratio E_b/I_{req}. Capacity degradation has been defined relative to the maximum attainable capacity calculated with 100% loading of each spot-beam in the cellular layout. The simulations have indicated that, even introducing a slight PCE (e.g. standard deviation 0.5dB) causes almost 50% capacity reduction, comparison to PPC case (e.g., $E_b/I_{tot} \leq E_b/I_{req}$).

Finally, link budget analysis of the satellite systems with different loadings has been presented. Excess link margin (ELM) is defined and calculated for satellite systems operating at different PCEs. It has been shown that the increase of signal power variations due to system PCE causes to a decrease in the ELM of the system. The ELM has also been evaluated and compared for different beam loadings. It has been stated that higher ELM and system availability can be obtained by decreasing spot-beam loadings.

5.3 Contributions

The main contributions of this thesis can be summarized as follows:

i. It has been shown that in satellite CDMA systems 3 Cell frequency reuse cluster gives better performance than full frequency reuse by appropriately choosing system parameters. It has been explained that the OCI factor decreases as frequency reuse cluster increases. The OCI factor is calculated for different frequency reuse schemes and presented in Tables 4-5, 4-6 and 4-7. We have explained that in low beam isolations (e.g. smaller spot-beam contours), where we have high OCI factor, introducing 3-Cell or more frequency reuse clusters reduces the interference in such a degree that it can compensate the capacity loss due to reduced

spectral efficiency. However, as we increase the beam isolation, it is not sufficient enough to compensate.

ii. The reverse link capacity of CDMA multi-beam satellite systems has been analyzed with PPC and IPC. The considered spot-beam user E_b/I_{tot} values have been calculated and the beam capacity has been assessed with the condition that users' E_b/I_{tot} satisfies the required E_b/I_{req}. The probability density functions and cumulative density functions of user' E_b/I_{tot} have been used to analyze system performance. The system outage probability has been evaluated with PPC and IPC schemes. Simulations have been performed to verify the analytical results. In all cases, the outage probability is found to be very sensitive to the PCE. It has been explained that the outage probability increases as we increase the PCE. The investigation of loading effect in satellite beams explicitly displays the tradeoff between system reliability and system capacity. It has been illustrated in Figure 4-17 that as we increase the beam loadings, the percentage of the users that the system can supply a good communication link quality increases.

iii. It has been shown that the OCI in satellite CDMA uplinks is much more critical than it is in terrestrial cellular systems. It has been demonstrated that inter-cell interference is generally independent of the number of spot-beams for greater than 61 spot-beams. It has been illustrated in Figure 4-2 and Table 4-2 that 80% of the OCI is caused by the beams in the first ring in the cellular layout and the effect of the beams further than the 4^{th} ring is negligible.

iv. Another parameter determining MAI, the edge of spot-beam coverage has also been presented. It has been shown that higher beam isolation leading to less interference and increased capacity per beam can be achieved by choosing a larger gain decrease at spot-beam contour. The decrease in the OCI factor relative to the increase in the spot-beam contour is given in Table 4-3 and 4-4. It has also been indicated that the increase in the spot-beam

contour causes the increase in the spot-beam radius and the decrease in the spectral efficiency.

v. The excess link margin of the system has been calculated and compared for different PCEs and loadings. It has also been explained that in order to guarantee a target Quality of Service (QoS), one has to decrease the mobile user capacity (loading) with increasing PCE.

5.4 Recommendation for Future Work

The recommendations for future work are:

i. In this thesis the results are obtained assuming PPC and PCE. In order to have a realistic capacity calculation we have to consider power control mechanisms. Simulation of power control algorithms and calculated PCE values would increase the reliability of the capacity calculations.

ii. This study has illustrated that the return link capacity is very sensitive to adjacent beam loadings and this issue has to be addressed considering different traffic distributions in the cellular layout.

iii. In the simulations, the earth's curvature is neglected. This issue may be critical for some satellite systems which consider serving the regions away from equator.

iv. Other satellite systems, sharing the same frequency band, should be considered in the interference calculations.

v. In this thesis we concentrated on capacity calculations in the mobile reverse link because of the asynchronous uplink assumption. Quasi-synchronous schemes using spreading codes which have a very low correlation over small timing offsets [Deg92] should be considered in limiting the reverse link capacity calculations.

vi. The ability of a CDMA system to reuse the entire frequency band again by utilizing the two opposite senses of circular polarization (e.g. cross-polarization isolation) should be taken into account in the MAI attenuation.

REFERENCES

[Abu94] A.A. Abu-Dayya and N. C. Beaulieu, "Outage Probabilities in the Presence of Correlated Lognormal Interferers," IEEE Trans. Veh. Technol., Vol.43, pp. 164-173, Feb. 1994

[Clr68]. R.H. Clarke, "A statistical theory of mobile reception", Bell Sys. Tech. J., 47, 957-1000, 1968

[Cor94] G.E. Corazza and F. Vatalaro, "A statistical model for land mobile satellite channels and its application to nongeostationary orbit systems," IEEE Trans. Veh. Technol., vol.43, 738-742, 1994.

[Cox84]. Cox, D.C., Murray, R., and Norris,A., "800 MHz Attenuation Measured in and around Suburban Houses," AT&T Bell Laboratory Technical Journal, Vol.673, No.6, July-August 1984.

[Dav97] F. Davarian, S. Chen, M. Shihabi, "Channel Behaviour and Power Control in Handheld Mobile Satellite Links", IMSC'97,16-18 June 1997, Pasadena, California, USA

[Deg92] R.DeGaudenzi, C.Elia, and R.Viola, "Bandlimited quasi-synchronous CDMA: Anovel satellite access technique for mobile and personal communication systems," IEEE J. Select. Areas Comm., vol.10, pp.328-343, Feb. 1992.

[Fen60] L.F. Fenton, "The sum of Log-Normal Probability Distributions in Scatter Transmission Systems," IRE Trans. Commun. Systems, Vol.CS-8, pp.57-67, Mar. 1960

[Fra59] J. M. Fraser, "Engineering aspects of TASI," Bell Syst. Tech. J., vol. 38, pp. 353-365, Mar. 1959.

[Gil90]K. S. Gilhousen, I. M. Jacobs, R. PAdovani, and L. A. Weaver, "Increased capacity using CDMA for mobile satellite communications," IEEE Transactions on Selected Areas in

Communications, vol.8, pp.503-514, May 1990

[Gil91] K.S. Gilhousen, I.M. Jacobs, R. Padovani, A.J. Viterbi, L.A. Weaver, Jr., and C.E. Wheatley, III, "On the capacity of a cellular CDMA system," IEEE Trans. Veh. Technol.,vol.40, May 1991.

[Gol94]. A. J. Goldsmith, L. J. Greenstein, and G. J. Foschini, "Error statistics of real-time power measurements in cellular channels with multipath and shadowing," IEEE Trans. Veh. Technol., vol.43, pp. 439-446, Aug.1994.

[Gud91]. Gudmunson, "Correlation model for shadow fading in mobile radio systems," IEEE Electronics Letters vol.27, No.23, 7th Nov. 1991.

[Hwa92] Y. Hwang, "Satellite Antennas", Proc. of the IEEE Vol.80, No.1, Jan 1992

[Kim93] K. I. Kim, "CDMA Cellular Engineering Issues", IEEE Trans. Veh. Technol., vol. 42, No.3, pp. 345-350, Aug 1993

[Koo00] E. Kudoh, "Sensitivity of the system capacity with Respect to the System Reliability in a DS-CDMA Cellular System", IEICE Trans. Commun., Vol. E83-B, No.3, pages 742-745, Mar 2000

[Kud92] E. Kudoh and Tadashi Matsumoto, "Effects of Power Control Error on the System User Capacity of DS/CDMA Cellular Mobile Radios", IEICE Trans. Commun., Vol. E75-B, No.6, pages 524-529, Jun 1992

[Kud93] E. Kudoh, "On the capacity of DS/CDMA Cellular Mobile Radios under Imperfect Power Control", IEICE Trans. Commun., Vol. E76-B, No.8, pages 886-893, Aug. 1993

[Lee91] W. C. Y. Lee, "Overview of Cellular CDMA" IEEE Trans. Veh. Technol., vol. 40, No.2, pp. 291-302, May 1991

[Loo85] C. Loo, "A statistical model for a land mobile satellite link", IEEE Trans. Veh. Technol., vol.34, 122-127, 1985.

[Lut00] E. Lutz, M. Werner and A. Jahn, Satellite Systems for Personal and Broadband Communications. Springer-Verlag Berlin, 2000

[Lut91] E. Lutz, D. Cygan, M. Dippold, F. Dolainsky, and W. Papke, "The land mobile satellite communication channel – recording, statistics and channel model, " IEEE Trans. Veh. Technol., vol. 40, pp. 375-386, May 1991.

[Lut97]E.Lutz, "Other-cell interference in satellite power controlled CDMA uplink", In proceedings 5th International Mobile Satellite Conference (IMSC '97), pages 83-87, 1997

[Lyo97] B. Lyons, "A transmission system for future satellite mobile and personal communications", European Space Agency Contract No.:11515/95/NL/US, 1997

[Mar98] G. Maral and M. Bousquet, Satellite Communications Systems. John Wiley & Sons Ltd, Chichester, 1998.

[Moh97] M.Moher, R. G. Lyons and L. Erup "Power and Bandwidth Tradeoffs for a Third Generation Satellite Systems", IMSC'97,16-18 June 1997, Pasadena, California, USA

[Mon93] A.M. Monk and L.B. Milstein, "A CDMA cellular system in a mobile base station environment," in Proc. IEEE GLOBECOM, vol. 4, Nov. 1993, pp. 65-69

[Mon95] M. Monk, L. B. Milstein, "Open-Loop Power Control Error in Land Mobile Satellite System", IEEE Transactions on Selected Areas in Communications, vol.13, No.2, pp.205-212, Feb. 1995

[Pra93] R. Prasad, "Near-far-effects on performance of DS/SS CDMA systems for personal communication networks," IEEE 43rd Veh. Tech. Conf. 18-20 May 1993 , pp 710-713

[Sch82] S.Schwardz and Y.S. Yeh, "On the Distribution function and moments of power sums with log-normal components," Bell Syst. Tech. J., Vol.61, pp.1441-1462, Sep. 1982

[Ska88], B. Sklar, digital Communications: Fundamentals and Applications, Ch. 4, Englewood Cliffs, NJ: Prentice Hall, 1988.

[Taa97] P.Taaghol, R. Tafazolli, B.G. Evans, "Power Control Performance in Measurement-based S-PCN Channel", IMSC'97,16-18 June 1997, Pasadena, California, USA

[Taa99] P.Taaghol, S. Nourizadeh, R. Tafazolli, "An Advanced Power Control Scheme for CDMA-based Satellite Communication Systems", IMSC'99, June 1999, Ottawa, Ontario, CANADA

[Taa99]. P. Taaghol and R. Tafazolli, "Correlation model for shadow fading in land-mobile satellite systems," IEEE Electronics Letters vol.33, No.15, 17th Jul. 1997.

[Tam97] W. M. Tam and F.C. M. Lau, "Analysis of imperfect power control in CDMACellular Systems," in Proc. PIMRC'97, pages 892-897, 1997

[Tam99] W. M. Tam and F.C. M. Lau, "Analysis of Power Control and Its Imperfections in CDMA Cellular Systems," IEEE Trans. Veh. Technol., vol. 48, No.5, pp. 1706-1717, Sep 1999

[Ven95] J. Ventura-Traveset, I. Stojkovic, F. Coromina, J. Benedicto, and F. Petz. Key payload technologies for future satellite personal communications: a European perspective. International Journal of Satellite Communications, vol. 13, pages 117-135, 1995

[Vit85] A. J. Vitebi, "When not to spread spectrum- A sequel," IEEE Communications Mag. Vol. 23, pp. 12-17, Apr. 1985.

[Vit93] A. M. Viterbi and A. J. Viterbi, Erlang capacity of power controlled CDMA system, IEEE Journal on Selected Areas in Communications, Vol. 11, pages 892-900, 1993.

[Vit94] A. J. Viterbi, A. M. Viterbi, and E. Zehavi. Other-cell interference in cellular power controlled CDMA IEEE Trans. On Comm. , vol.42, pages 1501-1504 1994.